Novel Biochemical Signatures of Early Stages of Alzheimer's Disease

Del Campo Milan, M.

2015

document version
Publisher's PDF, also known as Version of record

Chapter 1

Introduction
Aims and outline

ALZHEIMER'S DISEASE

Alzheimer's disease (AD) is an age-related neurodegenerative disorder and the most common form of dementia. It is clinically characterized by a progressive impairment of cognitive functions (i.e. memory, reasoning, language, emotional control) ultimately disrupting daily life activities. It has been estimated that 36 million of people worldwide were suffering from dementia in 2010 and that, due to increasing life expectancy, the number of patients will double every 20 years. Thus, the increasing global prevalence of AD will pose a huge impact not only on the patients and their families, but also on the public healthcare and financial systems[1,2].

AD can be divided into Familial AD (FAD), characterized by a specific genetic predisposition, and sporadic AD, with no familial inheritance. FAD cases are predominantly early-onset (younger than 65 years old) and accounts only for 5-10% of all AD patients. Thus, more than 90% of the AD patients are sporadic and usually with an age over 65. Besides the age of onset, both types are often clinically undistinguishable, which strongly suggests that similar pathological mechanisms are involved in the development FAD and sporadic AD[3]. FAD is usually caused by high penetrant autosomal dominant mutations in one of three genes: amyloid precursor protein (APP)[4], presenilin 1 (PS1) [5] and presenilin 2 (PS2)[6]. Importantly, mutations in those genes affect the production of amyloid β (Aβ)[7,8], pinpointing the importance of this amyloidogenic peptide in AD pathogenesis[9]. The sporadic AD form, which likely results as a combination of genetic and environmental factors, is however much more complex, with an amalgam of age-related physiological changes and different disorders. To date, the best-known genetic risk factor for sporadic AD is the ε4 allele of the apolipoprotein E (APOE) gene, which increases the risk of developing AD by about 3-fold or greater than 10-fold when carrying one or both APOEε4 copies respectively[10,11]. Several studies suggest that APOE protein is involved in the clearance of Aβ[12,13], although other functions such as transport and metabolism of lipids have also been described[14].

UNCOVERING AD PATHOGENESIS

Ramon y Cajal predicted that dementia could result from the weakness of synapses, the molecular structures that allows the communication between neuronal cells and thus are essential for neuronal function[15]. Several studies have indeed indicated that synaptic failure is likely the underlying event leading to memory loss, even at early stages of AD[16]. AD is pathologically characterized by the accumulation and aggregation of the abnormally

hyperphosphorylated form of tau in neurofibrillary tangles (NFT)[17] and Aβ peptide in senile plaques[18]. Besides these two classical hallmarks, other proteins and mechanisms are known to play important roles in AD pathogenesis such as the unfolded protein response (UPR) or inflammation (Fig. 1). However, despite the great research efforts undertaken in the last decades, the etiological factors underlying AD neuropathology remain unknown.

Tau and neurofibrillary tangles

Tau is a microtubule-associated protein involved in the stabilization of microtubules, one of the major components of the neuronal cytoskeleton that provides structural support to the neurons and regulate essential cellular processes such as transport of molecules or cell division[19]. The association of tau to microtubules depends on its phosphorylation state. Hyperphosphorylation of tau (p-Tau) leads not only to a disorganization of the microtubule structure but also to a self-aggregation of the protein and subsequent formation of NFT[17] (Fig. 1). Compelling evidences from cell and animal models indicate that the presence of tau aggregates induces cell death and loss of synapses through different mechanisms including disruption of axonal transport, oxidative stress, mitochondrial impairment or DNA damage[20]. Several kinases are involved in tau (hyper)phosphorylation including the glycogen synthase kinase 3 β (GSK3β)[21], whose activity can be modulated by Aβ[22]. Interestingly, the formation of NFT strongly correlated with the development of cognitive deficits in AD, suggesting an important role of tau aggregates in the development of dementia[23,24]. Noteworthy, tau lesions, rather than being an exclusive hallmark of AD pathology, are also present in other neurodegenerative dementias named tauopathies, such as frontotemporal dementia[25]. Although several conditions can contribute to the dysregulation and dysfunction of tau (hyperphosphorylation, truncation, nitration), the exact mechanism initiating abnormal tau hyperphophorylation in AD and other tauopathies remains to be uncovered.

Aβ and senile plaques

Senile plaques are one of the first AD hallmarks described by Alois Alzheimer in 1906[26,27], and are found not only in the brain parenchyma but also in the cerebral vessel walls (cerebral amyloid angiopathy (CAA)). The main components of these plaques are the Aβ peptides, which accumulate and self-associate leading to the formation of various assembling forms, ranging from soluble aggregates (oligomers) to insoluble fibrils. Over the past decade, several studies have suggested that oligomers, rather than fibrillar Aβ forms, mediate the neuronal toxicity observed in AD tissue[16,28–30]. Several amyloid-associated proteins have also been identified in senile plaques such as agrin, APOE,

complement activation factors or pro-inflammatory cytokines and interleukines, which can influence the aggregation and toxicity of Aβ[31,32].

Aβ is produced after a regulated intramembrane proteolysis of APP by β- and γ-secretases[33]. APP is first cleaved by β-secretase 1 (BACE1), leading to the release of the sAPPβ fragment[34,35]. The remaining membrane-bound fragment is further cleaved by γ-secretase, leading to the release of Aβ peptide[36] (Fig. 1). The γ-secretase is a multimolecular complex including, among others, PS1 and PS2[37]. Different Aβ forms have been described depending on the exact cleaving site of the γ-secretases and the subsequent length of the Aβ peptide, being Aβ 1-40 ($A\beta_{40}$) and 1-42 ($A\beta_{42}$) the most common peptides. Although $A\beta_{40}$ is the most abundant form in the brain and likely reflects Aβ production, $A\beta_{42}$ is highly amyloidogenic and sets the seed for amyloid plaque formation[38–40]. APP can also be proteolysed via a non-amyloidogenic proteolytic pathway in which it is cleaved by α-secretase. The cleavage site of α-secretase resides within the Aβ domain, thus abrogating Aβ formation[33,41]. The major α-secretase identified in APP processing is ADAM10[42–44]. The underlying mechanism that determines whether APP is cleaved by α- or β-secretase has not been revealed yet[41].

Different processes are involved in the clearance of Aβ from the brain. Those mechanisms include the transport of Aβ through the blood-brain-barrier (BBB)[45] as well as its degradation via specific proteases such as the insuling degrading enzyme (IDE)[46] or via nervous phagocytic cells such as microglia[47]. Interestingly, recent research showed a decreased clearance of Aβ from the brain of sporadic AD patients, indicating that the mechanisms involved in the Aβ clearance are hampered in AD pathogenesis[48]. However, it remains unclear to date whether the accumulation of Aβ in sporadic AD cases results from an overproduction of this amyloidogenic peptide, a decrease clearance or a combination of both mechanisms.

The amyloid cascade hypothesis

Although the etiology of AD remains unknown, the prevailing theory about AD pathogenesis is the amyloid cascade hypothesis, which suggests that the accumulation of specific Aβ oligomers is the key event ultimately leading to neurodegeneration[9,49–51]. Although still under debate, several studies suggest that amyloid-induced toxicity may trigger neurofibrillary pathology [52,53]. However, the exact mechanism by which amyloidosis may facilitate NFT formation remains to be elucidated. The amyloid cascade hypothesis is supported by the increased Aβ load found in FAD[7,54,55] and by the genetic risk factors related to sporadic AD (i.e. APOEε4, APOJ or CR1), which are genes encoding proteins that are likely involved in Aβ clearance[10,56,57]. In addition, some neuropathological hallmarks of sporadic AD were replicated in transgenic AD mice models with FAD mutation [58,59]. However, deposition of Aβ in senile plaques is also observed in normal

aging, and its correlation with neuronal loss and cognitive decline is not strong[60,61]. In addition, the presence of aggregated extracellular Aβ was not sufficient by itself to induce cognitive deficits in transgenic mouse model[62]. In this context, genome-wide association studies have identified novel loci associated with sporadic AD that are not related to Aβ metabolism, but rather to immune system response, cellular stress, or synaptic and mitochondrial dysfunction[63,64]. For instance, a variant of TREM2 has been recently identified as an important risk factor for late-onset AD. TREM2 is a protein found in microglia, which might be involved in the clearance of apoptotic damage in neuronal tissue as well as in the development of an anti-inflammatory response[65–67]. These data have led many scientists to suggest that Aβ plaques might be disease bystanders rather than the cause of the disease[68,69].

Other mechanisms involved in AD pathology: unfolded protein response and inflammation

The presence of misfolded proteins (i.e. Aβ and p-Tau in AD or α-synuclein in Parkinson's disease (PD)) induces an adaptive reaction in the endoplasmic reticulum (ER) and the subsequent activation the UPR in order to restore unfolded protein load and cell homeostasis[70,71]. However, failure to restore proteostasis and the chronic activation of the UPR initiate an apoptotic cell signalling cascade, ultimately leading to cell death[70,72] (Fig. 1). Indeed, several studies have shown that Aβ can induce ER stress-mediated apoptosis[73–76]. Increased expression of UPR markers has been observed in early stages of AD and PD[77–79], which was also associated with tau pathology in different tauopathies[80,81]. Noteworthy, UPR markers were observed in neurons with a diffuse accumulation of the corresponding protein aggregate (i.e. tau or a-synuclein) but not in the corresponding aggregated structures (NFT in AD or Lewy body in PD), suggesting that the UPR might be involved in the initial steps up-stream protein aggregation[78,81]. This is further supported by recent studies showing that UPR promotes not only the activation of GSK3β[82,83] but also the phosphorylation of tau[84]. Moreover, decreasing the levels of different UPR related proteins improved cognitive deficits and neurodegeneration in transgenic mice models of AD[85] and prions' disease[86,87]. Those data strongly suggest that the UPR is an important mechanism and a causative contributor to the pathogenesis not only of AD but also of other protein-misfolding disorders.

Similar to the UPR, inflammation is an adaptive response to harmful stimuli, but prolonged activation of the inflammatory process may play a role in the neurodegenerative process. A relationship between inflammation and AD was unraveled more than 20 years ago when the first studies showed an association between Aβ plaques and activated microglia[88]. Indeed, amyloid plaques co-localize with multiple inflammatory molecules such as

cytokines and interleukines (i.e. tumor necrosis factor a) or complement factors[89,90], which are already changed in early stages of AD[91,92] (Fig. 1). The involvement of inflammation in early pathological stages of AD is further supported by clinical studies using positron emission tomography (PET), which showed activated microglia in patients with mild cognitive impairment that had also amyloid deposition[93]. Epidemiological studies have reported that nonsteroidal anti-inflammatory drugs (NSAIDs) reduced the risk of AD, although clinical trials using these drugs in AD patients have not been so far successful[94]. In transgenic mice models, changes in inflammatory markers were observed even before Aβ deposition[95]. In addition, recent animal studies showed that the inflammatory pathway IL12/IL23 is crucially involved in the development not only of Aβ plaques but

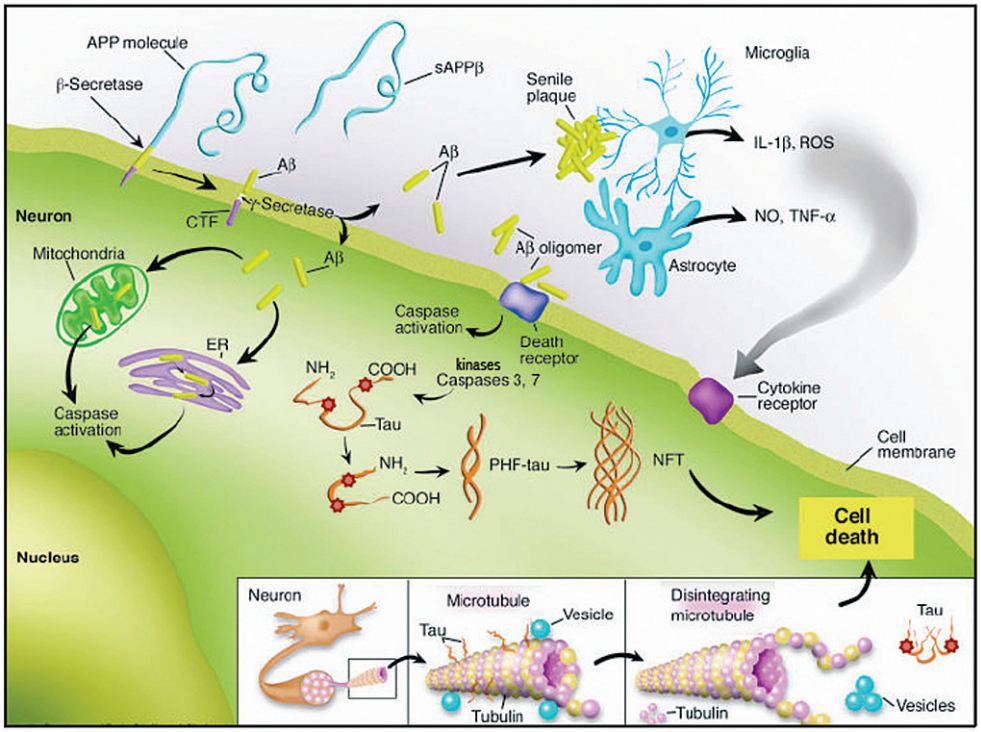

Fig 1. Classical characteristics of AD neuropathology

Aβ is produced after the sequential cleavage of APP by β- and γ-secretases. Aβ is highly prone to aggregate leading to the formation of extracellular senile plaques (top left corner). The presence of extracellular Aβ species triggers the activation of glia cells (microglia and astrocytes) initiating an inflammatory process in which different proinflammatory cytokines such as TNF-α are released (top right corner)**.** Intracellular Aβ can induce stress in the mitochondria and ER leading to the activation of caspases, downstream apoptotic effectors (left side). The activation of kinases and caspases induce the hyperphosphorylation and truncation of tau respectively. Abnormal tau disrupts cytoeskeleton (insert) and its accumulation lead to the formation of paired helical filaments (PHF) and NFT (bottom part). sAPPβ: soluble APPβ. Orange stars: Phosohorylated groups. Figure adapted from D. Dickson [98]

also of cognitive functions[96,97]. Taken together, those results support an important role of inflammation in early stages of AD pathology.

In summary, although the importance of the different hallmarks described above in the pathogenesis of AD is undeniable, it remains unclear whether these mechanisms are causative factors of the disease or the result of an ongoing up-stream pathological process. Thus, the understanding of AD pathogenesis is still a challenging field.

AD DIAGNOSIS

Diagnosis of probable or possible AD is made by neurologist following the new diagnostic criteria established by the National Institute on Aging and the Alzheimer's Association (NIA-AA)[99,100].

The neurodegenerative processes and the clinical manifestations of AD occurs gradually, where dementia is an endstage in which massive neuronal damage has already taken place[101]. Therefore, the pathophysiological changes leading to AD start decades before clinical symptoms appear[102], providing a good time-frame to detect biomarkers predicting the development of AD (preclinical AD). Early diagnosis is of great importance since it will likely enable to prevent, slow down or halt the disease before extensive neurodegeneration occurs[103,104]. Thus, interest in biomarkers able to detect the earliest phase is continuously high. Ideally, biomarkers should reflect the underlying molecular pathology related to the disease[105]. Cerebrospinal fluid (CSF) is considered one of the main sources for the discovery of biomarkers for the central nervous system, since it directly interacts with the extracellular space of the brain and mirrors biochemical alterations occurring in the parenchyma[106]. The current core CSF biomarkers for AD diagnosis represent the classical AD hallmarks: a decrease in $A\beta_{42}$ levels reflects senile plaque pathology, and the increase in total tau (t- Tau) and p-Tau levels reflect axonal degeneration and NFT formation[107–110]. Their sensitivity and specificity for AD is high and they can also reasonably predict the transition of mild cognitive impairment (MCI) to AD[111–113]. Nevertheless, AD CSF biomarker patterns are also present in cognitive normal subjects and influenced by the age of the patient, resulting in loss of sensitivity at higher age where the prevalence of sporadic AD is higher[114,115]. In addition, the measurements of the dinamyc changes on those biomarkers are not sensitive enough, which is a prerequisite for monitoring treatment effects. In the last years, novel candidate CSF biomarkers related to AD pathology have been identified although the initial promising findings have not been able to be replicated or validated[110]. In a recent lipidomics study, a panel of plasma phospholipds successfully predicted preclinical AD with an accuracy of 90%. However, further validation studies in larger and

different population are needed[116]. Thus, the quest for the earliest, and most sensitive and dynamic markers to AD pathology is ongoing. Noteworthy, an important issue that should not be underestimated for the discovery of novel CSF biomarkers is the effect of the pre-analytical confounding factors, which are already known to dramatically influence the real measurement of the current core AD CSF biomarkers[117,118]. Therefore, CSF should be stored and handled according to the established guidelines in order to obtain accurate diagnostic conclusions[119,120].

PROTEOMICS: A GATEWAY TO EXPLORE DISEASES

Proteomics is the analysis of all detectable proteins or peptides in an organism or in different subdivisions including tissue, organelles or body fluids such as CSF. The proteome of an entity varies according to the physiological and pathological conditions[121]. Thus, the detection of changes in the protein composition through proteomics approaches may reflect different stages of the disease or unravel novel players in the pathology, leading to the discovery of novel potential biomarkers, molecular networks, pathological processes and new targets for future therapies. The field of proteomics in neurodegenerative disorders is growing rapidly and the sensitivity, speed and the practicability of the different proteomics approaches is getting better. In fact, proteomics approaches are starting to be widely applied in the study of neurodegenerative disorders[122]. Generally, the identification of novel proteins through proteomics approaches goes through different phases. First, hypothesis-free (unbiased) proteomics approach (i.e. 2D-LC/MS) is applied in order to identify potential candidates related to the pathology. The selected candidates can then be further validated using not only targeted proteomics (i.e. MRM) but also other different immunoassay techniques (i.e. ELISA, multiplex platforms, western blotting, immunohistochemistry). Depending on the goal of the study (i.e. biomarker validation, pathological characterization) one specific technology or a combination of techniques can be used. The human CSF proteome described so far has been mapped and the information is accessible online[123,124]. In addition, several studies have already used proteomics-based approaches to identify AD CSF biomarkers, although further validation is still needed[125].

In summary, the worldwide research efforts in the Alzheimer's field have revealed the high complexity of this disorder, likely exacerbated in the sporadic forms due to the late age of onset and the subsequent combination with other disorders and the physiological processes of aging. Despite the tremendous progress that has been achieved in the understanding of AD pathology, we are still unable to effectively halt, delay or prevent

the development of AD. Thus, the quest for novel proteins involved in AD pathogenesis is still ongoing. In view of the potential of unbiased proteomics approaches for the discovery of novel CSF proteins, which may reflect unknown neuropathological processes and be useful as early biomarkers, a European consortium was established (clinical NEUroPROteomics of neurodegenerative diseases, cNEUPRO)[126]. As part of this consortium we previously analyzed CSF samples of non-demented controls (subjective memory complaints, SMC) and AD patients by a hypothesis-free proteomics approach. In order to find protein candidates reflecting changes in early stages of AD pathology, patients with mild cognitive impairment (MCI) who within two years follow-up developed AD (MCI-AD) or remained stable (MCI-S) were also included (Chiasserini et al., manuscript submitted). From that study, several and different potential protein signatures of early AD pathology were identified including the protein causing familial British and Danish dementias, named BRI2 (Integral membrane protein 2B, *Itm2B*), and agrin, the main heparin sulfate proteoglycan associated with Aβ plaques. Both proteins were increased in the CSF of MCI-AD and AD patients compared to control cases.

AIMS AND OUTLINE

The main focus of this thesis was to explore the involvement of BRI2 and related proteins in AD pathology as well as the potential of both BRI2 and agrin as early biomarkers for AD diagnosis. To this end, the following aims were formulated:

- Extensively investigate the expression of BRI2 and its processing enzymes in post-mortem tissue at different stages of the disease.
- Study the effects of abnormal BRI2 forms in cellular processes involved in AD pathogenesis.
- Investigate the potential of BRI2 and agrin as early biomarkers for AD.

The first part of the thesis addresses the importance that dysfunction of BRI2 protein could have in the main molecular pathways involved in AD, leading to the formulation of a modified hypothesis about AD etiology (**chapter 2**). In line with this hypothesis, we next investigated the expression of BRI2 and its processing enzymes in postmortem tissue from controls and AD cases at different stages of the disease. In addition, we analyzed whether the formation of BRI2-APP complexes, which was previously reported in cellular and mice models, occurred also in human tissue and if it was modified in AD cases (**chapter 3**). Since BRI2 has been shown to regulate also the levels of IDE in cell culture, we also analyzed in human hippocampus a possible relationship between changes in IDE and BRI2 (**chapter 4**). The results in chapter 3 unraveled larger BRI2 structures in AD tissue and set the

basis for our next study in which we investigated the effects of large recombinant BRI2 structures on molecular pathways involved in AD pathogenesis such as apoptosis, UPR or tau truncation and phosphorylation (**chapter 5**). The results of **chapter 3** additionally revealed that in AD the levels of one of the BRI2 processing enzymes, named SPPL2b, were dramatically changed. SPPL2b is a relatively new transmembrane protease and its relationship with AD had not been anticipated yet. Thus, in **chapter 6** we extensively analyzed the expression of SPPL2b not only in post-mortem tissue from control and AD cases but also in tissue from patients with other protein-misfolded dementias such as frontotemporal dementias and Parkinson's disease. In addition, an initial evaluation of SPPL2b in CSF from non-demented controls and AD cases was also performed.

In the last part of the thesis we aimed to investigate the potential of BRI2 and agrin as early CSF biomarkers for AD since changes in the levels of both proteins were previously detected in either AD brain tissue[127] or CSF[128]. The study of CSF biomarkers requires the use of standardized operating procedures (SOP) for the handling and biobanking of large cohorts of CSF samples in order to increase the accuracy of the results and ease its replication by other groups. As part of the BIOMARKAPD consortium focused on the formulation of international SOPs, we have updated and merged previous recommendations for the analysis of CSF biomarkers in AD and PD (**chapter 7**). In **chapter 8** we developed a new specific immunoassay able to measure the levels of BRI2 in CSF. Then, BRI2 levels were analyzed using a case-control study with CSF from non-demented controls and AD as well as a longitudinal approach in which patients with MCI-S and MCI-AD were also included. In addition, the association between the levels of BRI2 CSF and the classical AD biomarkers was also analyzed. **Chapter 9** evaluates whether the changes of agrin in AD tissue were reflected in CSF and its relationship with the classical AD markers using a commercially available immunoassay.

References

1. Alzheimer's disease International. *World Alzheimer Report 2009*. *World* (2009).

2. World Health Organization & Alzheimer's disease International, . *Dementia: A public health priority*. (2012).

3. Selkoe, D. J. Alzheimer ' s Disease : Genes , Proteins , and Therapy. **81,** 741–766 (2001).

4. Goate, A. *et al.* Segregation of a missense mutation in the amyloid precursor protein gene with familial Alzheimer's disease. *Nature* **349,** 704–6 (1991).

5. Sherrington, R. *et al.* Cloning of a gene bearing missense mutations in early-onset familial Alzheimer's disease. *Nature* **375,** 754–60 (1995).

6. Levy-Lahad, E. *et al.* Candidate gene for the chromosome 1 familial Alzheimer's disease locus. *Science* **269,** 973–7 (1995).

7. Citron, M. *et al.* Mutation of the beta-amyloid precursor protein in familial Alzheimer's disease increases beta-protein production. *Nature* **360,** 672–4 (1992).

8. Scheuner, D. *et al.* Secreted amyloid beta-protein similar to that in the senile plaques of Alzheimer's disease is increased in vivo by the presenilin 1 and 2 and APP mutations linked to familial Alzheimer's disease. *Nat Med* **2,** 864–70 (1996).

9. Hardy, J. & Allsop, D. Amyloid deposition as the central event in the aetiology of Alzheimer's disease. *Trends Pharmacol Sci* **12,** 383–8 (1991).

10. Corder, E. H. *et al.* Gene dose of apolipoprotein E type 4 allele and the risk of Alzheimer's disease in late onset families. *Science* **261,** 921–3 (1993).

11. Verghese, P. B., Castellano, J. M. & Holtzman, D. M. Apolipoprotein E in Alzheimer's disease and other neurological disorders. *Lancet Neurol* **10,** 241–52 (2011).

12. DeMattos, R. B. *et al.* ApoE and clusterin cooperatively suppress Abeta levels and deposition: evidence that ApoE regulates extracellular Abeta metabolism in vivo. *Neuron* **41,** 193–202 (2004).

13. Bales, K. R. *et al.* Apolipoprotein E is essential for amyloid deposition in the APP(V717F) transgenic mouse model of Alzheimer's disease. *Proc Natl Acad Sci U S A* **96,** 15233–8 (1999).

14. Wolf, A. B., Caselli, R. J., Reiman, E. M. & Valla, J. APOE and neuroenergetics: an emerging paradigm in Alzheimer's disease. *Neurobiol Aging* **34,** 1007–17 (2013).

15. Ramon y Cajal, S. Degeneration and Regeneration of the Nervous System. *J Neurol Psychopathol* **9,** 378 (1929).

16. Shankar, G. M. & Walsh, D. M. Alzheimer's disease: synaptic dysfunction and Abeta. *Mol Neurodegener* **4,** 48 (2009).

17. Grundke-Iqbal, I. *et al.* Abnormal phosphorylation of the microtubule-associated protein tau (tau) in Alzheimer cytoskeletal pathology. *Proc Natl Acad Sci U S A* **83,** 4913–7 (1986).

18. Masters, C. L. *et al.* Amyloid plaque core protein in Alzheimer disease and Down syndrome. *Proc Natl Acad Sci U S A* **82,** 4245–9 (1985).

19. Mandelkow, E.-M. *et al.* Tau domains, phosphorylation, and interactions with microtubules. *Neurobiol Aging* **16,** 355–362 (1995).

20. Frost, B., Götz, J. & Feany, M. B. Connecting the dots between tau dysfunction and neurodegeneration. *Trends Cell Biol* 1–8 (2014). doi:10.1016/j.tcb.2014.07.005

21. Gong, C. & Iqbal, K. Hyperphosphorylation of microtubule-associated protein tau: A Promising Therapeutic Target for Alzheimer Disease. *Curr Med Chem* **15,** 2321–2328 (2008).

22. Takashima, A. *et al.* Exposure of rat hippocampal neurons to amyloid fl peptide (25-35) induces the inactivation of phosphatidyl inositol-3 kinase and the activation of tau protein kinase I/ glycogen synthase kinase-3fl. *Neurosci Lett* **203,** 33–36 (1996).

23. Gold, G. *et al.* Clinical validity of Braak neuropathological staging in the oldest-old. *Acta Neuropathol* **99,** 579–82; discussion 583–4 (2000).

24. Nelson, P. T. *et al.* Clinicopathologic Correlations in a Large Alzheimer Disease Center Autopsy Cohort: Neuritic Plaques and Neurofibrillary Tangles "Do Count" When Staging Disease Severity. *J Neuropathol Exp Neurol* **66,** 1136–1146 (2007).

25. Lee, V. M., Goedert, M. & Trojanowski, J. Q. Nurodegenerative Tauopathies. *Annu Rev Neurosci* **24,** 1121–159 (2001).

26. Alzheimer, A. Uber eine eigenartige Erkrankung der Hirnrinde. *Allg Z Psychiatr Psych Med* 146–148 (1907).

27. Stelzma, R. A., Schnitzlein, H. N. & Murllagh, F. R. An English I ' ranslation of Alzheimer ' s 1907 Paper , " ijber eine eigenartige Erlranliung der Hirnrinde ." *Clin Anat* 429–431 (1995).

28. Walsh, D. M. & Selkoe, D. J. A beta oligomers - a decade of discovery. *J Neurochem* **101,** 1172–84 (2007).

29. Lesné, S. E. *et al.* Brain amyloid-β oligomers in ageing and Alzheimer's disease. *Brain* **136,** 1383–98 (2013).

30. Zahs, K. R. & Ashe, K. H. β-Amyloid oligomers in aging and Alzheimer's disease. *Front Aging Neurosci* **5,** 28 (2013).

31. Zhan, S.-S., Veerhuis, R., Kamphorst, W. & Eikelenboom, P. Distribution of beta amyloid associated proteins in plaques in Alzheimer's disease and in the non-demented elderly. *Neurodegeneration* **4,** 291–297 (1995).

32. Veerhuis, R., Boshuizen, R. S. & Familian, A. Amyloid Associated Proteins in Alzheimer ' s and Prion Disease. 235–248 (2005).

33. Chow, V. W., Mattson, M. P., Wong, P. C. & Gleichmann, M. An Overview of APP Processing Enzymes and Products. *Neuromolecular Med* 1–12 (2009). doi:10.1007/s12017-009-8104-z

34. Cai, H. *et al.* BACE1 is the major beta-secretase for generation of Abeta peptides by neurons. *Nat Neurosci* **4,** 233–4 (2001).

35. Luo, Y. *et al.* Mice deficient in BACE1 , the Alzheimer ' s β-secretase , have normal phenotype and abolished β-amyloid generation. **4,** 231–2 (2001).

36. Passer, B. *et al.* Generation of an Apoptotic Intracellular Peptide by γ-Secretase Cleavage of Alzheimer ' s Amyloid β Protein Precursor. **2,** 289–301 (2000).

37. Strooper, B. De. Aph-1, Pen-2, and Nicastrin with Presenilin Generate an Active Æ-Secretase Complex. *Neuron* **38,** 9–12 (2003).

38. Suzuki, N. *et al.* An increased percentage of long amyloid beta protein secreted by familial amyloid beta protein precursor (beta APP717) mutants. *Science* **264,** 1336–40 (1994).

39. Bitan, G. *et al.* Amyloid beta-protein (Abeta) assembly : Abeta 40 and Abeta 42 oligomerize through distinct pathways. *PNAS* **100,** 330–35 (2003).

40. Iwatsubo, T. *et al.* Visualization of A beta 42(43) and A beta 40 in senile plaques with end-specific A beta monoclonals: evidence that an initially deposited species is A beta 42(43). *Neuron* **13,** 45–53 (1994).

41. O'Brien, R. & Wong, P. Amyloid Precursor Protein Processing and Alzheimer's Disease. *Annu Rev Neurosci* **34,** 185–204 (2011).

42. Endres, K. & Fahrenholz, F. Regulation of alpha-secretase ADAM10 expression and activity. *Exp Brain Res* **217,** 343–52 (2012).

43. Kuhn, P.-H. *et al.* ADAM10 is the physiologically relevant, constitutive alpha-secretase of the amyloid precursor protein in primary neurons. *EMBO J* **29,** 3020–32 (2010).

44. Lammich, S. *et al.* Constitutive and regulated -secretase cleavage of Alzheimer's amyloid precursor protein by a disintegrin metalloprotease. *Proc Natl Acad Sci* **96,** 3922–3927 (1999).

45. Shibata, M. *et al.* Clearance of Alzheimer's amyloid-ss(1-40) peptide from brain by LDL receptor-related protein-1 at the blood-brain barrier. *J Clin Invest* **106,** 1489–99 (2000).

46. Farris, W. *et al.* Insulin-degrading enzyme regulates the levels of insulin, amyloid beta-protein, and the beta-amyloid precursor protein intracellular domain in vivo. *Proc Natl Acad Sci U S A* **100,** 4162–7 (2003).

47. Paresce, D., Ghosh, R. & Maxfield, F. Microglial Cells Internalize Aggregates of the Alzheimer ' s Disease Amyloid NL -Protein Via a Scavenger Receptor. *Neuron* **17,** 553–565 (1996).

48. Mawuenyega, K. G. *et al.* Decreased Clearance of CNS b -Amyloid in Alzheimer ' s Disease. *Science (80-)* **330,** 1774 (2010).

49. Haass, C. & Selkoe, D. J. Soluble protein oligomers in neurodegeneration: lessons from the Alzheimer's amyloid beta-peptide. *Nat Rev Mol Cell Biol* **8,** 101–12 (2007).

50. Hardy, J. & Selkoe, D. J. The amyloid hypothesis of Alzheimer's disease: progress and problems on the road to therapeutics. *Science* **297,** 353–6 (2002).

51. Karran, E., Mercken, M. & De Strooper, B. The amyloid cascade hypothesis for Alzheimer's disease: an appraisal for the development of therapeutics. *Nat Rev Drug Discov* **10,** 698–712 (2011).

52. Reitz, C. Alzheimer's disease and the amyloid cascade hypothesis: a critical review. *Int J Alzheimers Dis* **2012,** 11 (2012).

53. Götz, J., Chen, F., van Dorpe, J. & Nitsch, R. M. Formation of neurofibrillary tangles in P301l tau transgenic mice induced by Abeta 42 fibrils. *Science* **293,** 1491–5 (2001).

54. Tomita, T. *et al.* The presenilin 2 mutation (N141I) linked to familial Alzheimer disease (Volga German families) increases the secretion of amyloid beta protein ending at the 42nd (or 43rd) residue. *Proc Natl Acad Sci U S A* **94,** 2025–30 (1997).

55. Citron, M. *et al.* Mutant presenilins of Alzheimer's disease increase production of 42-residue amyloid beta-protein in both transfected cells and transgenic mice. *Nat Med* **3,** 67–72 (1997).

56. Jiang, Q. *et al.* ApoE promotes the proteolytic degradation of Abeta. *Neuron* **58,** 681–93 (2008).

57. Lambert, J.-C. *et al.* Genome-wide association study identifies variants at CLU and CR1 associated with Alzheimer's disease. *Nat Genet* **41,** 1094–9 (2009).

58. Hsiao, K. *et al.* Correlative memory deficits, Abeta elevation, and amyloid plaques in transgenic mice. *Science* **274,** 99–102 (1996).

59. Chishti, M. A. *et al.* Early-onset Amyloid Deposition and Cognitive Deficits in Transgenic Mice Expressing a Double Mutant Form of Amyloid Precursor Protein 695 *. **276,** 21562–21570 (2001).

60. Davies, L. *et al.* A4 amyloid protein deposition and the diagnosis of Alzheimer's disease: prevalence in aged brains determined by immunocytochemistry compared with conventional neuropathologic techniques. *Neurology* **38,** 1688–93 (1988).

61. Schmitt, F. A. *et al.* "Preclinical" AD revisited: neuropathology of cognitively normal older adults. *Neurology* **55,** 370–6 (2000).

62. Kim, J. *et al.* Normal cognition in transgenic BRI2-Aβ mice. *Mol Neurodegener* **8,** 15 (2013).

63. Morgan, K. The three new pathways leading to Alzheimer's disease. *Neuropathol Appl Neurobiol* **37,** 353–7 (2011).

64. Boada, M. *et al.* ATP5H/KCTD2 locus is associated with Alzheimer's disease risk. *Mol Psychiatry* 1–6 (2013). doi:10.1038/mp.2013.86

65. Guerreiro, R. *et al.* TREM2 variants in Alzheimer's disease. *N Engl J Med* **368,** 117–27 (2013).

66. Jonsson, T. *et al.* Variant of TREM2 Associated with the Risk of Alzheimer's Disease. *N Engl J Med* 121114152813005 (2012). doi:10.1056/NEJMoa1211103

67. Neumann, H. & Daly, M. J. Variant TREM2 as Risk Factor for Alzheimer's Disease. *N Engl J Med* 121114152740008 (2012). doi:10.1056/NEJMe1213157

68. Lee, H. *et al.* Amyloid- $_{NL}$ in Alzheimer Disease : The Null versus the Alternate Hypotheses. *J Pharmacol Exp Ther* **321,** 823–829 (2007).

69. Golde, T. E., Schneider, L. S. & Koo, E. H. Anti-aβ therapeutics in Alzheimer's disease: the need for a paradigm shift. *Neuron* **69,** 203–13 (2011).

70. Rutkowski, D. T. & Hegde, R. S. Regulation of basal cellular physiology by the homeostatic unfolded protein response. *J Cell Biol* **189,** 783–94 (2010).

71. Ferreiro, E., Oliveira, C. R. & Pereira, C. Involvement of endoplasmic reticulum Ca2+ release through ryanodine and inositol 1,4,5-triphosphate receptors in the neurotoxic effects induced by the amyloid-beta peptide. *J Neurosci Res* **76,** 872–80 (2004).

72. Walter, P. & Ron, D. The unfolded protein response: from stress pathway to homeostatic regulation. *Science* **334,** 1081–6 (2011).

73. Costa, R. O. *et al.* Amyloid β-induced ER stress is enhanced under mitochondrial dysfunction conditions. *Neurobiol Aging* **33,** 824.e5–16 (2012).

74. Resende, R., Ferreiro, E., Pereira, C. & Resende de Oliveira, C. Neurotoxic effect of oligomeric and fibrillar species of amyloid-beta peptide 1-42: involvement of endoplasmic reticulum calcium release in oligomer-induced cell death. *Neuroscience* **155,** 725–37 (2008).

75. Chafekar, S. M., Hoozemans, J. J. M., Zwart, R., Baas, F. & Scheper, W. Abeta 1-42 induces mild endoplasmic reticulum stress in an aggregation state-dependent manner. *Antioxid Redox Signal* **9,** 2245–54 (2007).

76. Ferreiro, E., Resende, R., Costa, R., Oliveira, C. R. & Pereira, C. M. F. An endoplasmic-reticulum-specific apoptotic pathway is involved in prion and amyloid-beta peptides neurotoxicity. *Neurobiol Dis* **23,** 669–78 (2006).

77. Unterberger, U. *et al.* Endoplasmic reticulum stress features are prominent in Alzheimer disease but not in prion diseases in vivo. *J Neuropathol Exp Neurol* **65,** 348–57 (2006).

78. Hoozemans, J. J. M., van Haastert, E. S., Nijholt, D. A. T., Rozemuller, A. J. M. & Scheper, W. Activation of the unfolded protein response is an early event in Alzheimer's and Parkinson's disease. *Neurodegener Dis* **10,** 212–5 (2012).

79. Hoozemans, J. J. M. *et al.* The unfolded protein response is activated in Alzheimer's disease. *Acta Neuropathol* **110,** 165–72 (2005).

80. Hoozemans, J. J. M. *et al.* The unfolded protein response is activated in pretangle neurons in Alzheimer's disease hippocampus. *Am J Pathol* **174,** 1241–51 (2009).

81. Nijholt, D. a T., van Haastert, E. S., Rozemuller, A. J. M., Scheper, W. & Hoozemans, J. J. M. The unfolded protein response is associated with early tau pathology in the hippocampus of tauopathies. *J Pathol* **226,** 693–702 (2012).

82. Song, L., De Sarno, P. & Jope, R. S. Central role of glycogen synthase kinase-3beta in endoplasmic reticulum stress-induced caspase-3 activation. *J Biol Chem* **277,** 44701–8 (2002).

83. Nijholt, D. A. T. *et al.* Unfolded protein response activates glycogen synthase kinase-3 via selective lysosomal degradation. *Neurobiol Aging* **34,** 1759–71 (2013).

84. Van der Harg, J. M. *et al.* The unfolded protein response mediates reversible tau phosphorylation induced by metabolic stress. *Cell Death Dis* **5,** e1393 (2014).

85. Duran-Aniotz, C., Martínez, G. & Hetz, C. Memory loss in Alzheimer's disease: are the alterations in the UPR network involved in the cognitive impairment? *Front Aging Neurosci* **6,** 8 (2014).

86. Moreno, J. A. *et al.* Oral treatment targeting the unfolded protein response prevents neurodegeneration and clinical disease in prion-infected mice. *Sci Transl Med* **5,** 206ra138 (2013).

87. Moreno, J. a *et al.* Sustained translational repression by eIF2α-P mediates prion neurodegeneration. *Nature* **485,** 507–11 (2012).

88. McGeer, P. L., Itagaki, S., Tago, H. & McGeer, E. G. Reactive microglia in patients with senile dementia of the Alzheimer type are positive for the histocompatibility glycoprotein HLA-DR. *Neurosci Lett* **79,** 195–200 (1987).

89. Eikelenboom, P. *et al.* The significance of neuroinflammation in understanding Alzheimer's disease. *J Neural Transm* **113,** 1685–95 (2006).

90. Akiyama, H. *et al.* Inflammation and Alzheimer's disease. *Neurobiol Aging* **21,** 383–421

91. Hoozemans, J. J. M., Veerhuis, R., Rozemuller, J. M. & Eikelenboom, P. Neuroinflammation and regeneration in the early stages of Alzheimer's disease pathology. *Int J Dev Neurosci* **24,** 157–65 (2006).

92. Tarkowski, E., Andreasen, N., Tarkowski, A. & Blennow, K. Intrathecal inflammation precedes development of Alzheimer's disease. *J Neurol Neurosurg Psychiatry* **74,** 1200–05 (2003).

93. Okello, a *et al.* Microglial activation and amyloid deposition in mild cognitive impairment: a PET study. *Neurology* **72,** 56–62 (2009).

94. Szekely, C. A. & Zandi, P. P. Non-steroidal anti-inflammatory drugs and Alzheimer's disease: the epidemiological evidence. *CNS Neurol Disord Drug Targets* **9,** 132–9 (2010).

95. Sheng, J. G. *et al.* Overexpression of the Neuritotrophic Cytokine S100 NL Precedes the Appearance of Neuritic NL -Amyloid Plaques in APPV717F Mice. 295–301 (2000).

96. Vom Berg, J. *et al.* Inhibition of IL-12/IL-23 signaling reduces Alzheimer's disease-like pathology and cognitive decline. *Nat Med* **18,** 1812–9 (2012).

97. Tan, M.-S. *et al.* IL12/23 p40 inhibition ameliorates Alzheimer's disease-associated neuropathology and spatial memory in SAMP8 mice. *J Alzheimers Dis* **38,** 633–46 (2014).

98. Dickson, D. W. Apoptotic mechanisms in Alzheimer neurofibrillary degeneration : cause or effect ? *J Clin Invest* **114,** 23–27 (2004).

99. McKhann, G. M. *et al.* The diagnosis of dementia due to Alzheimer's disease: recommendations from the National Institute on Aging-Alzheimer's Association workgroups on diagnostic guidelines for Alzheimer's disease. *Alzheimers Dement* **7,** 263–9 (2011).

100. Albert, M. S. *et al.* The diagnosis of mild cognitive impairment due to Alzheimer's disease: recommendations from the National Institute on Aging-Alzheimer's Association workgroups on diagnostic guidelines for Alzheimer's disease. *Alzheimers Dement* **7,** 270–9 (2011).

101. Jack, C. R. *et al.* Hypothetical model of dynamic biomarkers of the Alzheimer's pathological cascade. *Lancet, The* **9,** 1–20 (2010).

102. Morris, C. Early-Stage and Preclinical Alzheimer Disease. *Alzheimer Dis Assoc Disord* **19,** 163–65 (2005).

103. Das, P., Murphy, M. P., Younkin, L. H., Younkin, S. G. & Golde, T. E. Reduced effectiveness of Abeta1-42 immunization in APP transgenic mice with significant amyloid deposition. *Neurobiol Aging* **22,** 721–7 (2001).

104. Lansbury, P. T. Back to the future: the "old-fashioned" way to new medications for neurodegeneration. *Nat Med* **10 Suppl,** S51–7 (2004).

105. THE RONALD AND NANCY REAGEAN RESEARCH INSTITUTE OF THE ALZHEIMER'S ASSOCIATION AND THE NATIONAL INSTITUTE ON AGING WORKING GROUP, 123. Consensus Report of the Working Group on : " Molecular and Biochemical Markers of Alzheimer ' s Disease ." *Neurobiol Aging* **19,** 109–116 (1998).

106. Reiber, H. & Peter, J. B. Cerebrospinal fluid analysis: disease-related data patterns and evaluation programs. *J Neurol Sci* **184,** 101–22 (2001).

107. Tapiola, T. *et al.* Cerebrospinal fluid {beta}-amyloid 42 and tau proteins as biomarkers of Alzheimer-type pathologic changes in the brain. *Arch Neurol* **66,** 382–9 (2009).

108. Buerger, K. *et al.* CSF phosphorylated tau protein correlates with neocortical neurofibrillary pathology in Alzheimer's disease. *Brain* **129,** 3035–41 (2006).

109. Strozyk, D., Blennow, K., White, L. R. & Launer, L. J. CSF Abeta 42 levels correlate with amyloid-neuropathology in a population-based autopsy study. *Neurology* **60,** 652–6 (2003).

110. Blennow, K., Hampel, H., Weiner, M. & Zetterberg, H. Cerebrospinal fluid and plasma biomarkers in Alzheimer disease. *Nat Rev Neurol* **6,** 131–44 (2010).

111. Blennow, K. & Hampel, H. CSF markers for incipient Alzheimer's disease. *Lancet Neurol* **2,** 605–613 (2003).

112. Mattsson, N., Zetterberg, H. & Blennow, K. Lessons from Multicenter Studies on CSF Biomarkers for Alzheimer's Disease. *Int J Alzheimers Dis* **2010,** 1–5 (2010).

113. Mulder, C. *et al.* Amyloid-beta(1-42), total tau, and phosphorylated tau as cerebrospinal fluid biomarkers for the diagnosis of Alzheimer disease. *Clin Chem* **56,** 248–53 (2010).

114. Mattsson, N. *et al.* Age and diagnostic performance of Alzheimer disease CSF biomarkers. *Neurology* **78,** 468–76 (2012).

115. Bouwman, F. H. *et al.* CSF biomarker levels in early and late onset Alzheimer's disease. *Neurobiol Aging* **30,** 1895–901 (2009).

116. Mapstone, M. *et al.* Plasma phospholipids identify antecedent memory impairment in older adults. *Nat Med* 4–9 (2014). doi:10.1038/nm.3466

117. Verwey, N. A. *et al.* A worldwide multicentre comparison of assays for cerebrospinal fluid biomarkers in Alzheimer's disease. *Ann Clin Biochem* **46,** 235–40 (2009).

118. Sperling, R. a *et al.* Toward defining the preclinical stages of Alzheimer's disease: recommendations from the National Institute on Aging-Alzheimer's Association workgroups on diagnostic guidelines for Alzheimer's disease. *Alzheimers Dement* **7,** 280–92 (2011).

119. Del Campo, M. *et al.* Recommendations to standardize preanalytical confounding factors in Alzheimer's and Parkinson's disease cerebrospinal fluid biomarkers: an update. *Biomark Med* **6,** 419–30 (2012).

120. Teunissen, C. E., Tumani, H., Engelborghs, S. & Mollenhauer, B. Biobanking of CSF: international standardization to optimize biomarker development. *Clin Biochem* **47,** 288–92 (2014).

121. Wilkins, M. *et al.* From proteins to proteomes: Large scale protein identification by two-dimensional elec- trophoresis and amino acid analysis. *Nat Biotechnol* **14,** 61–5 (1996).

122. Craft, G. E., Chen, A. & Nairn, A. C. Recent advances in quantitative neuroproteomics. *Methods* **61,** 186–218 (2013).

123. Guldbrandsen, A. *et al.* In-depth characterization of the cerebrospinal fluid proteome displayed through the CSF Proteome Resource (CSF-PR). *Mol Cell proteomics* (2014).

124. Schutzer, S. E. *et al.* Establishing the proteome of normal human cerebrospinal fluid. *PLoS One* **5,** e10980 (2010).

125. Ghidoni, R., Paterlini, A. & Benussi, L. Translational proteomics in Alzheimer's disease and related disorders. *Clin Biochem* **46,** 480–6 (2013).

126. Spitzer, P. *et al.* cNEUPRO: Novel Biomarkers for Neurodegenerative Diseases. *Int J Alzheimers Dis* **2010,** (2010).

127. Berzin, T. M. *et al.* Agrin and microvascular damage in Alzheimer's disease. *Neurobiol Aging* **21,** 349–355 (2000).

128. Jahn, H. *et al.* Peptide Fingerprinting of Alzheimer's Disease in Cerebrospinal Fluid: Identification and Prospective Evaluation of New Synaptic Biomarkers. *PLoS One* **6,** e26540 (2011).

Chapter 2

Role of BRI2 in dementia

J Alzheimers Dis. 2014;40(3):481-94.

Marta Del Campo
Charlotte E. Teunissen

Abstract

Alzheimer's disease (AD), the most common form of dementia, shares clinical and pathological similarities with Familial British and Danish (FBD and FDD). Whereas the aetiology of sporadic AD remains unclear, Familial AD is linked to mutations in the amyloid β precursor protein (AβPP), presinilin 1 (PS1) and presinilin 2 (PS2). Similarly, FBD and FDD originate from mutations in the BRI2 gene (or *ITM2b*), causing amyloid angiopathy and neurofibrillary tangles analogous to those observed in AD. Recent studies on the role of BRI2 in FBD and FDD have revealed that the three diseases may share pathophysiological pathways leading to dementia. Interestingly, BRI2 is a potential regulator of AβPP processing, and it can inhibit the production and fibrillation of Aβ. This suggests a role of BRI2 in the amyloid cascade, which is the prevailing hypothesis about AD pathogenesis. To understand a possible relationship of BRI2 with AD, we reviewed the relevant studies on this protein. The data included not only the protein's structure, expression pattern, function and involvement in FBD and FDD, but also its relationship with memory deficits and the main pathological proteins involved in AD. Thus, we highlight and discuss the potential links between BRI2 and AD, leading to the formulation of a modified hypothesis about AD aetiology.

Key words: Integral membrane protein 2B (ITM2B/BRI2), Familial British dementia (FBD), Familial Danish dementias (FDD), Alzheimer's disease, Amyloid precursor protein, Amyloid-β

Introduction

BRI2 (Integral membrane protein 2B or Itm2B) is a type II transmembrane protein that is mutated in Familial British and Danish dementias (FBD and FDD, respectively) causing amyloid angiopathy and neurofibrillary tangles in the hippocampus[1–3]. These extremely rare dementias share pathological and clinical similarities with Alzheimer's disease (AD)[4,5]. Interestingly, recent studies have shown a relationship between BRI2 and the main proteins involved in AD pathology, suggesting that BRI2 may play an important role in the development of neurodegenerative dementias[6–9]. To assess the possible involvement of BRI2 in AD pathology, we reviewed the research on this topic. After a general introduction to the structure, expression and function of BRI2 and the main molecular, pathological and clinical features of AD, FBD and FDD, we discuss the studies performed on FBD and FDD mouse models. Next, we describe the function of BRI2 in the regulation of critical proteins involved in AD pathogenesis, e.g. amyloid precursor protein (AβPP) and amyloid β (Aβ). We finish with a hypothesis about AD aetiology and pose new research questions for understanding the possible role of BRI2 in AD.

BRI2

In 1998, the BRI2 coding gene was first subcloned and located on human chromosome 13q14.3[10]. BRI2 belongs to a family of transmembrane proteins containing two additional members, BRI1 (Itm2A) and BRI3 (Itm2C)[4]. The three BRI proteins share an amino acid sequence identity of 27%, and their expression patterns differ. While BRI2 is ubiquitously expressed[10], BRI1 is mainly expressed in osteogenic and chondrogenic tissues[11], and BRI3 is exclusively expressed in the brain[12]. However, this family of proteins contains an evolutionary conserved BRICHOS domain that is present in a superfamily of proteins with 309 members grouped into 12 families with diverse functions[13–15]. Experimental data have indicated that the BRICHOS domain can act as a chaperone by binding to regions of precursor proteins that are prone to form β-sheet structures, thereby preventing the fibrillation of amyloid proteins[9,14]. Indeed, it was recently shown that the BRI2-BRICHOS domain delayed fibrillation of the Aβ peptide[16].

BRI2 is a transmembrane protein with 266 amino acids (aa) (Fig. 1). It contains a cytosolic N-terminal domain of 54-aa followed by an additional 21-aa in the plasmatic membrane. The BRI2 luminal domain (BRI276-266) contains the BRICHOS domain (aa 137-231), an N-glycosylation site at asparagine residue 170 (Asn170) and several cysteines[5,15,17]. Two of the cysteines are present at the C-terminus (C248 and C265), and these are able to

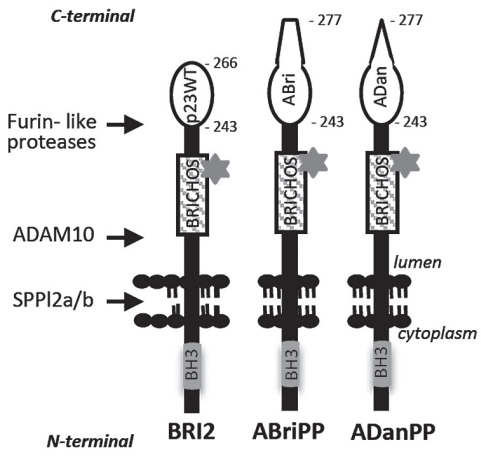

Fig. 1. Schematic representation of the BRI2 protein and its mutated forms, ABriPP and AdanPP. BRI2 and its mutated forms AbriPP and AdanPP are transmembrane proteins with a BH3 domain (grey rectangle) within the cytosolic part. The ectodomain of these proteins contains a BRICHOS domain (striped rectangle) and an N-glycosylation site at asparagine 170 (star). BRI2, AbriPP and AdanPP can be processed by Furin-like proteases, ADAM10 and SPPL2$_{a/b}$. The mutated forms are 11 aa longer than BRI2 and thus, while BRI2 processing by furin-like proteases leads to the secretion of a 23-aa peptide (p23WT), the processing of AbriPP and AdanPP leads to the secretion of peptides of 34-aa (Abri and Adan). The first 22-aa of Abri and Adan are identical to those of p23WT. However, the 12 additional aa in the C-terminal segments of Abri and Adan are completely different from each other.

form intramolecular disulfide bonds. Two other cysteines are located within the BRICHOS domain (C164 and C223), generating a loop-like conformation[3,15,18]. Studies on transfected human cells and mice brains revealed that an additional cysteine residue within the luminal domain (C89) is involved in homodimerization of BRI2 through non-covalent interactions and disulfide bonds. Dimers of BRI2 are formed within the endoplasmatic reticulum (ER) and appear at the cell surface together with monomers[19]. Interestingly, BRI2 undergoes consecutive maturation and processing cleavages in the cis or medial-Golgi, which leads to the formation of various secreted peptides, as will be discussed in more detail below[20]. Thus, BRI2 undergoes post-translational modifications leading to various forms of BRI2 that may have different cellular locations and physiological functions.

Given the aa sequence, the theoretical molecular weight of BRI2 is 30 kDa. Previous western blot studies have shown a 38kDa BRI2 band in samples from human brain tissue[21–24]. In mouse brains, a BRI2 band migrating at 44 kDa has been observed[19]. Moreover, several cell transfection studies have reported a BRI2 band migrating between 40-50 kDa in SDS-PAGE gels[19,25–27]. Dimerization should not account for the higher than expected molecular weights in these studies, since all experiments were carried out under reducing conditions. Post-translational modifications of BRI2 have been analyzed, but the presence of an N-glycosylation inhibitor or mutation of the BRI2 N-glycosylation site at Asn170 reduced BRI2 molecular weight only by 2kDa. This suggests the involvement of additional post-translational modifications that lead to forms of BRI2 with higher molecular masses[17]. Further experiments addressing the molecular isoforms and presentations of BRI2 are needed in order to better understand the physiological functions of BRI2.

BRI2 processing

During BRI2 maturation within the cis-medial-Golgi, proteolytic cleavage results in the release of a 23-aa C-terminal peptide (p23WT). p23WT may act as a signal peptide, since deletion of the C-terminal peptide prevented BRI2 from moving forward through the ER-Golgi network[28]. The remaining membrane-bound N-terminal part of BRI2 is known as the mature form of BRI2 (mBRI2)[27].

Several proteases, including furin, have been suggested to be involved in C-terminal processing of BRI2. Furin was able to cleave a transfected recombinant BRI2 between Arg243 and Glu244[27]. However, the BRI2 cleavage site ($_{238}$KGIQKR$_{243}$) is an atypical furin recognition sequence[29], In addition, furin activity is confined to the trans-Golgi[30], whereas BRI2 shedding was observed in the cis-medial-Golgi. Moreover, BRI2 processing in the cis-medial Golgi was not abrogated by use of a furin inhibitor[20]. Therefore, it remains unclear whether furin is the main physiological BRI2-cleavage enzyme. Other candidates include enzymes from the same family, i.e. the ubtilisin/kexin-like proprotein convertase (PC) family, such as the type 5 (PC6A) and the type 7 (LPC). These enzymes have also been shown to process BRI2, albeit more inefficiently[31].

mBRI2 can be further processed by the α-secretase ADAM10 leading to the secretion of a 25kDa peptide containing the BRICHOS domain[26]. The specific cleavage site of ADAM10 remains unknown, but it occurs between aa 76 and the BRI2 glycosylation site (Asn170)[20]. Besides ADAM10 cleavage, the remaining membrane-bound N-terminal fragment (NTF) of BRI2 undergoes an additional proteolysis by SPPL2a/b, leading to the release of a small, secreted C-peptide and the liberation of a 10kDa intracellular domain (ICD) in the cytosol. SPPL2a/b cleavage has several substrate requirements including shedding performed by ADAM10 and amino-acid sequence determinants of BRI2 in the luminal juxtamembrane, transmembrane and cytosolic domains. Although the absence of each of these requirements does not halt BRI2 processing, the combination of these four requirements enhances efficient intramembrane proteolysis of BRI2[25]. Both ADAM10 and SPPL2$_{a/b}$ cleavages occur independently of furin-like protease activity, and they may occur prior to arrival in the Golgi[26]. The ICD fragment, which contains a characteristic pro-apoptotic BH3 domain[32], may have important intracellular signaling functions as it is similar to the ICD domain in other proteins, e.g. Notch, that have such a role[33]. Therefore, further research on BRI2 ICD may lead to new insights into the physiological function of BRI2.

Physiological BRI2 expression in the brain

Two mRNA transcripts of BRI2 have been identified, but only one single-DNA fragment was detected, so the two BRI2 mRNA transcripts (2 and 1.6 kb) probably represent different polyadenylation isoforms[1]. Both mRNA transcripts have a ubiquitous expression, being highly expressed in kidney, pancreas, placenta and brain. Within the brain, the heaviest BRI2 mRNA transcript (2 Kb) has a similar high expression in the cerebellum, subthalamic nucleus, substantia nigra and hippocampus[1]. Immunohistochemistry of post-mortem human brain tissue showed that BRI2 was expressed as fine granules in the neuronal cytoplasm. BRI2 was found in dystrophic neurites of senile plaques, lewy neurites, ballooned neurons and in neurons following ischemia and/or hypoxia cases in different neuropathological conditions (e.g. AD, dementia with Lewy bodies, Parkinson's disease, alcoholism and corticobasal degeneration). This association suggests that this protein is related to neurodegeneration[22].

BRI2 function

Although the physiological function of BRI2 remains unknown, several functions have been proposed. It has been suggested that BRI2 is involved in apoptosis and mitochondrial dysfunction via its BH3 domain. For example, in a pro-apoptotic cell line, a splice variant of BRI2 (BRI2$_{S;}$ aa 1-210) was up-regulated, and experimental overexpression of BRI2$_S$ induced apoptosis via its BH3 domain independently from p53 tumor suppressor protein expression[32,34,35]. A prostate cancer study revealed that BRI2 is a potential candidate tumor suppressor gene[36]. Recently, it has been reported that BRI2 can form complexes with ADAM7 on membrane lipid rafts at the sperm surface, and that these complexes are increased during sperm capacitation, suggesting a role of BRI2 in male reproduction[37].
With respect to brain cells, BRI2 was able to promote neurite outgrowth in BRI2-overexpressing human neuronal cells[20]. BRI2 staining was observed in abnormal neurites in different neuropathological brain tissues, suggesting that BRI2 is transported through axons and that it has a role at the nerve terminal and may also be involved in the plasticity of neuronal processes[22]. The ability of BRI2 to constitute homodimers via disulfide bonds also suggests that BRI2 could act as a receptor, thus being involved in signal transduction and/or cell adhesion[19]. Interestingly, BRI2 null mice showed a link between BRI2 and AD pathology[38], which has not been extensively investigated yet.

Alzheimer's disease

AD is the most common type of dementia and is characterized by loss of cognitive functions[39]. In 1928, Ramon y Cajal[40] predicted that dementia could result from the weakness of synapses, and several studies have indeed indicated that synaptic dysfunction is likely the underlying event leading to memory loss, even at early stages of AD[40,41].

The main pathological hallmarks of AD are the presence of intraneuronal neurofibrillary tangles (NFTs), consisting of the phosphorylated protein tau (p-Tau)[42], and the accumulation of amyloid β ($Aβ_{42}$), which leads to the development of extracellular amyloid plaques[43,44]. Aβ can self-associate, leading to the formation of various assembling forms, ranging from soluble aggregates (oligomers) to insoluble fibrils. Over the past decade, several studies have suggested that oligomers, rather than fibrillar Aβ forms, mediate the neuronal toxicity observed in AD tissue[41,45–47].

$Aβ_{42}$ is a 42-aa peptide produced after the sequential cleavage of amyloid precursor protein (AβPP) by β- and γ-secretases[48]. AβPP is first cleaved by β-secretase 1 (BACE1), leading to the release of the sAβPPβ fragment[49,50]. The remaining membrane-bound C-terminal fragment of 99-aa (C99) is further cleaved by γ-secretase, leading to the release of Aβ peptide and the APP Intracellular Domain (AICD)[51]. The γ-secretase is a multimolecular complex including, among others, presenilins (PS1 and PS2)[52]. AβPP can also be proteolysed via a non-amyloidogenic proteolytic pathway in which it is cleaved by α-secretase, leading to the release of the sAβPPα fragment and the formation of a membrane-bound C-terminal fragment of 83-aa (C83). The cleavage site of α-secretase resides within the Aβ domain, thus abrogating Aβ formation[48,53]. C83 is subsequently cleaved by γ-secretase into the p3 and AICD peptides. The major α-secretase identified in AβPP processing is ADAM10[54–56], which is also involved in BRI2 processing, as mentioned above[26]. The underlying mechanism that determines whether AβPP is cleaved by α- or β-secretase has not been revealed yet[53].

Although the etiology of AD remains unknown, the prevailing theory about AD pathogenesis is the amyloid cascade hypothesis, which suggests that the accumulation of specific Aβ oligomers is the key event ultimately leading to neurodegeneration[57–60]. An important goal in current AD research is to discover which specific Aβ oligomers trigger the amyloid cascade response[46,47]. The amyloid cascade hypothesis is supported by the increased Aβ load found in familial forms, which are caused by mutations in AβPP or presenilins genes[61–63]. Moreover, transgenic AD mouse models that express mutant forms of AβPP found in familial AD mimic some of the neuropathological hallmarks of AD[64,65]. Additionally, genetic risk factors related to sporadic AD (which accounts for 90% of AD cases) have been identified. These include the Apolipoprotein E ε4 allele variant

(*APOEε4*), *APOJ* or *CR1*, which are genes encoding proteins that are likely involved in Aβ clearance[66–68]. However, deposition of Aβ in amyloid plaques is also observed in normal aging, and its correlation with neuronal loss and cognitive decline is not strong[69,70]. In this context, genome-wide association studies have identified novel loci associated with AD that are not related to Aβ metabolism, but rather to immune system response, cellular stress, or synaptic and mitochondria dysfunction[71,72]. For instance, a variant of TREM2 has been recently identified as an important risk factor for late-onset AD (frequency 0.63%; odds ratio 2.92; 95% confidence interval [CI] 2.09 to 4.09; $p = 3.42 \times 10^{-10}$). TREM2 is a protein found in microglia, which might be involved in the clearance of apoptotic damage in neuronal tissue as well as in the development of an anti-inflammatory response[73–75]. These data have led many scientists to suggest an alternative hypothesis: Aβ plaques are disease bystanders rather than the cause of the disease[76]. Despite the substantial progress that has been made in AD research, understanding of AD pathogenesis remains a challenging field.

FBD and FDD

FBD and FDD are caused by different autosomal dominant mutations in the BRI2 gene. These early-onset diseases share several clinical characteristics such as gradual progressive dementia and cerebellar ataxia. FBD, with an age of onset in the fourth to fifth decade of life, is clinically characterized by gradually progressive dementia, spastic tetraparesis and cerebellar ataxia, and lasts approximately ten years until death. In a study of five affected FBD patients, MRI scans revealed white matter hyperintensities[77,78]. In FDD, cataracts are the first symptom of the disease, with an onset in the second decade. Later on, patients develop hearing loss and other symptoms also common to FBD, such as cerebellar ataxia and memory loss[79]. Neuropathological studies of FBD revealed the presence of parenchymal pre-amyloid (non-fibrillar) and amyloid (fibrillar) lesions, while in FDD the parenchymal deposits were predominantly of the pre-amyloid type. Additional neuropathological characteristics in both diseases are the presence of an extensive cerebral amyloid angiopathy (CAA), the formation of NFTs, an astrocytic and activated microglia response as well as activation of the complement pathway[23,79–81]. Regarding the similarities and differences between FBD, FDD and AD, a number of interesting observations have been made. Although the basic neuropathological and clinical characteristics of FBD and FDD - including amyloid angiopathy, parenchymal deposits and NFTs - are also present in AD, the extracellular $A\beta_{42}$ plaques - a classical characteristic of AD - are not[4] (Table 1). Moreover, several amyloid-associated proteins have been found in all three disorders, including apolipoproteins E and J, agrin and glypican-1[82]. This suggests that the high

complexity of amyloid plaques in AD is also a characteristic of amyloid and pre-amyloid lesions in both FBD and FDD. In up to 60% of AD cases, TDP-43 pathology is present and it has also been observed in FBD cases, although the exact frequency of TDP-43 in FBD could not be established due to the low number of cases analyzed[83,84].

In FBD, a point mutation in the stop codon lengthens the reading frame of the cDNA, resulting in the production of a longer BRI2 precursor protein (ABriPP) of 277-aa[1]. In FDD cases, an elongated mutated protein of 277-aa (ADanPP) is also generated, which is produced by a decamer duplication insertion (TTTAATTTGT) between codons 265 and 266 of the wild-type BRI2 (*wtBRI2*) cDNA[2]. Both mutations lead to a 34-aa C-terminal sequence of ABriPP and ADanPP of which the first 22-aa are identical to that of wild type BRI2. However, the 12 additional aa in the C-terminal segment within the mutated proteins are completely different from each other (Fig. 1).

Similar to wtBRI2, ABriPP and ADanPP undergo the same furin-like proteolytic processing at positions 243-244, leading to the secretion of 34-aa peptides. These are called British

Table 1. Main clinical and pathological similarities between FBD, FDD and AD

	FBD	FDD	AD
Clinical symptoms			
Progressive dementia	X	X	X
Spastic paraparesis	X		X
Apraxia			X
Cerebellar ataxia	X	X	
Pseudobulbobar palsy	X		
Language problems	X		X
Personality changes (apathy)	X	X	X
Cataracts		X	
Deafness		X	
Pathological characteristics			
Amyloid angiopathy	X	X	X
Parenchymal amyloid plaques	X		X
Parenchymal pre-amyloid plaques	X	X	X
Amyloid co-deposition (ABri, ADan, Aβ)*		X	
Neurofibrillary tangles	X	X	X
Periventricular white matter changes	X	X	X
Activation of complement proteins	X	X	X
Amyloid associated proteins	X	X	X

FBD: Familial British dementia, FDD: Familial Danish dementia, AD: Alzheimer's disease, ABri: Amyloid British peptide, ADan: Amyloid Danish peptide, Aβ: Amyloid β peptide, *: Refers to the association of ABri or ADan with Aβ in the corresponding disease.

amyloid (ABri) in FBD and Danish amyloid (ADan) in FDD[27,31]. These peptides have been isolated from amyloid deposits in FBD and FDD cases[1,2]. Interestingly, Aβ was also found in vascular and parenchymal ADan depositions in FDD cases[79]. Similarly to Aβ, soluble monomeric circulating forms of ABri and ADan have been found in plasma of FBD and FDD patients, respectively[85–87]. Unlike AD, systemic ABri deposits in different organs have been described in FBD[86,88].

It has been shown that both ABri and ADan have a high tendency to aggregate and oligomerize *in vitro* and *in vivo*[4]. Those peptides form a short loop by means of a disulfide bond between the cysteines C248 and C265; consequently, they can exist in both oxidized and reduced forms. For ABri it has been shown that only the oxidized form aggregates in very toxic soluble oligomers[89]. In contrast, both oxidized and reduced forms of ADan are able to form oligomers, but the reduced form is more neurotoxic[90]. This indicates that similarly to AD, soluble oligomers, and not highly fibrillized amyloid peptides, are involved in the neurodegeneration process in FBD and FDD. ABri and ADan can undergo cyclization of the N-terminal glutaminyl residue[1,87], a characteristic also observed in 15-20% of the total Aβ fragments found in the Aβ deposits of AD cases[91]. Cyclization of the various amyloid peptides may confer protection against proteolysis, thus promoting its aggregation[18,92]. Due to the conformational homology between Aβ, ABri and ADan, immunization with a polymerized peptide that corresponds to the C-terminus of ABri in an AD mouse model induced a humoral immune response to toxic Aβ and to paired helical filaments[93]. Thus, despite the lack of primary sequence homology between ABri, ADan and Aβ, all three peptides can trigger similar molecular responses. This suggests that common end-stage molecular pathways triggered by some conformational structure rather than a specific sequence may be involved in FBD, FDD and AD.

Modeling FBD and FDD

Mouse models are important tools to understand the pathogenesis and therapy of human diseases. The initial studies with FBD mouse models were disappointing because overexpression of ABriPP (MoPrP- mtBRI2 and Thy-1.2-mtBRI2), did not show extracellular ABri aggregation[94]. However, promising results were obtained with transgenic FDD mice (tg-FDD), although overexpression of ADanPP did not completely resemble the characteristics of the disease: no neuronal loss (with the exception of cerebellar Purkinje cells) and, similar to transgenic AD mouse models, tangle formation was observed only when animals were crossed with a mouse model of human tau pathology (tg-FDD-tau)[95–97]. Interestingly, the amyloid deposits of tg-FDD mice were surrounded by dystrophic neurites containing the mature wild-type BRI2, which was attributed to

a disruption in axonal transport[96]. Cognitive deficits in this mouse model could not be analyzed due to the abnormal movements and arched backs of the animals. In another study, overexpressing ADanPP (ADanPP-tg) recapitulated the amyloid lesions, but not the characteristic ADan/Aβ mixed amyloid angiopathy, when the ADanPP-tg mice were crossed with an Aβ-depositing mouse model (ADanPP7/APPPS1)[98]. Absence of cognitive or memory defects was observed in animals at 6 months of age, despite the high ADan amyloid load, suggesting that amyloidosis itself is not sufficient to cause cognitive decline. Deficits in memory and cognition were only observed in transgenic mice at 18-20 months of age.

The remarkable loss of body weight in ADanPP-tg mice together with premature death, alopecia and kyphosis was attributed to possible ADanPP expression outside the central nervous system[98]. Tau pathology was not observed in ADanPP-tg mice unless the animals were crossed with a mouse model of human tau pathology. Interestingly, in both tg-FDD-tau and ADanPP-tg/tau mouse models, expression of ADanPP enhanced tau phosphorylation, suggesting that amyloidosis or mBRI2 overexpression may facilitate tau pathology, as discussed below[96,98]. Thus, both tg-FDD and ADanPP-tg mouse models are useful tools to study the effects of amyloidosis, although animals overexpressing wild-type BRI2 might be needed for proper comparison. Additionally, these transgenic mice can be useful to unravel the possible common molecular pathways leading to neurodegeneration in FBD, FDD and AD[95,98].

The current transgenic models are based on the hypothesis that the cognitive changes in human dementias are directly related to amyloid plaque and neurofibrillary tangle formation. However, despite the presence of severe amyloidosis, no cognitive deficits are observed in these models, raising the question whether these transgenic mice are suitable to study the mechanisms leading to cognitive decline and dementia. However, it has been suggested that loss of the physiological function of a protein (e.g. BRI2) as a result of a mutation can also account for the pathogenesis in human dementias[99,100]. In this situation, mouse models overexpressing the mutated protein (e.g. ABriPP or ADanPP) cannot precisely reproduce the disease features due to the constitutively normal – or at least not reduced - expression levels of the endogenous wild-type proteins (e.g. BRI2). To solve this problem, FBD_{KI} and FDD_{KI} mouse models have been developed in which the ABri and ADan mutation are inserted in the endogenous mouse BRI2 allele. FBD_{KI}, FDD_{KI} and $BRI2^{+/-}$ mice did not show the FBD and FDD neuropathological features such as cerebral amyloidosis and tauopathy[100,101]. However, the levels of mBRI2 were drastically reduced in the total brain and synaptic membranes, a characteristic also observed in one FBD and two FDD human cases. Moreover, the decreased mBRI2 levels correlated with hippocampal memory deficits and impaired synaptic plasticity, which supports the possible synaptic function of BRI2[22,101,102]. These data suggest that loss of BRI2 function may

play an important role not only in FBD and FDD pathogenesis, but also in the development of cognitive impairment and synaptic dysfunction, and thus, in dementia[101,102]. A recent study of cerebrospinal fluid from patients with Multiple Sclerosis revealed decreased levels of p23WT, which was associated with cerebellar dysfunction and cognitive decline. Moreover a decreased expression of BRI2 mRNA was also found in the cerebellum of those patients, again suggesting a close relationship between BRI2 function and cognitive impairment[103].

Role of BRI2 in AD

I) How can BRI2 regulate AβPP processing?

Although the shedding of AβPP plays an essential role in AD pathogenesis, the complete molecular mechanism that regulates AβPP processing remains unknown. Transgenic cell culture experiments showed that BRI2 binds AβPP, thereby downregulating the production of Aβ[6,7]. Downregulating endogenous BRI2 expression using shRNA or null BRI2 mice (BRI2$^{-/-}$) showed significant increased levels of the endogenous sAβPPα, sAβPPβ and Aβ, indicating that BRI2 is a physiological inhibitor of AβPP processing, probably by masking the α, β and γ-secretase cleavage sites[38,104]. AD mouse models crossed with BRI2$^{+/-}$ mice (APP-PS1/ BRI2$^{+/-}$) showed increased $A\beta_{40}$ and $A\beta_{42}$ levels compared to those crossed with BRI2$^{+/+}$ (APP-PS1/ BRI2$^{+/+}$)[38]. In addition, both viral delivery of wtBRI2 and crossing an AD mouse model with wtBRI2 mice reduced AD pathology[8,38,105]. Biochemical analysis of brain homogenates revealed that the levels of $A\beta_{38}$, $A\beta_{40}$ and $A\beta_{42}$ were significantly decreased in these models[105]. Together, these data suggest that wtBRI2 is able to regulate AβPP processing *in vivo*, attenuating the development of AD pathology. Therefore, altered BRI2 function may also have an effect on AD pathology.

Maturation of both BRI2 and AβPP are needed to form the BRI2-AβPP complexes, which are observed in the plasma membrane and endocytic compartments[28]. In line with this observation, brains of FDD_{KI} mice, which contain reduced levels of mature BRI2[102], also have a 75% reduction in the levels of mBRI2/mAβPP complexes together with increased levels of sAβPPα, sAβPPβ and AICD in the total brains and in synaptic membranes. Moreover, blocking β but not γ-secretase activity or halving AβPP expression prevented synaptic and memory dysfunctions in FBD_{KI} and FDD_{KI} mice[104,106–108]. These data confirm that BRI2 is a regulator of AβPP *in vivo* and suggest that memory deficits in FBD and FDD are caused by toxic AβPP products. Increased levels of $A\beta_{40}$ and $A\beta_{42}$, sAβPPα and sAβPPβ were also found in human brain tissue of one FDD case[24]. Although these analyses should be extended to include larger numbers of FBD and FDD cases, the results strongly support

the hypothesis that cognitive impairment and synaptic dysfunction in FDD and FBD are caused by loss of BRI2 function and the subsequent release of toxic AβPP metabolites, rather than by amyloidosis. Interestingly, this hypothesis has also been recently suggested to explain the cognitive decline observed in AD[106,109,110]. For example, no memory or cognitive impairment was found in mouse models in which an amyloid pathology was developed through the overexpression of $A\beta_{40}$ or $A\beta_{42}$ using BRI2-Aβ fusion protein transgenes, and thus in the absence of AβPP overexpression[110]. Strikingly, a recent study showed that BRI2 is also able to bind BACE1, promoting BACE1 degradation and reducing its mRNA levels[111]. Therefore, BRI2 could also regulate the amyloidogenic processing of AβPP by controlling the levels of BACE1, which appear to be increased in post-mortem human AD brain tissue[112–114].

These data suggest that intact BRI2 function may play an essential role not only in FBD and FDD development, but also in AD pathogenesis, since it is a potential regulator of AβPP and BACE1 and thus, of Aβ production. Therefore, FBD, FDD and AD may share common molecular pathways leading to dementia, which may be prompted by aberrant regulation of AβPP due to impaired BRI2 functionality.

II) BRI2 and Aβ aggregation

Besides a role in the regulation of AβPP processing, BRI2 may also inhibit aggregation of $A\beta_{42.}$ *In vitro* experiments showed that p23WT, the peptide released during BRI2 maturation, is able to inhibit $A\beta_{42}$ aggregation[8]. The viral delivery of BRI2 lacking the p23WT did not suppress Aβ deposition in an AD mouse model indicating that p23WT is critical for the inhibitory effect on $A\beta_{42}$ *in vivo*[8]. However, those results could also be attributed to the fact that the presence of the p23WT sequence in the wild-type protein is necessary to move into the Golgi compartment. The absence of this sequence may promote BRI2 accumulation within the ER, thereby preventing its inhibitory effect on AβPP[28].

In addition to the role of the C-terminal p23WT fragment, the BRICHOS domain can also inhibit aggregation. Direct anti-amyloid activity has been reported *in vitro* for the BRICHOS domains of both the prosurfactant protein C and BRI2[14]. In line with these results, incubation of $BRI2_{90\text{-}236}$, which contains the BRICHOS domain, together with $A\beta_{40}$ prevented Aβ aggregation and fibril formation[9]. Moreover, it has been observed that the BRI2 BRICHOS domain delays $A\beta_{40}$ and $A\beta_{42}$ fibril formation in a concentration-dependent manner by interfering with nucleation processes[16]. These data suggest that the BRI2 BRICHOS domain and p23WT may both have physiologically protective effects against the development of AD pathology by preventing Aβ aggregation and fibrillation.

III) BRI2 and NFT formation

As mentioned above, NFTs are one of the main hallmarks of AD, FBD and FDD. Interestingly, the analysis of NFTs isolated from cases of both FBD and FDD showed that these NFTs are ultrastructurally and biochemically indistinguishable from those observed in AD, since they are composed of paired helical filaments and have a similar western blot banding profile[79,80]. Although still subject to debate, the observed association between amyloid deposits and NFTs suggests that neurofibrillary pathology could be caused by amyloid induced toxicity[115]. Several studies have reported an enhanced tau pathology in mice either injected with $A\beta_{42}$ or co-expressing mutant AβPP or BRI2, suggesting that amyloidosis may promote tauopathy[98,116,117]. However, the exact mechanism by which amyloidosis may facilitate NFT formation remains to be elucidated.

In AD it has been suggested that Aβ peptides may promote pathological filament assembly through the proteolysis of tau by caspases[118]. The recently characterized double-transgenic tg-FDD-tau mice showed enhanced tau phosphorylation prior to ADan deposition, suggesting that either soluble ADan, human mutant BRI2 or abnormal BRI2 function is involved in the development of tau pathology. These mice also showed an earlier and stronger synaptic degeneration before amyloid and tau deposition, indicating that the combination of truncated ADan and tau may initiate the cognitive decline[96]. Therefore, understanding the relationship between amyloid deposition, NFT formation and synaptic loss in FBD, FDD and AD may help to reveal the mechanisms leading to cognitive decline, warranting further research on this topic.

IV) BRI2 and Insulin-degrading enzyme (IDE)

Reduced clearance of Aβ was found to be the likely culprit in sporadic AD cases[119]. Several Aβ-degrading enzymes in the brain have been described, including IDE and neprilysin among others[120]. IDE is present in the cellular cytoplasm where it degrades AICD, but it can also be secreted to degrade Aβ peptides extracellularly[121,122]. *In vitro* experiments showed that IDE is also capable of degrading ABri and ADan, and it degrades monomers more efficiently than oligomers. Moreover, ABri and ADan were more resistant to degradation than p23WT[123]. It remains to be elucidated whether other enzymes are also involved in the degradation of ABri and ADan.

Strikingly, the levels of the AβPP and AβPP C-terminal fragments were unchanged in AD mouse models crossed with mice expressing wtBRI2 in which a reduced amyloid plaque load was observed. It was therefore concluded that BRI2, rather than having an effect on AβPP processing and Aβ production, may have an effect on the enzymes degrading Aβ or other mechanism of Aβ clearance[105]. However, those results were not in agreement with previous cell culture studies in which BRI2 transfection modified the levels of AβPP

C-terminal fragments[6,7,38]. Noteworthy, the AD mouse model that was used (APPS1-21) contains mutations, which alter the activity of γ-secretase. In addition, the AβPP is cleaved by β-secretase[124–126] in Golgi-derived vesicles in these mice instead of endosomes[127], which may halt the posterior binding of BRI2 to AβPP in the plasma membrane or in endocitic compartments[28]. Consequently, this AD mouse model may not be a good tool to unravel the involvement of BRI2 expression in AβPP processing.
Nevertheless, the study importantly revealed that the levels of secreted IDE were increased after BRI2 transfection, unlike the levels of neprilysin, which remained unchanged. The increased levels of secreted IDE in those cells enhanced Aβ degradation thereby reducing the levels of Aβ[105]. Since BRI2 positively regulates IDE, impaired functionality of BRI2 may also contribute to the development of FBD, FDD and AD via diminished IDE secretion and subsequent reduced degradation of the amyloid peptides, i.e. ABri, ADan and Aβ. Whether BRI2 can regulate other Aβ-degrading enzymes such as endothelin or angiotensin-converting enzymes, or plasmin[120] remains to be elucidated .

Concluding remarks

AD, the most common form of dementia[39], shares clinical and pathological characteristics with FBD and FDD such as memory decline, amyloid angiopathy and tangle formation, which are caused by autosomal mutations in the BRI2 gene[1,2]. The data summarized in this review indicate that BRI2, which is present in human control brain tissue, probably performs a critical physiological neuronal function.
To unravel the physiological function of BRI2, several issues need to be clarified, including (i) the prevalence, the location and the function of the different BRI2 forms (dimers, monomers and peptides) under physiological conditions, (ii) the presence of high molecular weight BRI2 forms and (iii) the effect of ADAM10 cleavage on the BRI2 BRICHOS functionality. One of the main hallmarks shared by AD, FBD and FDD is the presence of amyloid deposits, suggesting that the accumulation of amyloid peptides is the initiating event leading to neuronal loss and dementia. However, an alternative hypothesis about AD suggests that Aβ, although it is clearly involved in the disease, is not the causative event of AD pathogenesis, since amyloid load does not strongly correlate with memory deficits[76]. In line with this hypothesis, recent studies on FBD and FDD have indicated that the cognitive impairment and synaptic dysfunction in these disorders are not caused by amyloidosis, but rather by a loss of BRI2 function, preventing its binding to AβPP[104,107]. Additionally, the ABri, ADan and Aβ peptides trigger similar pathological and clinical outcomes despite their different amino acidic sequences, highlighting the importance

of protein structure in the development of these disorders. These data suggest that FBD, FDD and AD may share common molecular pathways leading to dementia.

A diagram summarizing possible interactions of BRI2 in AD pathology is presented in Figure 2. BRI2 is a physiological inhibitor of AβPP processing, but it can also regulate the levels of BACE1, likely affecting the amyloidogenic processing of AβPP and thus Aβ production. p23WT and the BRI2 BRICHOS domain, which are released after BRI2 processing, are both able to inhibit Aβ aggregation, delaying Aβ fibrillation and the subsequent formation of Aβ plaques. Additionally, BRI2 up-regulates the secretion of IDE, one of the main enzymes involved in Aβ degradation. Thus, BRI2 may also be involved in AD pathogenesis and may have a regulatory role in several aspects of the amyloid cascade.

The data presented in this review suggest that a lack of BRI2 or reduced BRI2 functionality plays an essential role in FBD and FDD development. Moreover, in view of the possible relationship between BRI2 and AD pathology, defective on BRI2 function may also contribute for the development of AD. A recent proteomic study has revealed higher levels of the BRI2 C-terminal part ($BRI2_{254-262}$) in cerebrospinal fluid of AD patients compared to controls[128], supporting the hypothesis that BRI2 change during disease development, and thus may have a role in AD. Therefore, an extensive analysis of this protein in AD may open new insights into AD aetiology.

Acknowledgments

This work was supported by the Erasmus Mundus Joint Doctorate Program (EMJD 2009-2013, Action 1B, Grant 159302-1-2009-1-NL-ERA, European Neuroscience Campus Network) and was executed in the Neurodegeneration research program of the Neuroscience Campus Amsterdam, the Netherlands.

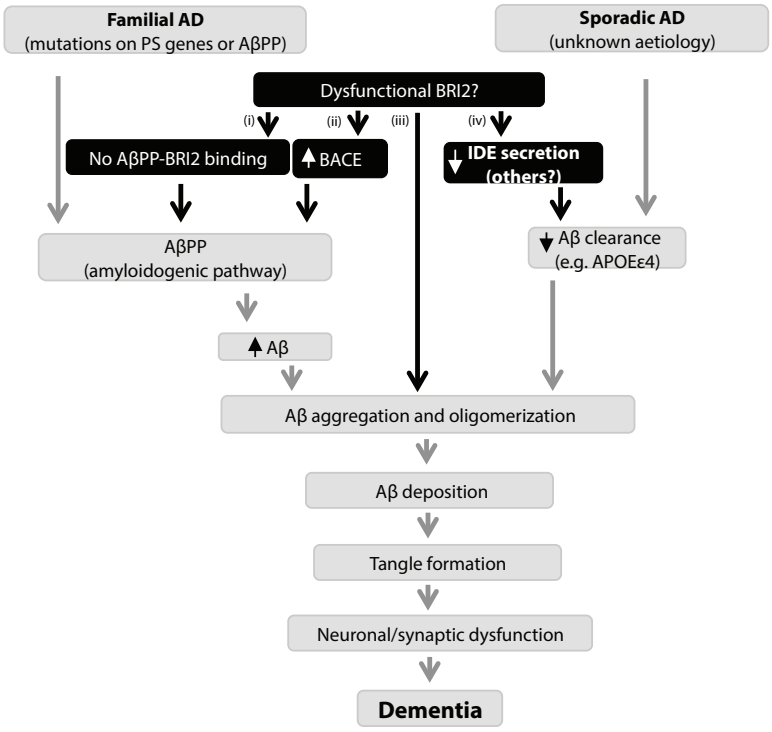

Fig. 2. Hypothetical role of BRI2 within the amyloid cascade hypothesis. According to the amyloid cascade hypothesis (in grey) [129], AD pathogenesis is caused by an imbalance between Aβ production and clearance. In familial AD, mutations in PS or AβPP genes lead to increased production and amyloidogenic processing of AβPP, which increases Aβ *production*. Although the aetiology of sporadic AD remains unknown, the genome-wide associated studies suggest that in sporadic AD a decrease in *clearance* of Aβ beta is the likely culprit [68]. The accumulation of Aβ leads to its oligomerization, aggregation and deposition, which also promote tangle formation. All these events lead to neuronal and synaptic dysfunction and dementia. The described results suggest that in sporadic AD a loss of BRI2 function (dark grey rectangles and black lines) may lead to (i) the diminished formation of AβPP-BRI2 complexes and (ii) increasedlevels of BACE1, which can ultimately promote Aβ production, (iii) disinhibition of Aβ aggregation and fibrillation by BRI2 and (iv) decreased secretion of the IDE enzyme, thereby impairing extracellular Aβ clearance. Thus, the loss of BRI2 functionality can lead to an imbalance between Aβ production and clearance, which may promote the development of AD.

References

1. Vidal, R. *et al.* A stop-codon mutation in the BRI gene associated with familial British dementia. *Nature* **399,** 776–81 (1999).

2. Vidal, R. *et al.* A decamer duplication in the 3' region of the BRI gene originates an amyloid peptide that is associated with dementia in a Danish kindred. *Proc Natl Acad Sci U S A* **97,** 4920–5 (2000).

3. Garringer, H. J., Murrell, J., D'Adamio, L., Ghetti, B. & Vidal, R. Modeling familial British and Danish dementia. *Brain Struct Funct* **214,** 235–44 (2010).

4. Rostagno, A. *et al.* Chromosome 13 dementias. *Cell Mol Life Sci* **62,** 1814–25 (2005).

5. Tsachaki, M., Ghiso, J. & Efthimiopoulos, S. BRI2 as a central protein involved in neurodegeneration. *Biotechnol J* **3,** 1548–54 (2008).

6. Fotinopoulou, A. *et al.* BRI2 interacts with amyloid precursor protein (APP) and regulates amyloid beta (Abeta) production. *J Biol Chem* **280,** 30768–72 (2005).

7. Matsuda, S. *et al.* The familial dementia BRI2 gene binds the Alzheimer gene amyloid-beta precursor protein and inhibits amyloid-beta production. *J Biol Chem* **280,** 28912–6 (2005).

8. Kim, J. *et al.* BRI2 (ITM2b) inhibits Abeta deposition in vivo. *J Neurosci* **28,** 6030–6 (2008).

9. Peng, S., Fitzen, M., Jörnvall, H. & Johansson, J. The extracellular domain of Bri2 (ITM2B) binds the ABri peptide (1-23) and amyloid beta-peptide (Abeta1-40): Implications for Bri2 effects on processing of amyloid precursor protein and Abeta aggregation. *Biochem Biophys Res Commun* **393,** 356–61 (2010).

10. Pittois, K., Deleersnijder, W. & Merregaert, J. cDNA sequence analysis, chromosomal assignment and expression pattern of the gene coding for integral membrane protein 2B. *Gene* **217,** 141–149 (1998).

11. Deleersnijder, W. *et al.* Isolation of Markers for Chondro-osteogenic Differentiation Using cDNA Library Subtraction. **271,** 19475–19482 (1996).

12. Vidal, R. *et al.* Sequence, genomic structure and tissue expression of Human BRI3, a member of the BRI gene family. *Gene* **266,** 95–102 (2001).

13. Hedlund, J., Johansson, J. & Persson, B. BRICHOS - a superfamily of multidomain proteins with diverse functions. *BMC Res Notes* **2,** 180 (2009).

14. Willander, H., Hermansson, E., Johansson, J. & Presto, J. BRICHOS domain associated with lung fibrosis, dementia and cancer--a chaperone that prevents amyloid fibril formation? *FEBS J* **278,** 3893–904 (2011).

15. Sánchez-Pulido, L., Devos, D. & Valencia, A. BRICHOS: a conserved domain in proteins associated with dementia, respiratory distress and cancer. *Trends Biochem Sci* **27,** 329–32 (2002).

16. Willander, H. *et al.* BRICHOS Domains Efficiently Delay Fibrillation of Amyloid β-Peptide. *J Biol Chem* **287,** 31608–17 (2012).

17. Tsachaki, M. *et al.* Glycosylation of BRI2 on asparagine 170 is involved in its trafficking to the cell surface but not in its processing by furin or ADAM10. *Glycobiology* **21,** 1382–8 (2011).

18. Vidal, R., Delisle, M. B. & Ghetti, B. Neurodegeneration caused by proteins with an aberrant carboxyl-terminus. *J Neuropathol Exp Neurol* **63,** 787–800 (2004).

19. Tsachaki, M., Ghiso, J., Rostagno, A. & Efthimiopoulos, S. BRI2 homodimerizes with the involvement of intermolecular disulfide bonds. *Neurobiol Aging* **31,** 88–98 (2010).

20. Choi, S., Vidal, R., Frangione, B., Levy, E. & Alzheimer, I. Axonal transport of British and Danish amyloid peptides via secretory vesicles. *FASEB J* **18,** 373–5 (2003).

21. Pickford, F., Onstead, L., Camacho-prihar, C., Hardy, J. & Mcgowan, E. Expression of mBRI 2 in mice. **338,** 95–98 (2003).

22. Akiyama, H. *et al.* Expression of BRI, the normal precursor of the amyloid protein of familial British dementia, in human brain. *Acta Neuropathol* **107,** 53–8 (2004).

23. Lashley, T. *et al.* Expression of BRI2 mRNA and protein in normal h1. Lashley T, Revesz T, Plant G, Bandopadhyay R, Lees A, et al. (2008) Expression of BRI2 mRNA and protein in normal human brain and familial British dementia: its relevance to the pathogenesis of disease. Ne. *Neuropathol Appl Neurobiol* **34,** 492–505 (2008).

24. Matsuda, S., Tamayev, R. & D'Adamio, L. Increased AβPP Processing in Familial Danish Dementia Patients. *J Alzheimers Dis* **27,** 385–91 (2011).

25. Martin, L., Fluhrer, R. & Haass, C. Substrate requirements for SPPL2b-dependent regulated intramembrane proteolysis. *J Biol Chem* **284,** 5662–70 (2009).

26. Martin, L. *et al.* Regulated intramembrane proteolysis of Bri2 (Itm2b) by ADAM10 and SPPL2a/SPPL2b. *J Biol Chem* **283,** 1644–52 (2008).

27. Kim, S. H. *et al.* Furin mediates enhanced production of fibrillogenic ABri peptides in familial British dementia. *Nat Neurosci* **2,** 984–8 (1999).

28. Matsuda, S., Matsuda, Y., Snapp, E. L. & D'Adamio, L. Maturation of BRI2 generates a specific inhibitor that reduces APP processing at the plasma membrane and in endocytic vesicles. *Neurobiol Aging* **32,** 1400–8 (2009).

29. Nakayama, K. Furin: a mammalian subtilisin/Kex2p-like endoprotease involved in processing of a wide variety of precursor proteins. *Biochem J* **327,** 625–35 (1997).

30. Molloy, S. S., Anderson, E. D., Jean, F. & Thomas, G. Bi-cycling the furin pathway: from TGN localization to pathogen activation and embryogenesis. *Trends Cell Biol* **9,** 28–35 (1999).

31. Kim, S.-H., Creemers, J. W. M., Chu, S., Thinakaran, G. & Sisodia, S. S. Proteolytic processing of familial British dementia-associated BRI variants: evidence for enhanced intracellular accumulation of amyloidogenic peptides. *J Biol Chem* **277,** 1872–7 (2002).

32. Fleischer, A., Ayllón, V., Dumoutier, L., Renauld, J.-C. & Rebollo, A. Proapoptotic activity of ITM2B(s), a BH3-only protein induced upon IL-2-deprivation which interacts with Bcl-2. *Oncogene* **21,** 3181–9 (2002).

33. Selkoe, D. & Kopan, R. Notch and Presenilin: regulated intramembrane proteolysis links development and degeneration. *Annu Rev Neurosci* **26,** 565–97 (2003).

34. Fleischer, A., Ayllon, V. & Rebollo, A. ITM2BS regulates apoptosis by inducing loss of mitochondrial membrane potential. *Eur J Immunol* **32,** 3498–505 (2002).

35. Fleischer, A. & Rebollo, A. Induction of p53-independent apoptosis by the BH3-only protein ITM2Bs. *FEBS Lett* **557,** 283–287 (2004).

36. Latil, A. *et al.* Extensive analysis of the 13q14 region in human prostate tumors: DNA analysis and quantitative expression of genes lying in the interval of deletion. *Prostate* **57,** 39–50 (2003).

37. Han, C. *et al.* Identification of heat shock protein 5, calnexin and integral membrane protein 2B as Adam7-interacting membrane proteins in mouse sperm. *J Cell Physiol* **226,** 1186–95 (2011).

38. Matsuda, S., Giliberto, L., Matsuda, Y., McGowan, E. M. & D'Adamio, L. BRI2 inhibits amyloid beta-peptide precursor protein processing by interfering with the docking of secretases to the substrate. *J Neurosci* **28,** 8668–76 (2008).

39. Blennow, K., de Leon, M. J. & Zetterberg, H. Alzheimer's disease. *Lancet* **368,** 387–403 (2006).

40. Ramon y Cajal, S. Degeneration and Regeneration of the Nervous System. *J Neurol Psychopathol* **9,** 378 (1929).

41. Shankar, G. M. & Walsh, D. M. Alzheimer's disease: synaptic dysfunction and Abeta. *Mol Neurodegener* **4,** 48 (2009).

42. Grundke-Iqbal, I. *et al.* Abnormal phosphorylation of the microtubule-associated protein tau (tau) in Alzheimer cytoskeletal pathology. *Proc Natl Acad Sci U S A* **83,** 4913–7 (1986).

43. Masters, C. L. *et al.* Amyloid plaque core protein in Alzheimer disease and Down syndrome. *Proc Natl Acad Sci U S A* **82,** 4245–9 (1985).

44. Braak, H. & Braak, E. Neuropathological stageing of Alzheimer-related changes. *Acta Neuropathol* **82,** 239–59 (1991).

45. Walsh, D. M. & Selkoe, D. J. A beta oligomers - a decade of discovery. *J Neurochem* **101,** 1172–84 (2007).

46. Lesné, S. E. *et al.* Brain amyloid-β oligomers in ageing and Alzheimer's disease. *Brain* **136,** 1383–98 (2013).

47. Zahs, K. R. & Ashe, K. H. β-Amyloid oligomers in aging and Alzheimer's disease. *Front Aging Neurosci* **5,** 28 (2013).

48. Chow, V. W., Mattson, M. P., Wong, P. C. & Gleichmann, M. An Overview of APP Processing Enzymes and Products. *Neuromolecular Med* 1–12 (2009). doi:10.1007/s12017-009-8104-z

49. Cai, H. *et al.* BACE1 is the major beta-secretase for generation of Abeta peptides by neurons. *Nat Neurosci* **4,** 233–4 (2001).

50. Luo, Y. *et al.* Mice deficient in BACE1 , the Alzheimer ' s β-secretase , have normal phenotype and abolished β-amyloid generation. **4,** 231–2 (2001).

51. Passer, B. *et al.* Generation of an Apoptotic Intracellular Peptide by γ-Secretase Cleavage of Alzheimer ' s Amyloid β Protein Precursor. **2,** 289–301 (2000).

52. Strooper, B. De. Aph-1, Pen-2, and Nicastrin with Presenilin Generate an Active Ŝ-Secretase Complex. *Neuron* **38,** 9–12 (2003).

53. O'Brien, R. & Wong, P. Amyloid Precursor Protein Processing and Alzheimer's Disease. *Annu Rev Neurosci* **34,** 185–204 (2011).

54. Endres, K. & Fahrenholz, F. Regulation of alpha-secretase ADAM10 expression and activity. *Exp Brain Res* **217,** 343–52 (2012).

55. Kuhn, P.-H. *et al.* ADAM10 is the physiologically relevant, constitutive alpha-secretase of the amyloid precursor protein in primary neurons. *EMBO J* **29,** 3020–32 (2010).

56. Lammich, S. *et al.* Constitutive and regulated -secretase cleavage of Alzheimer's amyloid precursor protein by a disintegrin metalloprotease. *Proc Natl Acad Sci* **96,** 3922–3927 (1999).

57. Hardy, J. & Allsop, D. Amyloid deposition as the central event in the aetiology of Alzheimer's disease. *Trends Pharmacol Sci* **12,** 383–8 (1991).

58. Haass, C. & Selkoe, D. J. Soluble protein oligomers in neurodegeneration: lessons from the Alzheimer's amyloid beta-peptide. *Nat Rev Mol Cell Biol* **8,** 101–12 (2007).

59. Hardy, J. & Selkoe, D. J. The amyloid hypothesis of Alzheimer's disease: progress and problems on the road to therapeutics. *Science* **297,** 353–6 (2002).

60. Karran, E., Mercken, M. & De Strooper, B. The amyloid cascade hypothesis for Alzheimer's disease: an appraisal for the development of therapeutics. *Nat Rev Drug Discov* **10,** 698–712 (2011).

61. Tomita, T. *et al.* The presenilin 2 mutation (N141I) linked to familial Alzheimer disease (Volga German families) increases the secretion of amyloid beta protein ending at the 42nd (or 43rd) residue. *Proc Natl Acad Sci U S A* **94,** 2025–30 (1997).

62. Citron, M. *et al.* Mutant presenilins of Alzheimer's disease increase production of 42-residue amyloid beta-protein in both transfected cells and transgenic mice. *Nat Med* **3,** 67–72 (1997).

63. Citron, M. *et al.* Mutation of the beta-amyloid precursor protein in familial Alzheimer's disease increases beta-protein production. *Nature* **360,** 672–4 (1992).

64. Hsiao, K. *et al.* Correlative memory deficits, Abeta elevation, and amyloid plaques in transgenic mice. *Science* **274,** 99–102 (1996).

65. Chishti, M. A. *et al.* Early-onset Amyloid Deposition and Cognitive Deficits in Transgenic Mice Expressing a Double Mutant Form of Amyloid Precursor Protein 695 *. **276,** 21562–21570 (2001).

66. Jiang, Q. *et al.* ApoE promotes the proteolytic degradation of Abeta. *Neuron* **58,** 681–93 (2008).

67. Corder, E. H. *et al.* Gene dose of apolipoprotein E type 4 allele and the risk of Alzheimer's disease in late onset families. *Science* **261,** 921–3 (1993).

68. Lambert, J.-C. *et al.* Genome-wide association study identifies variants at CLU and CR1 associated with Alzheimer's disease. *Nat Genet* **41,** 1094–9 (2009).

69. Davies, L. *et al.* A4 amyloid protein deposition and the diagnosis of Alzheimer's disease: prevalence in aged brains determined by immunocytochemistry compared with conventional neuropathologic techniques. *Neurology* **38,** 1688–93 (1988).

70. Schmitt, F. A. *et al.* "Preclinical" AD revisited: neuropathology of cognitively normal older adults. *Neurology* **55,** 370–6 (2000).

71. Morgan, K. The three new pathways leading to Alzheimer's disease. *Neuropathol Appl Neurobiol* **37,** 353–7 (2011).

72. Boada, M. *et al.* ATP5H/KCTD2 locus is associated with Alzheimer's disease risk. *Mol Psychiatry* 1–6 (2013). doi:10.1038/mp.2013.86

73. Guerreiro, R. *et al.* TREM2 variants in Alzheimer's disease. *N Engl J Med* **368,** 117–27 (2013).

74. Jonsson, T. *et al.* Variant of TREM2 Associated with the Risk of Alzheimer's Disease. *N Engl J Med* 121114152813005 (2012). doi:10.1056/NEJMoa1211103

75. Neumann, H. & Daly, M. J. Variant TREM2 as Risk Factor for Alzheimer's Disease. *N Engl J Med* 121114152740008 (2012). doi:10.1056/NEJMe1213157

76. Lee, H. *et al.* Amyloid- in Alzheimer Disease : The Null versus the Alternate Hypotheses. *J Pharmacol Exp Ther* **321,** 823–829 (2007).

77. Plant, G. T., Révész, T., Barnard, R. O., Harding, A. E. & Gautier-Smith, P. C. Familial cerebral amyloid angiopathy with nonneuritic amyloid plaque formation. *Brain* **113,** 721–47 (1990).

78. Mead, S. *et al.* Familial British dementia with amyloid angiopathy: early clinical, neuropsychological and imaging findings. *Brain* **123,** 975–91 (2000).

79. Holton, J. L. *et al.* Familial Danish dementia: a novel form of cerebral amyloidosis associated with deposition of both amyloid-Dan and amyloid-beta. *J Neuropathol Exp Neurol* **61,** 254–67 (2002).

80. Holton, J. L. *et al.* Regional distribution of amyloid-Bri deposition and its association with neurofibrillary degeneration in familial British dementia. *Am J Pathol* **158,** 515–26 (2001).

81. Rostagno, A. *et al.* Complement activation in chromosome 13 dementias. Similarities with Alzheimer's disease. *J Biol Chem* **277,** 49782–90 (2002).

82. Lashley, T. *et al.* Molecular chaperons, amyloid and preamyloid lesions in the BRI2 gene-related dementias: a morphological study. *Neuropathol Appl Neurobiol* **32,** 492–504 (2006).

83. Schwab, C. *et al.* TDP-43 pathology in familial British dementia. *Acta Neuropathol* **118,** 303–11 (2009).

84. Lashley, T., Holton, J. L. & Revesz, T. TDP-43 pathology may occur in the BRI2 gene-related dementias. *Acta Neuropathol* **121,** 559–60 (2011).

85. Seubert, P. *et al.* Isolation and quantification of soluble Alzheimer's beta-peptide from biological fluids. *Nature* **359,** 325–7 (1992).

86. Ghiso, J. a *et al.* Systemic amyloid deposits in familial British dementia. *J Biol Chem* **276,** 43909–14 (2001).

87. Tomidokoro, Y. *et al.* Familial Danish dementia: co-existence of Danish and Alzheimer amyloid subunits (ADan AND A{beta}) in the absence of compact plaques. *J Biol Chem* **280,** 36883–94 (2005).

88. Holton, J. L. *et al.* Familial British dementia (FBD): a cerebral amyloidosis with systemic amyloid deposition. *Neuropathol Appl Neurobiol* **28,** 148–148 (2002).

89. El-Agnaf, O. M., Nagala, S., Patel, B. P. & Austen, B. M. Non-fibrillar oligomeric species of the amyloid ABri peptide, implicated in familial British dementia, are more potent at inducing apoptotic cell death than protofibrils or mature fibrils. *J Mol Biol* **310,** 157–68 (2001).

90. Gibson, G. *et al.* Oligomerization and neurotoxicity of the amyloid ADan peptide implicated in familial Danish dementia. *J Neurochem* **88,** 281–290 (2003).

91. Mori, H., Takio, K., Ogawara, M. & Selkoe, D. J. Mass spectrometry of purified amyloid beta protein in Alzheimer's disease. *J Biol Chem* **267,** 17082–6 (1992).

92. Saul, A. *et al.* Abundant pyroglutamate-modified ABri and ADan peptides in extracellular and vascular amyloid deposits in familial British and Danish dementias. *Neurobiol Aging* **34,** 1416–25 (2013).

93. Goñi, F. *et al.* Immunomodulation targeting abnormal protein conformation reduces pathology in a mouse model of Alzheimer's disease. *PLoS One* **5,** e13391 (2010).

94. Pickford, F., Coomaraswamy, J., Jucker, M. & McGowan, E. Modeling familial British dementia in transgenic mice. *Brain Pathol* **16,** 80–5 (2006).

95. Vidal, R., Barbeito, A. G., Miravalle, L. & Ghetti, B. Cerebral amyloid angiopathy and parenchymal amyloid deposition in transgenic mice expressing the Danish mutant form of human BRI2. *Brain Pathol* **19,** 58–68 (2009).

96. Garringer, H. J. *et al.* Increased tau phosphorylation and tau truncation, and decreased synaptophysin levels in mutant BRI2/tau transgenic mice. *PLoS One* **8,** e56426 (2013).

97. Pérez, M., Morán, M. A., Ferrer, I., Avila, J. & Gómez-Ramos, P. Phosphorylated tau in neuritic plaques of APP(sw)/Tau (vlw) transgenic mice and Alzheimer disease. *Acta Neuropathol* **116,** 409–18 (2008).

98. Coomaraswamy, J. *et al.* Modeling familial Danish dementia in mice supports the concept of the amyloid hypothesis of Alzheimer's disease. *Proc Natl Acad Sci U S A* **107,** 7969–74 (2010).

99. Saura, C. a *et al.* Loss of presenilin function causes impairments of memory and synaptic plasticity followed by age-dependent neurodegeneration. *Neuron* **42,** 23–36 (2004).

100. Giliberto, L., Matsuda, S., Vidal, R. & D'Adamio, L. Generation and initial characterization of FDD knock in mice. *PLoS One* **4,** e7900 (2009).

101. Tamayev, R. *et al.* Memory Deficits Due to Familial British Dementia BRI2 Mutation Are Caused by Loss of BRI2 Function Rather than Amyloidosis. *J Neurosci* **30,** 14915–14924 (2010).

102. Tamayev, R., Matsuda, S., Fà, M., Arancio, O. & Adamio, L. D. Danish dementia mice suggest that loss of function and not the amyloid cascade causes synaptic plasticity and memory deficits. *PNAS* **107,** 20822–27 (2010).

103. Harris, V. K. *et al.* Bri2-23 is a potential cerebrospinal fluid biomarker in multiple sclerosis. *Neurobiol Dis* **40,** 331–9 (2010).

104. Tamayev, R., Matsuda, S., Giliberto, L., Arancio, O. & D'Adamio, L. APP heterozygosity averts memory deficit in knockin mice expressing the Danish dementia BRI2 mutant. *EMBO J* **30,** 2501–9 (2011).

105. Kilger, E. *et al.* BRI2 regulates {beta}-amyloid degradation by increasing levels of secreted insulin degrading enzyme (IDE). *J Biol Chem* **286,** 37446–37457 (2011).

106. Tamayev, R., Matsuda, S., Arancio, O. & D'Adamio, L. β- but not γ-secretase proteolysis of APP causes synaptic and memory deficits in a mouse model of dementia. *EMBO Mol Med* **4,** 171–9 (2012).

107. Tamayev, R. & D'Adamio, L. Memory deficits of British Dementia knock-in mice are prevented by APP haploinsufficiency. *J Neurosci* **32,** 5481–5485 (2012).

108. Tamayev, R. & D'Adamio, L. Inhibition of γ-secretase worsens memory deficits in a genetically congruous mouse model of Danish dementia. *Mol Neurodegener* **7,** 19 (2012).

109. Melnikova, T. *et al.* Reversible pathologic and cognitive phenotypes in an inducible model of Alzheimer-amyloidosis. *J Neurosci* **33,** 3765–79 (2013).

110. Kim, J. *et al.* Normal cognition in transgenic BRI2-Aβ mice. *Mol Neurodegener* **8,** 15 (2013).

111. Tsachaki, M. *et al.* BRI2 interacts with BACE1 and regulates its cellular levels by promoting its degradation and reducing its mRNA levels. *Curr Alzheimer Res* **10,** 532–41 (2013).

112. Zhao, J. *et al.* Beta-site amyloid precursor protein cleaving enzyme 1 levels become elevated in neurons around amyloid plaques: implications for Alzheimer's disease pathogenesis. *J Neurosci* **27,** 3639–49 (2007).

113. Zhang, X.-M. *et al.* Beta-secretase-1 elevation in transgenic mouse models of Alzheimer's disease is associated with synaptic/axonal pathology and amyloidogenesis: implications for neuritic plaque development. *Eur J Neurosci* **30,** 2271–83 (2009).

114. Coulson, D. T. R. *et al.* BACE1 mRNA expression in Alzheimer's disease postmortem brain tissue. *J Alzheimers Dis* **22,** 1111–22 (2010).

115. Reitz, C. Alzheimer's disease and the amyloid cascade hypothesis: a critical review. *Int J Alzheimers Dis* **2012,** 369808 (2012).

116. Lewis, J. *et al.* Enhanced neurofibrillary degeneration in transgenic mice expressing mutant tau and APP. *Science* **293,** 1487–91 (2001).

117. Götz, J., Chen, F., van Dorpe, J. & Nitsch, R. M. Formation of neurofibrillary tangles in P301l tau transgenic mice induced by Abeta 42 fibrils. *Science* **293,** 1491–5 (2001).

118. Gamblin, T. C. *et al.* Caspase cleavage of tau: linking amyloid and neurofibrillary tangles in Alzheimer's disease. *Proc Natl Acad Sci U S A* **100,** 10032–7 (2003).

119. Mawuenyega, K. G. *et al.* Decreased Clearance of CNS Amyloid-β in Alzheimer's Disease. *Science (80-)* **330,** 1774 (2010).

120. Miners, J. S. *et al.* Abeta-degrading enzymes in Alzheimer's disease. *Brain Pathol* **18,** 240–52 (2008).

121. Qiu, W. Q. *et al.* Insulin-degrading enzyme regulates extracellular levels of amyloid beta-protein by degradation. *J Biol Chem* **273,** 32730–8 (1998).

122. Farris, W. *et al.* Insulin-degrading enzyme regulates the levels of insulin, amyloid beta-protein, and the beta-amyloid precursor protein intracellular domain in vivo. *Proc Natl Acad Sci U S A* **100,** 4162–7 (2003).

123. Morelli, L. *et al.* Insulin-degrading enzyme degrades amyloid peptides associated with British and Danish familial dementia. *Biochem Biophys Res Commun* **332,** 808–16 (2005).

124. Moehlmann, T. *et al.* Presenilin-1 mutations of leucine 166 equally affect the generation of the Notch and APP intracellular domains independent of their effect on Abeta 42 production. *Proc Natl Acad Sci U S A* **99,** 8025–30 (2002).

125. Radde, R. *et al.* Abeta42-driven cerebral amyloidosis in transgenic mice reveals early and robust pathology. *EMBO Rep* **7,** 940–6 (2006).

126. Haass, C. *et al.* The Swedish mutation causes early-onset Alzheimer's disease by β-secretase cleavage within the secretory pathway. *Nat Med* **1,** 1291–1296 (1995).

127. Kinoshita, A. *et al.* Demonstration by FRET of BACE interaction with the amyloid precursor protein at the cell surface and in early endosomes. *J Cell Sci* **116,** 3339–46 (2003).

128. Jahn, H. *et al.* Peptide Fingerprinting of Alzheimer's Disease in Cerebrospinal Fluid: Identification and Prospective Evaluation of New Synaptic Biomarkers. *PLoS One* **6,** e26540 (2011).

129. Selkoe, D. J. The Molecular of Alzheimer ' s Pathology Disease Review. *Neuron* **6,** 487–498 (1991).

Chapter 3

BRI2-BRICHOS is increased in human amyloid plaques in early stages of Alzheimer's disease

Neurobiol Aging. 2014 Jul;35(7):1596-604.

Marta Del Campo
Jeroen J.M Hoozemans
Lois-Lee Dekkers
Annemieke J Rozemuller
Carsten Korth
Andreas Müller-Schiffmann
Philip Scheltens
Marinus A. Blankenstein
Connie R. Jimenez
Robert Veerhuis
Charlotte E. Teunissen

Abstract

BRI2 protein binds amyloid precursor protein (APP) to halt amyloid-β production and inhibits amyloid-β aggregation via its BRICHOS-domain suggesting a link between BRI2 and Alzheimer's disease (AD). Here, we investigate the possible involvement of BRI2 in human AD pathogenesis. BRI2 containing BRICHOS-domain was increased up to 3-fold in AD hippocampus (p=0.003,n=14/group). Immunohistochemistry showed BRI2 deposits associated with amyloid-β plaques in early pathological stages (Braak-III;Thal-2/3). We observed a decrease in the protein levels of ADAM10 (p=0.02) and furin (p=0.066), as well as an increase in SPPL2b (p<0.0001) in AD hippocampus. Since these enzymes are involved in BRI2 processing, their changes may lead to aberrant processing of BRI2 promoting its deposition and likely affecting BRI2 function. Loss of BRI2 function in AD was supported by the decreased presence of BRI2-APP complexes in hippocampus of AD patients compared to controls. In conclusion, our data obtained from human samples indicate that in early stages of AD there is an increased deposition of BRI2, which likely leads to impaired BRI2 function thereby influencing AD pathophysiology.

Key words: Alzheimer's disease, BRI2, amyloid plaques, human hippocampus, pathogenesis.

Introduction

Mutations in BRI2 (*ITM2B*) are involved in Familial British and Danish dementias (FBD and FDD respectively) causing amyloid deposits and neurofibrillary tangles similar to those observed in Alzheimer's disease (AD)[1–4]. BRI2 is a 266 amino-acid long transmembrane type II protein (Fig. 1*A*) with unknown physiological function[5]. During maturation, BRI2 can be cleaved by a furin-like protease in its C-terminal region which leads to the release of a 23 amino acid (AA) peptide ($BRI2_{23}$)[6](Choi et al., 2004; Kim et al., 1999). The remaining membrane-bound N-terminal part of BRI2 (mBRI2) contains an evolutionary conserved BRICHOS domain, which may function as a chaperone promoting the correct folding of BRI2 and preventing amyloid formation[7,8]. mBRI2 can be further processed by ADAM10 and SPPL2b leading to the secretion of a 25 and 10 kDa peptides[9].
(R Vidal et al., 1999, 2000)Recent studies revealed a possible link between BRI2 and the main proteins involved in AD pathogenesis, e.g. amyloid β precursor protein (APP) and amyloid beta 1-40 and 1-42 ($A\beta_{40}$ and $A\beta_{42}$) among others. $BRI2_{23}$ and the BRI2 BRICHOS domain inhibited $A\beta_{42}$ aggregation and delayed Aβ fibrillation *in vitro* and *in vivo*[7,10,11]. Moreover, mBRI2 bound APP, leading to decreased production of $A\beta_{40}$ and $A\beta_{42}$ in both transgenic mice and cell cultures[12–18]. In addition, BRI2 regulated the levels of the β-secretase 1 (BACE1)[19] as well as the levels of the insulin degrading enzyme (IDE) [20]; affecting the

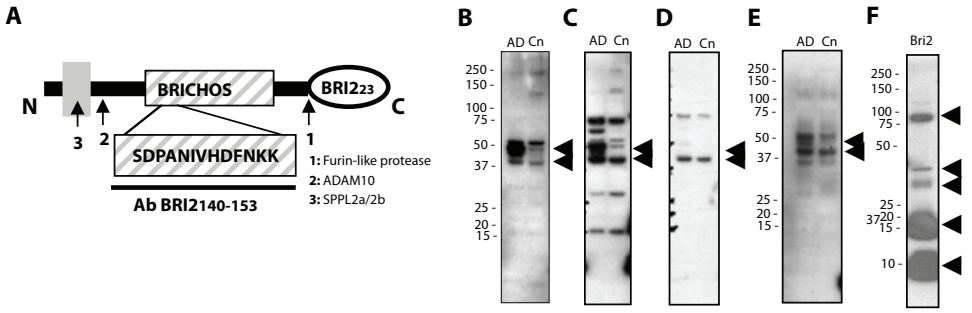

Fig. 1. Antibodies raised against human BRI2 were specific on Western Blot.
A, Schematic illustration of the BRI2 protein. The cell membrane, the BRICHOS domain and $BRI2_{23}$ peptide are presented. The numbers (1, 2 and 3) indicate the cleavage sites of BRI2 for different enzymes (furin, ADAM10 and $SPPL2_b$, respectively). The enlargement of the BRICHOS domain shows the AA sequence that is recognized by $BRI2_{140-153}$ antibody***. B-E:*** Western blot analysis of human brain homogenates from AD and Control (Cn) cases showed reactivity at bands of 40, 45 and 52 kDa using polyclonal antibodies raised against human $BRI2_{140-153}$ (***B***, affinity-purified and ***C***, protein A-purified). ***D,*** Pre-absorption of polyclonal protein A-purified $BRI2_{140-153}$ antibody with $BRI2_{140-153}$ peptide dramatically diminished or even abrogated the signal of all the bands. ***E,*** Similar reactivity against AD and Control cases was observed using the monoclonal IgM-purified anti-$BRI2_{111-153}$. ***F***, Several bands at different molecular weights were observed when recombinant $BRI2_{76-266}$ (Bri2) was analyzed using protein A-purified anti-$BRI2_{140-153}$ indicating that $BRI2_{76-266}$ can form aggregates of various sizes.

amyloidogenic processing of APP and the degradation of Aβ respectively. Interestingly, loss of wild-type BRI2 function rather than amyloidogenesis of the mutated fragments correlated with memory deficits and impaired synaptic plasticity in FBD and FDD mice models suggesting that BRI2 has a key role in memory performance [21,22]. Noteworthy, increased BRI2 levels prevented AD pathology in AD mice models when these were either crossed with mice expressing human BRI2 or when BRI2 was injected[10,14,20]. Thus, previous studies importantly related BRI2 not only with the main proteins involved in AD pathology but also with memory functioning and synaptic plasticity, which suggest that BRI2 has protective effects and that the lack of this protein leads to impaired memory and cognition.

We previously identified increased levels of BRI2 containing BRICHOS ectodomain in human cerebrospinal fluid (CSF) of AD patients compared to controls using a hypothesis-free proteomics approach (Chiasserini *et al.*, manuscript submitted), which further supports a link between BRI2 and AD. Taking into account the BRI2 increase observed in the CSF proteomic study, the association of BRI2 with FBD and FDD, and the inhibitory effect of BRI2 on several key steps of the amyloid cascade (i.e. APP processing and Aβ aggregation), we hypothesized that BRI2 might be a relevant protein in early stages of AD pathophysiology. Thus, here we extensively analyzed the levels of BRI2 in human brain tissue from controls and AD patients and the relation of BRI2 with amyloid pathology. Furthermore, we studied if BRI2 protein changes in hippocampus of AD patients were related to concentrations of its processing enzymes, including furin, ADAM10 and SPPL2b. Lastly, we questioned if the binding of BRI2 to APP occurred in human tissue and if it was preserved in AD.

Materials and Methods

Post-mortem brain tissue

Post-mortem brain material was obtained from the Netherlands Brain Bank (Amsterdam, The Netherlands). All donors (n = 35) or their next of kin provided written informed consent for brain autopsy and use of tissue and medical records for research purposes. Clinical and neuropathological evaluation as well as sample processing are described in detail in Supplementary data (materials and methods, page 1-2). Clinical and pathological diagnosis, gender, age, post-mortem interval, Braak and Thal scores for NFTs and amyloid load of all cases are listed in Supplementary Table I. Both clinical and pathological diagnoses were used as outcome data to analyze the results.

Antibody purification and characterization.

Five different purified anti-BRI2 antibodies detecting BRICHOS domain have been used: Polyclonal protein A-purified anti-$BRI2_{140-153}$, Polyclonal affinity-purified anti-$BRI2_{140-153}$, Monoclonal Protein G-purified anti-$BRI2_{140-153,}$ Polyclonal protein G-purified anti-$BRI2_{113-231}$ and Monoclonal immunoglobulin M-purified anti-$BRI2_{111-153}$. Detailed information regarding antibody generation, purification and characterization is given in Supplementary data (materials and methods, page 1).

Western blotting.

Preparation of human brain tissue and $BRI2_{76-266}$ recombinant protein and western blotting procedures are presented in the Supplementary data (materials and methods, page 2). The following primary antibodies were used: affinity-purified polyclonal rabbit anti-$BRI2_{140-153}$ (2.3 µg/ml), monoclonal mouse anti-Furin B6 (1:1000, Santa Cruz Biothecnology, Santa Cruz, USA), polyclonal rabbit anti-ADAM10 ab1997 (1:2000, Abcam, Cambridge, UK), polyclonal rabbit anti-SPPL2b (1:1000, Aviva system biology, San Diego, USA), monoclonal mouse anti-APP clone 22C11 (1:10000, clone 22C11, Millipore, Bedford, USA) and monoclonal mouse anti-Actin (clone AC-40, 1:1000, Sigma-Aldrich, Saint Louis, USA).

BRI2 Immunoprecipitation.

In order to precipitate BRI2 from human hippocampus, individual human hippocampus homogenates (HHH; 100 µg) were pre-cleared with Protein G PLUS-Agarose beads (1:2, SantaCruz Biotechnology, USA) during 30 minutes at 4C. Loading buffer was added to half of the cleared HHH (untreated) and stored at -20C until further analysis. The other half was incubated with 5 µl Protein A-purified rabbit anti-$BRI2_{140-153}$ or control rabbit polyclonal antibody during 2 hours at 4°C. Antibody-bound protein complexes were then incubated with Protein G PLUS-Agarose beads (1:2) overnight at 4C. Beads were washed 4 times with M-PER buffer (Thermo Scientific, Waltham, USA) and resuspended in sample buffer. BRI2 precipitates and untreated samples were analyzed for APP immunoreactivity by Western blot as described above.

Immunohistochemistry

Formalin-fixed and paraffin-embedded hippocampus, parietal, occipital and temporal cortex sections (5µm) were mounted on Superfrost plus tissue slides (Menzel-Glaser, Braunschweig, Germany) and dried overnight at 37°C. Single and double immunohistochemistry procedures are described in detail in Supplementary data

(materials and methods, page 3-4). The following primary antibodies were used: Protein A-purified rabbit anti-BRI2$_{140-153}$ (9.2 µg/ml) and mouse anti-Aβ$_{1-17}$ (2.57 µg/ml, VUmc, [23]).

Evaluation of stainings.

Quantitative analysis of BRI2 immunoreactive plaques was performed on single stained slides by manually counting the number of BRI2 depositions in different regions of the hippocampus (CA4-CA2, CA1 and Subiculum) and correcting for the size of the area. Contiguous microscopic fields were evaluated using a 10 x objective (0.64 mm2). Double (BRI2 and Aβ) stainings were used to determine the association of BRI2 with individual Aβ containing plaques. Data were corrected for the size of the area and the percentage of individual BRI2 positive Aβ plaques was calculated for each hippocampus area. Staining and counting was performed twice by two independent researchers, who were unaware of the diagnosis and specifics of the cases.

Statistical analysis.

Statistical analyses were performed on SPSS version 16.0 (Chicago, USA) using non-parametric Student's *t*-test (two groups analysis) or one-way ANOVA (multiple group analysis) to analyze group differences. Correlation analysis were done using Spearman's test. Values with $p < 0.05$ were considered significant.

Results

Antibody characterization.

Analysis of BRI2$_{140-153}$ peptide using Basic Local Alignment Search Tool (BLAST, NCBI) showed an e-value of 3e-08 for BRI2. The e-values of other proteins were higher than 0.01 indicating that BRI2$_{140-153}$ is a unique sequence for human BRI2 within the BRI2-BRICHOS domain (AA 137-231). The affinity purified polyclonal antibody against BRI2$_{140-153}$ detected bands of 40, 45 and 52 kDa in AD and controls human brain homogenates on Western Blots (Fig. 1*B*). Additional bands were detected at 15, 25, 75 kDa using Protein A-purified BRI2$_{140-153}$ antibody (Fig. 1C) and the reactivity of all bands was dramatically decreased after peptide pre-absorption of the antibody (Fig. 1*D*). The same 40, 45 and 52 kDa bands were observed using a monoclonal antibody raised against BRI2$_{111-153}$ (Fig. 1*E*). The polyclonal antibodies against BRI2$_{140–153}$ (Fig. 1*F*) or BRI2$_{113–231}$ (Supplementary Fig. 1*B*) showed reactive at 10, 15, 20, 30, 40 and 90 kDa of a recombinant human BRI2$_{76-266}$ protein. Specificity of all other anti-BRI2 antibodies towards the 45 kDa band was further confirmed by a dramatic

decrease in immunoreactivity after pre-absorption with recombinant human $BRI2_{140-153}$ or $BRI2_{76-226}$ (Supplementary Fig. 1*A*).

Immunohistochemical examination of AD and control hippocampus tissue for the presence and localization of BRI2, showed similar BRI2 deposition in plaques using polyclonal protein A-purified anti-$BRI2_{140-153}$, monoclonal protein G-purified anti-$BRI2_{140-153,}$ monoclonal IgM-purified anti-$BRI2_{111-153}$ or polyclonal protein G-purified $BRI2_{113-231}$ antibodies (Supplementary Fig. 1*C-G*). Reactivity of the polyclonal protein A-purified anti-$BRI2_{140-153}$ antibody to amyloid plaques was abolished after peptide pre-absorption of the antibody (Supplementary Fig. 1*H*).

BRI2 levels are increased in hippocampus of AD patients compared to controls.

BRI2 was analyzed in homogenates of hippocampal specimens from 31 patients at different stages of AD using the affinity-purified anti-$BRI2_{140-153}$ antibody (Fig. 2*A*). The 45 kDa band was specifically increased in AD patients compared to controls, based on both pathological (Fig. 2*B*) and clinical (Supplementary Fig. 2) diagnosis.

BRI2 accumulates in AD hippocampus in early pathological stages and associates with amyloid plaques.

In order to analyze the location of the increase in BRI2 reactivity in AD subjects we performed BRI2 immunostainings on post-mortem hippocampus brain sections of 34 patients (30 of them were the same patients as analyzed by Western blot). Three different areas within the hippocampus (CA4 to 2, CA1 and Subiculum) were examined (Fig. 3*A*). BRI2 staining in control patients was mainly observed in neuronal cytosol or in astrocytes. In AD cases BRI2 immunoreactivity was observed in extracellular deposits. BRI2 deposits were observed in all hippocampal areas (Fig. 3*B,* second row). BRI2 immunoreactive deposits were not observed in the same areas in control cases (Fig. 3*B,* first row). We next asked whether extracellular BRI2 deposition was related to Aβ deposition. To this end, we performed double immunohistochemical stainings for BRI2 as well as for Aβ peptides. The results showed a clear association between BRI2 and Aβ immunoreactivity (Fig. 3*B-C,* third row). Detailed analysis of this association revealed that approximately 50% of the Aβ plaques were BRI2 positive (Supplementary Fig. 3). Quantification revealed a significant increase in BRI2 deposition in AD compared to control patients, when patients were grouped either to the pathological (Fig. 4) or clinical (Supplementary Fig. 4) diagnosis. In a subset of AD cases (n=5) we also evaluated the association of BRI2 deposition with Aβ plaques in additional brain areas, such as the temporal, occipital and parietal cortex. The co-localization of BRI2 deposits with Aβ plaques in these cortical areas was considerably lower (between 1 and 5%) compared to the hippocampal area (data not shown).

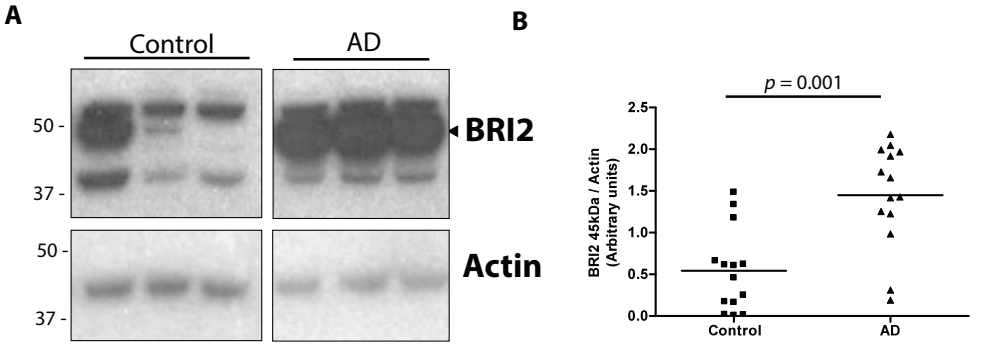

Fig. 2. BRI2 is increased in human hippocampus homogenates of AD patients compared to controls.
A, Representative Western blot of post-mortem human hippocampus from 3 Control and 3 AD cases indicating an increase of BRI2 in AD. Actin analysis showed equal protein concentrations in every lane. ***B,*** BRI2 reactivity against human brain homogenates from control (n = 14) and AD (n = 14) patients was quantified and corrected for actin levels. Data were compared based on pathological diagnosis.

There was a significant correlation between the extent of BRI2 staining and the levels of the 45kDa BRI2 observed by Western blot in all hippocampus areas (CA4-2: $p = 0.018$, CA1: $p = 0.03$, Subicullum: $p = 0.009$, Supplementary Fig. 5). We next questioned if BRI2 deposition starts in early stages of the AD pathology. The data in Fig. 5 show that BRI2 deposition in the hippocampus was present already in the early stages of AD (III/IV-3) and correlated with the increase in tangles and amyloid plaques. The maximal BRI2 values are found at Braak stages IV and V (Fig. 5*A*). BRI2 deposition also increased with amyloid progression (Amyloid staging according to Thal [24]), i.e. the highest amount of BRI2 deposition was observed in the most advanced stage of the disease (Fig. 5*B*). Collectively, these results revealed that in AD hippocampus there is a deposition of BRI2 protein associated with amyloid plaques, which is not present in control tissue. The data additionally showed that BRI2 deposition starts already in early stages of the AD pathology.

The levels of BRI2 processing enzymes furin, ADAM10 and SPPL2b are changed in AD human hippocampus.

BRI2 undergoes three consecutive cleavages performed by a furin-like protease, ADAM10 and SPPL2b leading to the secretion of different molecular weight peptides[6,9] (Fig. 1*A*). The higher intensity of the 45 kDa band on Western blot suggested higher levels of unprocessed BRI2 in AD patients (Fig. 2*A*). Thus, we hypothesized that the levels of furin, ADAM10 and SPPL2b were also different in AD compared to control cases. Therefore, we analyzed the levels of these proteins by Western blot in the same hippocampus homogenates as tested for BRI2 reactivity (Fig. 6*A*). Furin levels were 3–fold decreased

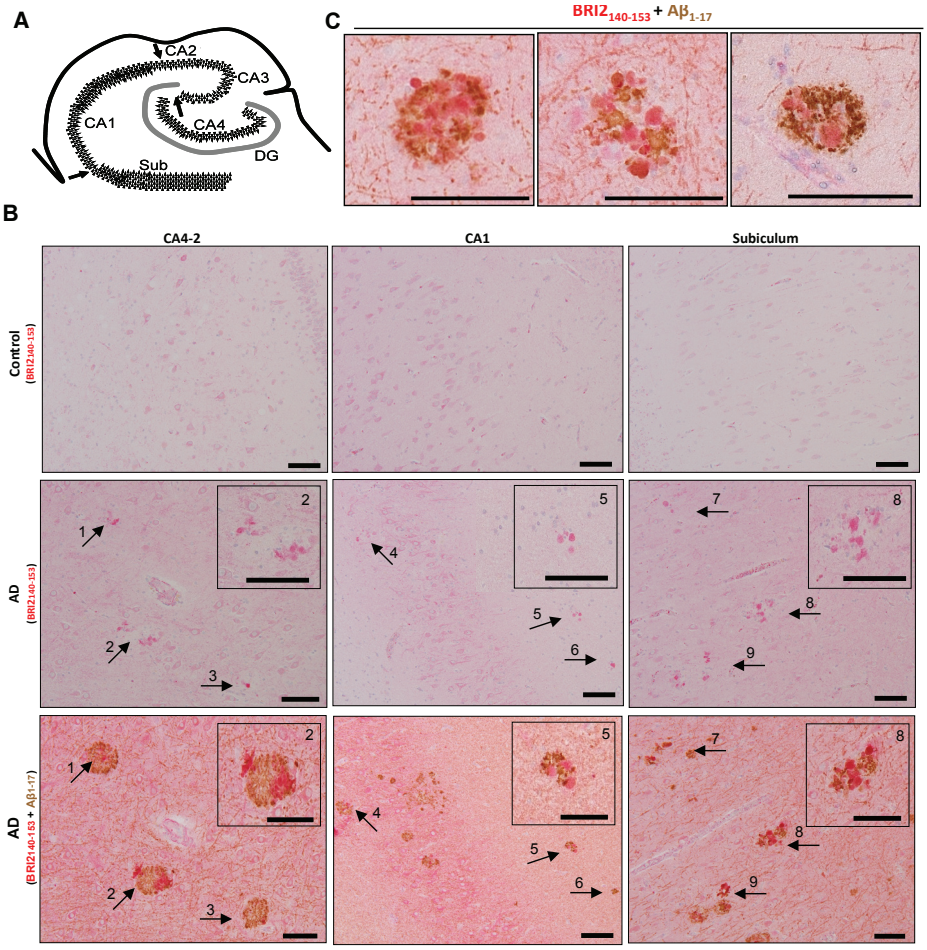

Fig. 3. BRI2 deposition in AD hippocampus is associated with amyloid plaques.
A, Schematic representation of human hippocampus. Arrows delimit the different areas analyzed: CA4-2, CA1 and Subiculum. ***B,*** Post-mortem hippocampus sections from control and AD cases were stained with anti-$BRI2_{140-153}$ (Red). AD cases were also simultaneously stained for anti-$BRI2_{140-153}$ (Red) and anti-$A\beta_{1-17}$ (Brown). BRI2 deposition in plaques is present (arrows with numbers) in all AD brain areas, but not in controls. Double immunohistochemistry showed that BRI2 deposition was associated with amyloid plaques. Squares within the sections represent the magnification of the corresponding plaque/deposit. ***C,*** Amyloid plaques (Brown) associated with BRI2 deposits in post-mortem hippocampus sections form AD cases with higher magnification. Scale bars: 100μm.

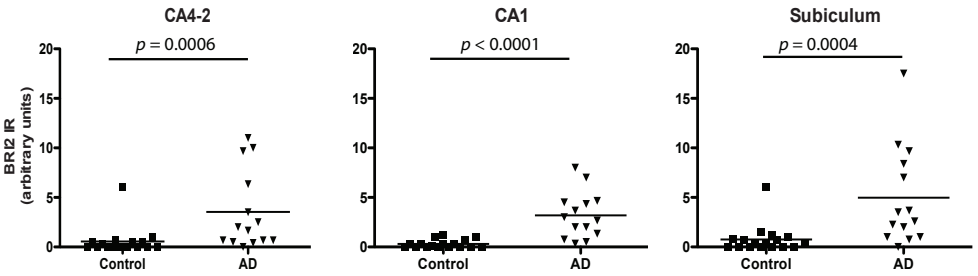

Fig. 4. BRI2 immunoreactivity is significantly more frequent in AD cases.
BRI2 immunoreactivity (IR) was semiquantitatively measured for each patient in each hippocampus area, and patients were grouped according to pathological diagnosis. Higher numbers of BRI2 deposits were found in AD patients (n = 14) compared to control (n = 14) cases in all the areas analyzed.

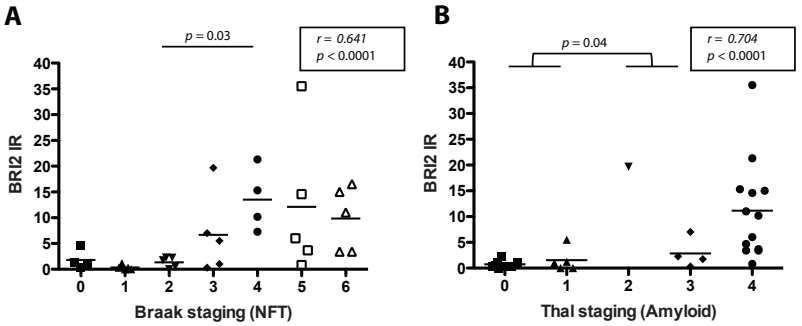

Fig. 5. **BRI2 deposition starts in early stages of the disease**.
Analysis of BRI2 immunoreactivity (IR) in human hippocampus according to Braak stage for NFTs (***A***) or Thal staging for amyloid pathology (***B***). BRI2 was increased already in early stages of the disease (Braak III-2/3). Pearson correlation coeficients for the relation between BRI2 deposition and NFT or amyloid plaque formation are presented in the inserts.

in AD patients although this difference did not reach significance (Fig. 6*B*). ADAM10 was 2-fold decreased in AD compared to control cases (Fig. 6*C*). SPPL2b was 10-fold increased in AD hippocampus homogenates (Fig. 6*D*). The levels of ADAM10 were negatively correlated with the levels of BRI2 (Fig. 6*E*). The decrease in furin and ADAM10 as well as the increase in SPPL2b observed in AD brain could lead to an alternative processing of BRI2.

BRI2 binding to APP is absent in hippocampus of AD patients

Since BRI2 is able to bind APP *in vitro* and in mice[12–15], we aimed to analyze if this binding also occurs in human brains and if this is preserved in AD cases. Immunoprecipitation of BRI2 from human hippocampus and analysis of APP levels in the precipitates revealed that BRI2 was associated with APP in the control cases. Interestingly, APP reactivity of captured BRI2 proteins was not present or considerably reduced in AD homogenates, indicating that there is a loss of BRI2-APP complexes in these AD cases (Fig. 7). Noteworthy, one of the AD patients analyzed (AD4) showed a similar APP-BRI2 reactivity to that in the control cases. Interestingly, AD4 case had one of the lowest values for both 45 kDa BRI2 reactivity and BRI2 deposits. These data indicate that in AD there is a decreased interaction between BRI2 and APP, which may affect the regulatory function of BRI2 in APP processing and thus in Aβ production.

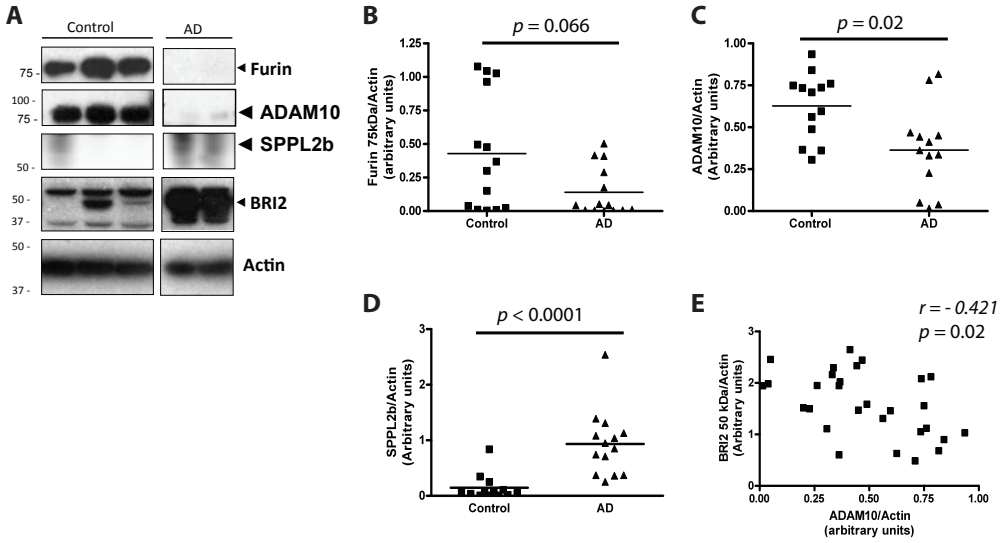

Fig. 6. The levels of the BRI2 processing enzymes furin, ADAM10 and SPPL2b are changed in AD human hippocampus.

A, Representative Western blot of human brain homogenates from 3 control and 2 AD patients shows the reactivity of furin, ADAM10, SPPL2b and BRI2 in the same samples. Actin analysis showed equal protein concentrations in every lane. ***B-D***: Significant differences between Control (n = 14) and AD (n = 14) patients are observed in the levels of ADAM10 (***C***) and SPPL2b (***D***) and a tendency for the levels of furin (***B***). Correlation analysis showed a significant negative correlation between ADAM10 and mBRI2 (***E***).

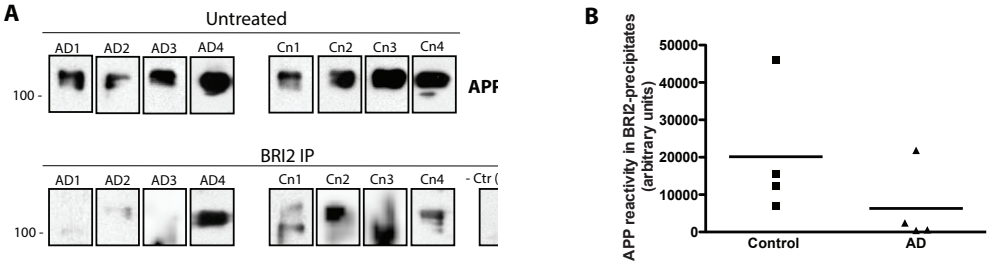

Fig. 7. BRI2-APP complexes are present in control but not in AD human hippocampus.

A, BRI2 was immunoprecipitated from human hippocampus of 4 controls and 4 AD cases using anti-$BRI2_{113-231}$. APP was analyzed by Western blot in the original samples (untreated) and in the immunoprecipitated-BRI2 samples (BRI2 IP). Negative control (- Ctr) is an immunoprecipitation performed with an irrelevant rabbit antibody. ***B***, APP reactivity in BRI2 immunprecipitated samples from human brain homogenates of control (n = 4) and AD (n = 4) patients was quantified and compared based on pathological diagnosis.

Discussion

In this study we importantly found that the levels of BRI2 containing BRICHOS domain were increased in human AD hippocampus homogenates compared to that of non-demented controls. We observed BRI2 deposits in the hippocampus already in early stages of the AD pathology, which were associated with Aβ plaques. Moreover, we observed that the levels of furin, ADAM10, and SPPL2b, the enzymes involved in BRI2 processing, were all modified in AD tissue. Additionally, we observed that BRI2 binding to APP was lost in AD patients. Taken together, these results obtained from human samples suggest that BRI2 accumulation in AD may lead to a decreased formation of BRI2-APP complexes and could thereby be involved in early stages of AD pathophysiology.

Four different antibodies (monoclonal, polyclonal and an additional affinity-purified antibody) recognizing three different epitopes covering the BRI2-BRICHOS domain were used to analyze the specificity by comparison of the signals on Western Blot and immunohistochemistry as well as by pre-absorbing the antibodies with their antigenic peptides; which led to a dramatically decreased, or complete absence, of signal. Antibody characterization showed specific BRI2 bands at 40, 45 and 52 kDa in hippocampus homogenates for all the antibodies tested which is in line with previous studies[6,9,25,26]. However, based on its AA sequence, the expected molecular weight of BRI2 is 30 kDa. In a recent transgenic cell culture study deglycosylation of BRI2 decreased its molecular weight by only 2 kDa [27] suggesting the involvement of other mechanisms in the generation of higher molecular weight forms of BRI2. Intriguingly, Western blot analysis of the recombinant BRI2 ectodomain under denatured conditions showed also bands of higher molecular weight, which suggests that BRI2 is able to aggregate, at least *in vitro*. We propose that BRI2 may undergo additional post-translational modifications or can constitute aggregates with itself and/or other proteins accounting for the relatively higher molecular bands of 45 and 52 kDa.

Our Western blot results showed specific increased levels of the 45 kDa BRI2 band in AD hippocampus compared to controls based on both clinical and pathological diagnosis of AD. Immunohistochemical BRI2 analysis in the different hippocampal areas confirmed those results, as we observed BRI2 deposition in all hippocampal areas of AD patients, but not in control cases. These results are in agreement with the BRI2 staining previously observed in the temporal cortex of one AD case [28]. A previous small-scale (n = 4) immunohistochemical study compared the presence of BRI2 in AD hippocampus and control cases but no difference was found [29]. The discrepancy found could be explained by the antibody used in the latter study, which was raised against the C-terminal part of the BRI2 BRICHOS domain ($BRI2_{223-233}$). $BRI2_{223}$ is involved in the formation of disulfide

bonds and loop like structures[4] that could mask the epitope recognized by that antibody when the protein is aggregated. There was a significant correlation between increased levels of the 45 kDa BRI2-positive bands in Western blot and the immunohistochemistry results, which suggest that BRI2 immunostaining represented deposition of the 45 kDa form of BRI2.

We also related BRI2 deposition to Braak and Thal stages [24,30,31]. The observed increase of BRI2 deposition in Braak stages III-IV indicates that BRI2 is already involved in the early stages of the pathology in which NFT can be also prominently observed in the hippocampal areas. Since the NFT-formation correlates well with the clinical diagnosis and dementia level[32], the results suggest that BRI2 changes take place in very early stages in which cognitive impairment is being developed and thus, it may have an involvement on AD etiology. Indeed, previous studies in FBD and FDD mice models showed that memory decline was caused by reduced levels and loss of function of wild-type BRI2 rather than by amyloidosis [21,22]. Further support for the relation between BRI2 and memory functioning comes from the recently characterized double BRI2/Tau transgenic mice in which synaptic loss was suggested to be partially caused by the accumulation of wild-type BRI2[33]. Thus, in our study the increased BRI2 deposition in early Braak stages may represent a change in BRI2 functionality, possibly leading to the memory decline observed in early stages of AD (i.e. mild cognitive impairment). In addition, the relation of BRI2 deposition with amyloid (Thal) staging shows that BRI2 deposition coincides and correlates with amyloid plaque formation in the hippocampus indicating a close relationship between BRI2 and APP processing and thus also, with AD pathology. However, it remains to be elucidated why BRI2 deposition was not considerably observed in other areas in which amyloid pathology is notably present in AD.

The specific increased levels of 45 kDa BRI2 in brain homogenates of AD cases led us to hypothesize that different concentrations or activity of furin, ADAM10 or SPPL2b could account for the increase in BRI2. A tendency for a decrease in the levels of furin was observed in AD homogenates compared to controls. In parallel, ADAM10 levels were significantly decreased in AD hippocampus compared to control, which is in agreement with previous mRNA and immunoshistological studies in AD[34–36]. Another recent study did not find differences in ADAM10 protein levels between AD and controls[37]. However, the significant higher age of the cases in the control group compared to the AD group may have hampered to observe the differences in ADAM10 levels in that study[35,37]. In addition, the correlation found between the levels of ADAM10 and BRI2 supports an involvement of BRI2 in early stages of AD since ADAM10 alterations have been found in platelets of patients in the earliest clinically detectable stages of AD[38]. Strikingly, the levels of SPPL2b were remarkably increased in AD patients. SPPL2b is a presenilin homologue which also processes tumor necrosis factor α (TNFα) and thus SPPL2b has a critical role regulating the

innate and adaptive immunity[39] which is an important feature of AD pathology. Therefore, the understanding of the SPPL2b increase in AD is an interesting topic that needs to be further investigated. In summary, we suggest that the observed modified levels of furin, ADAM10 and SPPL2b in AD may lead to an aberrant processing of BRI2, which would promote its deposition.

Several studies have previously reported that BRI2 is able to bind APP *in vitro* and in mice[12–15,40]. Moreover, this interaction seems to be crucial in the development of dementia since synaptic and memory dysfunction in mice that express reduced levels of endogenous BRI2 (FBD_{KI} and FDD_{KI} mice) was prevented by blocking β-secretase activity or by halving APP expression[17,18,40]. However, to the best of our knowledge BRI2-APP complexes have not been previously investigated in human tissue. The analysis of APP in immunoprecipitated-BRI2 protein from human hippocampus revealed that BRI2 was bound to APP in control cases. Interestingly, BRI2-APP complexes were not observed or considerably reduced in the AD patients analyzed (with the exception of AD4 that also had very low 45 kDa BRI2 levels). These data suggest that in AD, BRI2 does not bind to APP, which would prevent the regulatory function of BRI2 on APP processing and may hence the development of dementia.

The BRI2 increase and deposition in AD patients observed in this study was unexpected since BRI2 has positive anti-amyloidogenic effects[7,11–13] and its overexpression can halt AD pathology[14,20,41]. Moreover, BRI2 is an important protein preserving memory and cognition [21,22]. Thus, the increased of the 45 kDa BRI2 form in AD likely reflect changes in the BRI2 protein, which may affect its positive functioning. Fig. 8 represents a hypothetical model of the causes and consequences of increased levels of the 45 kDa BRI2 form in AD. In this model, the decreased levels of furin and ADAM10 together with the increased levels of SPPL2b would prevent the shedding of BRI2 in different peptides leading to the secretion of the whole BRI2 ectodomain, which is able to aggregate and thus, it may promote BRI2 deposition. Based on our results, we hypothesize that BRI2 deposition may prevent its binding to APP as shown by our immunoprecipitation experiments, thereby enhancing APP processing into amyloidogenic peptides. Moreover, the accumulation of the BRI2 containing the BRICHOS domain may lead also to a loss of its inhibitory function in Aβ aggregation and fibrillation. Additionally, the non-amyloidogenic pathway of APP processing might be also hampered in AD due to the decreased expression of ADAM10 via its direct effects on APP since ADAM10 is the major α-secretase involved in the non-amyloidogenic APP shedding[42,43]. Alterations in both pathways could increase the production and aggregation of $A\beta_{42,}$ ultimately resulting in amyloid plaque formation[7,10,43].

In conclusion, the novel results outlined in this study reveal an important relationship between BRI2 and AD. Our findings show that BRI2 is already increased in early stages, suggesting an involvement of BRI2 in AD pathogenesis. The modified levels of furin,

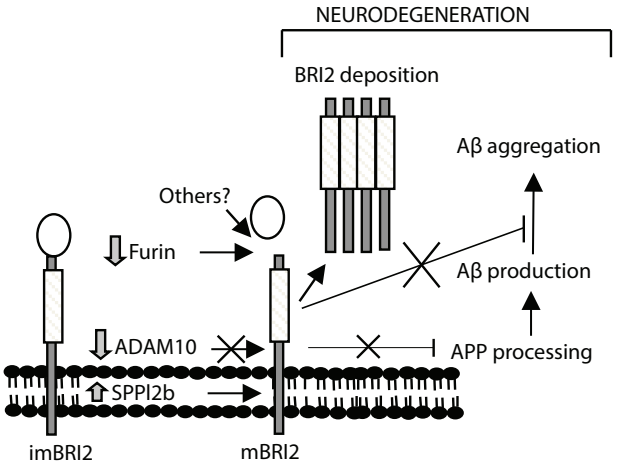

Fig. 8. Hypothetical model illustrating the possible causes and consequences of BRI2 deposition.
The reduce cleavage of BRI2 by furin and ADAM10 together with the increase of the BRI2 processing by SPPL2b leads to the release of the whole BRI2 ectodomain. BRI2 ectodomain has high aggregation propensities and thus, its release may lead to the observed accumulation and deposition of BRI2. BRI2 aggregation would lead to a loss of BRI2 function preventing the formation of BRI2-APP complexes and the subsequent inhibition of Aβ production and aggregation.

ADAM10 and SPPL2b likely lead to an alternative cleavage of BRI2 promoting its deposition and the subsequent loss of BRI2 function. The further understanding of the role of BRI2 in AD pathology may open new insights in the development of new preventive and disease-modifying therapies targeted to harness the normal processing of BRI2 and its positive effects in APP processing and Aβ aggregation.

Acknowledgment

We acknowledge the technical assistance of Elise S. van Haastert in the Neuropathology Laboratory at VU medical center, the Netherlands Brain Bank for providing human brain tissue, Dr. Jenny Presto and Janne Johansson (Sweden) for antibody donation and Dr. Paula Agostinho and Dr. Rodrigo A. Cunha from the Center for Neuroscience and Cell Biology (CNC, Portugal) for their counsel in the immunoprecipitation experiments.

Funding

This work was supported by the Erasmus Mundus Joint Doctorate Program (EMJD 2009-2013, Action 1B, Grant 159302-1-2009-1-NL-ERA, European Neuroscience Campus Network). We also acknowledge the grant from the German scientific network for dementia research (BMBF 01GI1010C) to C. K.

Disclosure statement

None of the authors with exception of Dr. Scheltens have any competing interest. Dr Scheltens serves/has served on the advisory boards of: Genentech, Novartis, Pfizer, Roche, Danone, Nutricia, Jansen AI, Baxter and Lundbeck. He has been a speaker at symposia organised by Lundbeck, Lilly, Merz, Pfizer, Jansen AI, Danone, Novartis, Roche and Genentech. He serves on the editorial board of Alzheimer's Research & Therapy and Alzheimer's Disease and Associated Disorders, is a member of the scientific advisory board of the EU Joint Programming Initiative and the French National Plan Alzheimer. The Alzheimer Center receives unrestricted funding from various sources through the VUmc Fonds. Dr Scheltens receives no personal compensation for the activities mentioned above.

Supplementary data

Materials and Methods

Post-mortem brain tissue

Clinical diagnosis was defined according to DSM-III-R criteria and the severity of dementia prior to death had been evaluated with the Global Deterioration Scale of Reisberg[44]. Neuropathological evaluation was performed on formalin-fixed, paraffin-embedded tissue from different brain areas. The distribution and the density of neurofibrillary tangles (NFTs) were determined using Bodian staining and immunohistochemistry for hyperphosphorylated tau. Senile plaques were stained with the methenamine silver method[45]. Staging of Alzheimer's disease was evaluated according to the Braak criteria for NFTs[30,31] and according to Thal criteria for amyloid deposition [24].
Frozen brain hippocampus tissue blocks were present from 31 of these cases. The tissue was homogenized with Mammalian Protein Extraction Reagent (M-PER, 0.1g/ml, Thermo Scientific, Waltham, USA) containing EDTA-free Protease Inhibitor Cocktail (1:25, Roche, Basel, Germany). Human hippocampus homogenates (HHH) were centrifuged at 10,500g for 30 min at 4°C. The protein content in the supernatant was quantified using bovine serum albumin (BSA) standards (Thermo Scientific, Waltham, USA) and the Bio-Rad Protein Assay (Bio-Rad, Hercules, USA). Samples were stored at -80ºC until further analysis.

Antibody purification and characterization.

Polyclonal and monoclonal antibodies against human BRI2 were raised by immunizing rabbits and mice with Limulus Polyphemus Hemocyanin (LPH) - conjugated synthetic peptides corresponding to the human BRI amino acids 140–153 (BioGenes GmbH, Berlin, Germany) which resides in the BRI2 BRICHOS domain (Fig. 1*A*). Antibodies were purified using HiTrap™ Protein A or Protein G HP Columns (GE Healthcare, Amersham, UK) on GE Pharmacia ÄKTA™ Purifier (GE Healthcare, Amersham, UK). Affinity purification of polyclonal antibody BRI2140-153 was performed using antigen-peptide-conjugated sepharose columns (BioGenes GmbH, Berlin, Germany). A monoclonal antibody (anti-$BRI2_{111-153,}$ IgM) was produced by immunizing mice with recombinant human BRI protein (76-266) expressed and purified from E. coli as described[46]. Monoclonal antibody was purified using HiTrap™ IgM HP Columns (GE Healthcare, Amersham, UK). Goat polyclonal antibody against $BRI2_{113-231}$ was a generous gift from Dr. Jenny Presto and Dr. Janne Johansson (Karolinska instituted, Stockholm, Sweden).

Antibody specificity on Western blot of the five different purified antibodies (Polyclonal protein A-purified anti-$BRI2_{140-153}$, Polyclonal affinity-purified anti-$BRI2_{140-153}$, Monoclonal Protein G-purified anti-$BRI2_{140-153,}$ Polyclonal protein G-purified anti-$BRI2_{113-231}$ and Monoclonal IgM-purified anti-$BRI2_{111-153}$) was analyzed through reactivity comparison towards BRI2 in HHH and recombinant BRI_{76-266}. Specificity was further tested by comparison with antibodies that were pre-absorbed with recombinant human $BRI2_{140-153}$ or $BRI2_{76-226}$ (1:10 w/w, 8 hours).

Western blotting

Human hippocampus homogenates (12 µg) or BRI_{76-266} recombinant protein (2 µg) were prepared in sample buffer (2% SDS, 0.03 M Tris, 5% 2-Mercaptoethanol, 10% glycerol, bromophenol blue) and heated 5 min at 95ºC. Electrophoresis of HHH was carried out using pre-cast NuPAGE Bis-Tris Mini Gels 4-12% (1 mm, 4-12%; Invitrogen, Carlsbad, USA) or 10% SDS-PAGE mini gels. Next, proteins were transferred to polyvinylidene fluoride membranes (PVDF; Millipore, Bedford, USA) that were subsequently blocked for 30 minutes with blocking buffer (5% (w/v) non fat dried milk in PBS-Tween 0.5% (v/v) (PBS-T)), and incubated with the corresponding primary antibody in blocking buffer overnight. After washing with washing buffer (0.05% (w/v) Milk in PBS-T), membranes were incubated during 1 hour with polyclonal swine anti-rabbit IgG/HRP (1:3000, DAKO, Glostrup, Denmark) or goat anti-mouse IgG/HRP (1:1000, DAKO, Glostrup, Denmark) in blocking buffer. Protein bands were detected with ECL™ Western Blotting detection kit (GE Healthcare, Amersham, UK). Samples were always randomly distributed within the gels and researcher was unaware to the diagnosis and specifics of the samples. Immunoblot films were scanned and signal quantification was performed using ImageJ 1.45 (NIH, Bethesda, USA). Signal intensity was normalized by the actin signal intensity.

Immunohistochemistry.

For all stainings, sections were deparaffinized and subsequently immersed in 0.3% H_2O_2 in methanol for 30 minutes to quench endogenous peroxidase activity. Sections were boiled in a microwave in 10 mmol/L pH 6.0 sodium citrate buffer during 10 minutes for antigen retrieval and incubated 10 minutes with normal swine serum (1:10; DAKO, Glostrup, Denmark). Phosphate-buffered saline (PBS) containing 1% (w/v) bovine serum albumin (Boehringer Mannheim, Germany) was used as diluent for normal swine serum and antibodies. Sections were incubated with protein A-purified rabbit anti-$BRI2_{140-153}$ (9.2 µg/ml) overnight at 4°C. After washing with PBS, sections were incubated with biotin-conjugated swine anti-rabbit F(ab)2 (1:300, DAKO, Glostrup, Denmark). Next, sections were incubated with streptavidin-biotin horseradish peroxidase complex (strept

ABComplex/HRP, 1:100; DAKO, Glostrup, Denmark) for 60 minutes. Sections were then stabilized for 5 minutes with Tris-HCl buffer (0.2 M pH 8.5). Color was developed using Liquid Permanent Red (LPR, 17 minutes, DAKO, Glostrup, Denmark) as chromogen. Nuclei were stained with hematoxylin and sections were mounted using Aquamount (BDH Laboratories Supplies, Dorset, UK). Antibody specificity was evaluated by comparing immunohistochemistry patterns using all except the polyclonal affinity-purified anti-$BRI2_{140-153}$. Antibody pre-absorption with the antigenic peptide was also performed for the polyclonal protein A-purified anti-$BRI2_{140-153}$ antibody. Negative controls for all single and double immunostainings were generated by omission of primary antibodies.

Double immunohistochemistry: BRI2 with Aβ

To determine co-localization of BRI2 with amyloid plaques, sections were incubated with rabbit protein A-purified anti-$BRI2_{140-153}$ (9.2 µg/ml) simultaneously with mouse anti-$A\beta_{1-17}$ (2.57 µg/ml; VUmc [23]) overnight at 4°C. After washing with PBS, sections were incubated with biotin-conjugated swine anti rabbit-F(ab)2 (1:300 dilution) together with EnVision solution (goat anti-mouse HRP, undiluted; DAKO, Glostrup, Denmark) during 60 minutes for the detection of primary antibodies. Further processing was performed as described above. Reactivity against $A\beta_{1-17}$ was developed using 3,3-diaminobenzidine (DAB, 0.1 mg/ml, 0.02% H_2O_2, 2 minutes; Sigma, St. Louis, MO) as chromogen. Sections were then intensively washed with MilliQ water and Tris-HCl buffer (0.2 M pH 8.5) during 5 minutes, before visualization of BRI2 using liquid permanent red.

Supplementary table and figures

Supplementary Table 1. Demographic data of patients used in this study.

Patient number	Clinical diagnosis	Pathological diagnosis	Gender	Age	PMI(h)	Grade (Braak, NFT)	Grade (Thal, Aβ)
1	Control	Control	M	56	5.50	0	0
2	Control	Control	M	80	10.00	0	0
3	Control	Control	M	56	5.50	0	4
4	Control	Control	M	66	9.15	0	1
5	Control	Control	M	96	6.30	I	0
6	Control	Control	F	84	6.55	I	0
7	Control	Control	F	94	6.25	I	0
8	Control	Control	F	77	2.55	I	1
9	Control	Control	F	73	7.45	I	3
10	Control	Control	M	81	5.30	II	0
11	Control	Control	F	93	7.15	II	0
12	Control	Control	M	88	4.43	II	1
13	Control	Control	M	71	8.55	II	3
14	Control	Control	F	89	6.05	II	3
15	Control	Control	F	89	3.52	III	0
16	Control	Control	M	88	7.00	III	1
17	Control	Control	M	74	5.00	III	3
18	Control	Uncertain	F	86	6.25	III	1
19	AD	Uncertain	F	83	4.05	III	2
20	AD	Uncertain	M	82	5.20	III	0
21	AD	AD	F	86	7.45	IV	4
22	AD	AD	F	93	2.30	IV	ND
23	AD	AD	M	93	5.50	IV	4
24	AD	AD	M	61	5.55	V	4
25	AD	AD	F	81	ND	V	4
26	AD	AD	F	78	4.50	V	4
27	AD	AD	M	93	4.30	V	4
28	AD	AD	M	74	5.35	VI	4
29	AD	AD	F	72	5.55	VI	4
30	AD	AD	F	68	3.50	VI	4
31	AD	AD	F	67	5.50	VI	4
32	AD	AD	F	91	5.45	VI	ND
33	VD	AD	F	92	4.00	IV	4
34	VD	AD	F	91	4.15	IV	4
35	VD	AD	F	78	4.35	V	4

Braak and Thal stages were established as described in the Materials and Methods section. Abbreviations: AD = Alzheimer's disease; F = Female; M = Male; PMI = Post-mortem interval (h = hours); VD = Vascular dementia; ND = Not determined; NA = Not applicable.

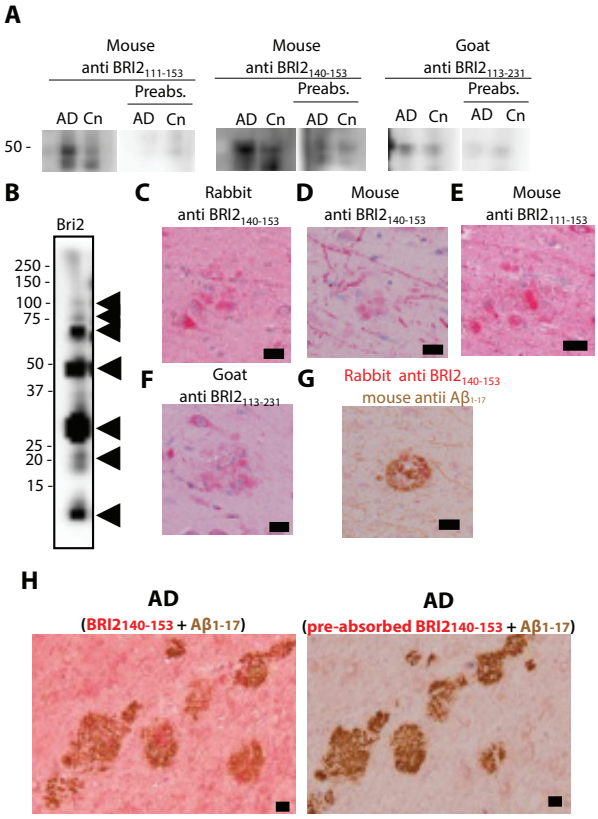

Supplementary Fig. 1. Antibodies raised against human BRI2 show that the observed 45 kDa band in Western blot and the BRI2 deposition in immunohistochemistry are specific.

A, The 45 kDa BRI2 band observed by western blot with the polyclonal anti $BRI2_{140\text{-}153}$ was specific for BRI2 as several antibodies raised against the BRICHOS domain (monoclonal protein G-purified anti-$BRI2_{111\text{-}153}$, monoclonal protein G-purified $BRI2_{140\text{-}153}$ and polyclonal protein G-purified $BRI2_{113\text{-}231}$) show a similar reactivity for Alzheimer's disease and controls (Cn) human hippocampus homogenates, and the signal disappeared after pre-absorbing each antibody (Preabs.) with $BRI2_{76\text{-}266}$ (for anti-$BRI2_{111\text{-}153}$ and $BRI2_{113\text{-}231}$) or $BRI2_{140\text{-}153}$ (for monoclonal anti-$BRI2_{140\text{-}153}$). ***B,*** Several bands at different molecular weights were observed when recombinant $BRI2_{76\text{-}266}$ (Bri2) was analyzed using protein G-purified goat anti $BRI2_{113\text{-}231}$ indicating that $BRI2_{76\text{-}266}$ can form aggregates of various sizes. ***C-F,*** A similar BRI2 deposition pattern in Alzheimer's disease was observed for all antibodies. ***C)*** polyclonal protein A-purified $BRI2_{140\text{-}153}$, ***D)*** monoclonal protein G-purified $BRI2_{140\text{-}153}$, ***E)*** monoclonal protein G-purified anti-$BRI2_{111\text{-}153}$ and ***F)*** polyclonal goat protein G-purified $BRI2_{113\text{-}231}$. ***G,*** An additional double staining using polyclonal protein A-purified $BRI2_{140\text{-}153}$ and mouse monoclonal $A\beta_{1\text{-}17}$ is shown to observe the association with an amyloid plaque. ***H,*** Pre-absorption of Protein A-purified $BRI2_{140\text{-}153}$ with its antigenic peptide completely abrogates the BRI2 reactivity observed by double immunohistochemistry analysis with monoclonal $A\beta_{1\text{-}17}$ in Alzheimer's hippocampus tissue.

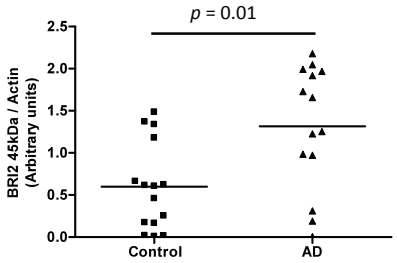

Supplementary Fig. 2. BRI2 is increased in human brain homogenates of Alzheimer's disease patients compared to controls.
BRI2 reactivity against human brain homogenates from control (n = 14) and Alzheimer's disease patients (n = 15) was measured and corrected for actin levels. Data were compared based on clinical diagnosis.

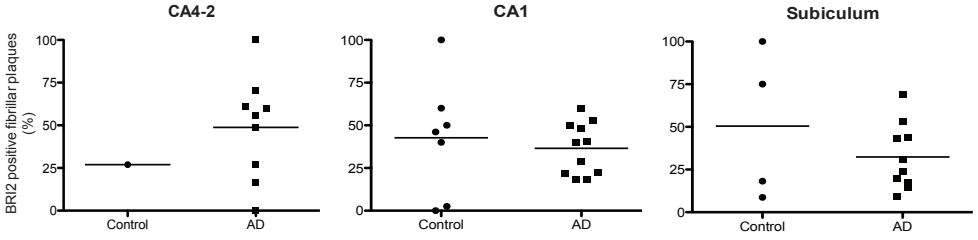

Supplementary Fig. 3. Approximately 50% of Aβ plaques are associated with BRI2 in human hippocampus. ***A***, The total amount of Aβ plaques was counted and the percentage of individual Aβ plaques which were BRI2 positive was calculated in CA4-2, CA1 and Subiculum in Alzheimer's disease and control human hippocampus sections. Approximately 50% of Aβ plaques are BRI2 positive. Only cases with Aβ plaques were analyzed, including control cases that developed a low number of Aβ plaques.

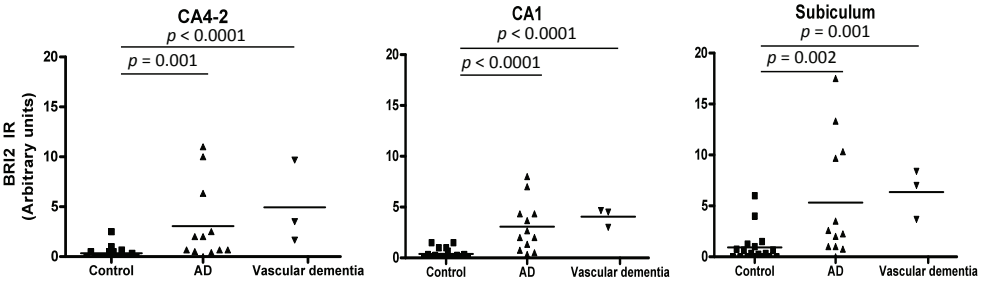

Supplementary Fig. 4. BRI2 deposition is significantly higher in Alzheimer's disease cases.
BRI2 immunoreactivity (IR) was quantified for each patient in each hippocampus area and levels were compared with clinical diagnosis as outcome measure. Alzheimer's disease patients (n = 12) showed higher BRI2 deposition compared to control cases (n = 18) in all analyzed areas.

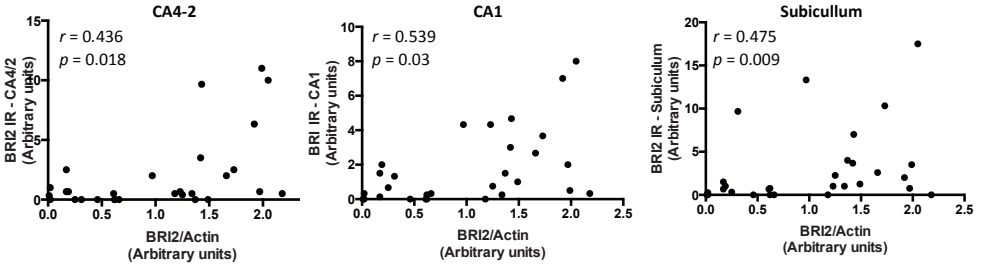

Supplementary Fig. 5. BRI2 45kDa increased correlates with the BRI2 deposition observed in all areas of human Alzheimer's disease hippocampus.

BRI2 immunoreactivity (IR) was quantified in each hippocampus area and correlated to the levels of BRI2 45 kDa for each patient (n = 29). There was a significant correlation between the levels of 45 kDa BRI2 band in Western blot and the immunohistochemistry results in every hippocampal area.

References

1. Vidal, R. *et al.* A stop-codon mutation in the BRI gene associated with familial British dementia. *Nature* **399,** 776–81 (1999).

2. Vidal, R. *et al.* A decamer duplication in the 3' region of the BRI gene originates an amyloid peptide that is associated with dementia in a Danish kindred. *Proc Natl Acad Sci U S A* **97,** 4920–5 (2000).

3. Rostagno, A. *et al.* Chromosome 13 dementias. *Cell Mol Life Sci* **62,** 1814–25 (2005).

4. Garringer, H. J., Murrell, J., D'Adamio, L., Ghetti, B. & Vidal, R. Modeling familial British and Danish dementia. *Brain Struct Funct* **214,** 235–44 (2010).

5. Tsachaki, M., Ghiso, J. & Efthimiopoulos, S. BRI2 as a central protein involved in neurodegeneration. *Biotechnol J* **3,** 1548–54 (2008).

6. Kim, S. H. *et al.* Furin mediates enhanced production of fibrillogenic ABri peptides in familial British dementia. *Nat Neurosci* **2,** 984–8 (1999).

7. Peng, S., Fitzen, M., Jörnvall, H. & Johansson, J. The extracellular domain of Bri2 (ITM2B) binds the ABri peptide (1-23) and amyloid beta-peptide (Abeta1-40): Implications for Bri2 effects on processing of amyloid precursor protein and Abeta aggregation. *Biochem Biophys Res Commun* **393,** 356–61 (2010).

8. Willander, H., Hermansson, E., Johansson, J. & Presto, J. BRICHOS domain associated with lung fibrosis, dementia and cancer--a chaperone that prevents amyloid fibril formation? *FEBS J* **278,** 3893–904 (2011).

9. Martin, L. *et al.* Regulated intramembrane proteolysis of Bri2 (Itm2b) by ADAM10 and SPPL2a/SPPL2b. *J Biol Chem* **283,** 1644–52 (2008).

10. Kim, J. *et al.* BRI2 (ITM2b) inhibits Abeta deposition in vivo. *J Neurosci* **28,** 6030–6 (2008).

11. Willander, H. *et al.* BRICHOS Domains Efficiently Delay Fibrillation of Amyloid β-Peptide. *J Biol Chem* **287,** 31608–17 (2012).

12. Fotinopoulou, A. *et al.* BRI2 interacts with amyloid precursor protein (APP) and regulates amyloid beta (Abeta) production. *J Biol Chem* **280,** 30768–72 (2005).

13. Matsuda, S. *et al.* The familial dementia BRI2 gene binds the Alzheimer gene amyloid-beta precursor protein and inhibits amyloid-beta production. *J Biol Chem* **280,** 28912–6 (2005).

14. Matsuda, S., Giliberto, L., Matsuda, Y., McGowan, E. M. & D'Adamio, L. BRI2 inhibits amyloid beta-peptide precursor protein processing by interfering with the docking of secretases to the substrate. *J Neurosci* **28,** 8668–76 (2008).

15. Matsuda, S., Matsuda, Y., Snapp, E. L. & D'Adamio, L. Maturation of BRI2 generates a specific inhibitor that reduces APP processing at the plasma membrane and in endocytic vesicles. *Neurobiol Aging* **32,** 1400–8 (2009).

16. Matsuda, S., Tamayev, R. & D'Adamio, L. Increased AβPP Processing in Familial Danish Dementia Patients. *J Alzheimers Dis* **27,** 385–91 (2011).

17. Tamayev, R., Matsuda, S., Giliberto, L., Arancio, O. & D'Adamio, L. APP heterozygosity averts memory deficit in knockin mice expressing the Danish dementia BRI2 mutant. *EMBO J* **30,** 2501–9 (2011).

18. Tamayev, R. & D'Adamio, L. Memory deficits of British Dementia knock-in mice are prevented by APP haploinsufficiency. *J Neurosci* **32,** 5481–5485 (2012).

19. Tsachaki, M. *et al.* BRI2 interacts with BACE1 and regulates its cellular levels by promoting its degradation and reducing its mRNA levels. *Curr Alzheimer Res* **10,** 532–41 (2013).

20. Kilger, E. *et al.* BRI2 regulates {beta}-amyloid degradation by increasing levels of secreted insulin degrading enzyme (IDE). *J Biol Chem* **286,** 37446–37457 (2011).

21. Tamayev, R., Matsuda, S., Fà, M., Arancio, O. & Adamio, L. D. Danish dementia mice suggest that loss of function and not the amyloid cascade causes synaptic plasticity and memory deficits. *PNAS* **107,** 20822–27 (2010).

22. Tamayev, R. *et al.* Memory Deficits Due to Familial British Dementia BRI2 Mutation Are Caused by Loss of BRI2 Function Rather than Amyloidosis. *J Neurosci* **30,** 14915–14924 (2010).

23. Verwey, N. A. *et al.* Immunohistochemical characterization of novel monoclonal antibodies against the N-terminus of amyloid β-peptide. *Amyloid* **20,** 179–87 (2013).

24. Thal, D. R., Capetillo-Zarate, E., Del Tredici, K. & Braak, H. The development of amyloid beta protein deposits in the aged brain. *Sci Aging Knowledge Environ* **6,** 1–9 (2006).

25. Martin, L., Fluhrer, R. & Haass, C. Substrate requirements for SPPL2b-dependent regulated intramembrane proteolysis. *J Biol Chem* **284,** 5662–70 (2009).

26. Tsachaki, M., Ghiso, J., Rostagno, A. & Efthimiopoulos, S. BRI2 homodimerizes with the involvement of intermolecular disulfide bonds. *Neurobiol Aging* **31,** 88–98 (2010).

27. Tsachaki, M. *et al.* Glycosylation of BRI2 on asparagine 170 is involved in its trafficking to the cell surface but not in its processing by furin or ADAM10. *Glycobiology* **21,** 1382–8 (2011).

28. Akiyama, H. *et al.* Expression of BRI, the normal precursor of the amyloid protein of familial British dementia, in human brain. *Acta Neuropathol* **107,** 53–8 (2004).

29. Lashley, T. *et al.* Expression of BRI2 mRNA and protein in normal h1. Lashley T, Revesz T, Plant G, Bandopadhyay R, Lees A, et al. (2008) Expression of BRI2 mRNA and protein in normal human brain and familial British dementia: its relevance to the pathogenesis of disease. Ne. *Neuropathol Appl Neurobiol* **34,** 492–505 (2008).

30. Braak, H. & Braak, E. Neuropathological stageing of Alzheimer-related changes. *Acta Neuropathol* **82,** 239–59 (1991).

31. Braak, H., Alafuzoff, I., Arzberger, T., Kretzschmar, H. & Del Tredici, K. Staging of Alzheimer disease-associated neurofibrillary pathology using paraffin sections and immunocytochemistry. *Acta Neuropathol* **112,** 389–404 (2006).

32. Nelson, P. T. *et al.* Clinicopathologic correlations in a large Alzheimer disease center autopsy cohort: neuritic plaques and neurofibrillary tangles "do count" when staging disease severity. *J Neuropathol Exp Neurol* **66,** 1136–46 (2007).

33. Garringer, H. J. *et al.* Increased tau phosphorylation and tau truncation, and decreased synaptophysin levels in mutant BRI2/tau transgenic mice. *PLoS One* **8,** e56426 (2013).

34. Marcinkiewicz, M. & Seidah, N. G. Coordinated expression of beta-amyloid precursor protein and the putative ß-secretase BACE and alpha-secretase ADAM10 in mouse and human brain. *J Neurochem* **75,** 2133–2143 (2000).

35. Bernstein, H.-G. *et al.* Comparative localization of ADAMs 10 and 15 in human cerebral cortex normal aging, Alzheimer disease and Down syndrome. *J Neurocytol* **32,** 153–60 (2003).

36. Bernstein, H.-G. *et al.* Reduced neuronal co-localisation of nardilysin and the putative alpha-secretases ADAM10 and ADAM17 in Alzheimer's disease and Down syndrome brains. *Age (Dordr)* **31,** 11–25 (2009).

37. Bekris, L. M. *et al.* ADAM10 expression and promoter haplotype in Alzheimer's disease. *Neurobiol Aging* **33,** 2229.e1–2229.e9 (2012).

38. Colciaghi, F. *et al.* Platelet APP, ADAM 10 and BACE alterations in the early stages of Alzheimer disease. *Neurology* **62,** 498–501 (2004).

39. Friedmann, E. *et al.* SPPL2a and SPPL2b promote intramembrane proteolysis of TNFalpha in activated dendritic cells to trigger IL-12 production. *Nat Cell Biol* **8,** 843–8 (2006).

40. Tamayev, R., Matsuda, S., Arancio, O. & D'Adamio, L. β- but not γ-secretase proteolysis of APP causes synaptic and memory deficits in a mouse model of dementia. *EMBO Mol Med* **4,** 171–9 (2012).

41. Kim, S. H. *et al.* Familial British dementia: expression and metabolism of BRI. *Ann N Y Acad Sci* **920,** 93–9 (2000).

42. Endres, K. & Fahrenholz, F. Regulation of alpha-secretase ADAM10 expression and activity. *Exp Brain Res* **217,** 343–52 (2012).

43. Kuhn, P.-H. *et al.* ADAM10 is the physiologically relevant, constitutive alpha-secretase of the amyloid precursor protein in primary neurons. *EMBO J* **29,** 3020–32 (2010).

44. Reisberg, B., Ferris, S. ., De Leon, M. ., Ed, D. & Crook, T. The Global Deterioration Scale for Assessment of Primary degenerative Dementia. *Am J Psychiatry* **139,** 1136–39 (1982).

45. Yamaguchi, H., Haga, C., Hirai, S., Nakazato, Y. & Kosaka, K. Distinctive, rapid, and easy labeling of diffuse plaques in the Alzheimer brains by a new methenamine silver stain. *Acta Neuropathol* **79,** 569–72 (1990).

46. Korth, C. *et al.* Prion (PrPSc)-specific epitope defined by a monoclonal antibody. *Nature* **390,** 74–7 (1997).

Chapter 4

Accumulation of BRI2-BRICHOS ectodomain correlates with a decreased clearance of Aβ by insulin degrading enzyme (IDE) in Alzheimer's disease.

Neurosci Lett. 2015 Jan 15; 589C:47-51.

Marta Del Campo
Anita Stargardt
Rob Veerhuis
Eric Reits
Charlotte E. Teunissen

Abstract

The precursor protein BRI2 that in its mutated form is associated with British and Danish dementia, can regulate critical processes involved in AD pathogenesis including not only the metabolism of amyloid precursor protein (APP) and formation of Aβ, but also the levels of secreted insulin degrading enzyme (IDE), an enzyme involved in Aβ clearance. We recently observed increased levels of a 45 kDa BRI2 form as well as BRI2 ectodomain deposits in Aβ plaques in human AD hippocampus, which may affect BRI2 functional activity. Since BRI2 regulated the levels of secreted IDE and subsequent degradation of Aβ in human cell culture models, we explored if BRI2 changes could affect the Aβ degradation capacity of IDE in human hippocampus (n = 28). We observed that IDE is the main enzyme involved in Aβ degradation, and both IDE levels as well as Aβ degradation tend to be decreased in AD. Interestingly, the levels of the 45 kDa BRI2 form and BRI2 deposits in hippocampal tissue were inversely correlated with IDE protein levels ($r = -0.52$, $p = 0.005$; $r = -0.4$, $p = 0.045$) and IDE activity ($r = -0.5935$, $p = 0.0004$; $r = -0.4$, $p = 0.03$). Taken together, the current results suggest a relationship between BRI2 protein changes, IDE activity and Aβ levels in human hippocampus. Thus, the formation and accumulation high molecular weight BRI2 forms observed in AD may impair IDE functioning and consequently lead to impaired Aβ clearance and to the accumulation of Aβ.

Key words: Alzheimer's disease, IDE, BRI2, pathogenesis, Aβ, hippocampus

Introduction

Mutations in BRI2 (*ITM2B*) are involved in Familial British and Danish dementias (FBD and FDD respectively) causing amyloid deposits and neurofibrillary tangles similar to those observed in Alzheimer's disease (AD)[1–4]. Interestingly, BRI2 can regulate the formation of amyloid β (Aβ) via different mechanisms including the binding to amyloid precursor protein (APP) and the subsequent down regulation of the processing of APP[5–11] or by regulating the levels of β-secretase 1[12]. BRI2 can additionally delay Aβ aggregation and fibril formation via its BRICHOS domain[13,14]. Moreover, overexpression of BRI2 was found to reduce amyloid load in AD mice models[7,15,16] likely by hampering the amyloidogenic processing of APP. Interestingly, loss of wild-type BRI2 function caused memory deficits and impaired synaptic plasticity in FBD and FDD mice models, suggesting that BRI2 plays a role in memory performance[17,18]. Taken together, the relative lack of BRI2 or reduced BRI2 functional activity could play an important role in AD (reviewed in[19]).

BRI2 is a type-II transmembrane protein of 30 kDa which is cleaved into shorter peptides by specific enzymes[20,21]. We recently found not only higher levels of a large BRI2 form (45 kDa) but also showed BRI2 deposits associated with Aβ plaques already in early stages of AD. Despite further characterization is needed, those BRI2 deposits likely represent the 45 kDa BRI2 form detected by western blot[22]. In addition, the levels of BRI2-processing enzymes were also significantly changed in post-mortem hippocampus of AD patients compared to controls. Those results led us to hypothesize that in AD there is an aberrant BRI2 processing, which enhances the release of an un-processed BRI2 ectodomain ($BRI2_{76-266}$) instead of shorter BRI2 peptides[22]. Previous analysis of recombinant BRI2 ectodomain ($rBRI2_{76–266}$) showed not only the expected band at 25 kDa but also at 50 kDa, suggesting that the 45 kDa BRI2 form observed in AD human hippocampus may represent aggregates of the un-processed BRI2 ectodomain[22,23]. We thus proposed that the un-processed BRI2 ectodomain promotes the formation of BRI2 aggregates/deposits[23], which may reduce BRI2 functionality as judged by the decrease of BRI2-APP complexes in AD hippocampus[22].

An additional function of BRI2 is to regulate the extracellular levels of one of the critical enzymes involved in Aβ clearance, the insulin degrading enzyme (IDE)[16,24,25]. IDE is a metalloproteinase primarily found in the cytosol, although it has been also detected at the plasma membrane and in peroxisomes. Moreover, a small fraction of this enzyme (between 3 - 10%) is also secreted to the extracellular space by an unconventional pathway[26], where it can degrade extracellular Aβ[27]. Noteworthy, despite the small fraction of secreted enzyme, IDE is so far the main enzyme identified to be involved in the degradation of extracellular Aβ[27]. Since IDE degradation activity has a preference for monomeric Aβ[25], decreased activity of this enzyme would likely increase monomeric

Aβ load, thus promoting the aggregation into oligomeric forms and the subsequent formation of amyloid plaques. Importantly, BRI2 transfection led to increased levels of secreted IDE and subsequent reduction of extracellular Aβ[16]. Thus, the lack or reduced functionality of BRI2 may alter the levels of secreted IDE thereby influencing Aβ clearance. Since the accumulation of the 45 kDa form and development of BRI2 deposits in early stages of AD may reflect a reduced BRI2 function[22], this might lead to altered IDE activity and impaired degradation of extracellular Aβ. Here, we explored the potential relationship between the intensity of BRI2 aggregates and the ability of IDE to degrade Aβ in the same post-mortem hippocampus homogenates from control and AD cases.

Materials and Methods

Post-mortem brain tissue

Post-mortem brain material was obtained from the Netherlands Brain Bank, Netherlands Institute for Neuroscience (Amsterdam, The Netherlands). All donors (n = 35) or their next of kin provided written informed consent for brain autopsy and use of the tissue and clinical information for research purposes. Clinical and neuropathological evaluation, sample processing and the demographic data of patients used (clinical and pathological diagnosis, gender, age, post-mortem interval, Braak and Thal scores for NFTs and amyloid load) have been described previously[22].

Western blotting

Human hippocampus homogenates (12 µg) were prepared in sample buffer (2% SDS, 0.03 M Tris, 5% 2-Mercaptoethanol, 10% glycerol, bromophenol blue) and heated 5 min at 95ºC. Electrophoresis was carried out using pre-cast NuPAGE Bis-Tris Mini Gels 4-12% (1 mm, 4-12%; Invitrogen, Carlsbad, USA) and immunoblotting was performed as previously described[22]. The following primary antibodies were used: Rabbit polyclonal anti-IDE (1:500, N3C1, GenTex, CA, USA) and monoclonal mouse anti-Actin (clone AC-40, 1:1000, Sigma-Aldrich, Saint Louis, USA).

Aβ peptide degradation assay

The ability of IDE to degrade Aβ was screened by the fluorescence emitted upon cleavage of an unique quenched Aβ peptide ($qA\beta_{40}$) as previously described[25]. Briefly, $qA\beta_{40}$ (340 nM) was added to 10 µg protein from human hippocampus in KMH buffer (110 mM KAc, 2 mM MgAc, and 20 mM Hepes-KOH, pH 7.2) and incubated for 30 min at 4 °C. Assays were

performed in the absence and presence of the IDE protease inhibitor bacitracin (200 μM, Sigma-Aldrich). Degradation of the peptide was analyzed at 37 °C using the FLUOstar OPTIMA (BMG Labtec., Jena, Germany) in which fluorescence was measured every 2 minutes for a total of 70 minutes. IDE activity was calculated as the difference in the Aβ degradation with and without the IDE inhibitor bacitracin.

Statistical analysis

Statistical analyses were performed on SPSS version 16.0 (Chicago, USA) using non-parametric Mann-whitney test. Correlation analyses were done using non-parametric Spearman's test. Values with $p < 0.05$ were considered significant.

Results

IDE is the main peptidase degrading monomeric Aβ in human hippocampus.

The degradation of $qA\beta_{40}$ in human hippocampus homogenates was drastically reduced by the presence of bacitracin, an IDE inhibitor (Fig 1A), indicating that IDE is the main Aβ degrading enzyme in these homogenates. In addition, a tendency for reduced IDE protein levels (Fig 1B,C) as well as activity of IDE (Fig 1D) was observed in AD hippocampus compared to control cases. When IDE activity was analyzed per individual Braak stage, we observed that IDE decreased along with disease progression (Fig. 1E). The IDE activity of two cases (Braak 0 and II) was below the detection limit. When those cases are excluded from the analysis, the differences between groups become significant. A significant correlation was observed between IDE protein concentration and IDE activity (Fig 1F). These results show that the concentration of IDE as well as the activity of this Aβ-degrading enzyme can be measured in human hippocampus and tend to be decreased as the disease progressed.

IDE protein concentration as well as protein activity correlate with increased levels of larger BRI2 forms and the development of BRI2 deposits in AD.

We next explored the possible association between the changes in BRI2 and the protein levels and activity of IDE in human hippocampus. We observed an inverse correlation between IDE protein levels as well as IDE activity with the formation not only of the large 45 kDa BRI2 form ($r = -0.52$ and $r = -0.59$ respectively, Fig. 2A,B) but also with the formation of BRI2 deposits (both $r = -0.4$, Fig. 2B,C).

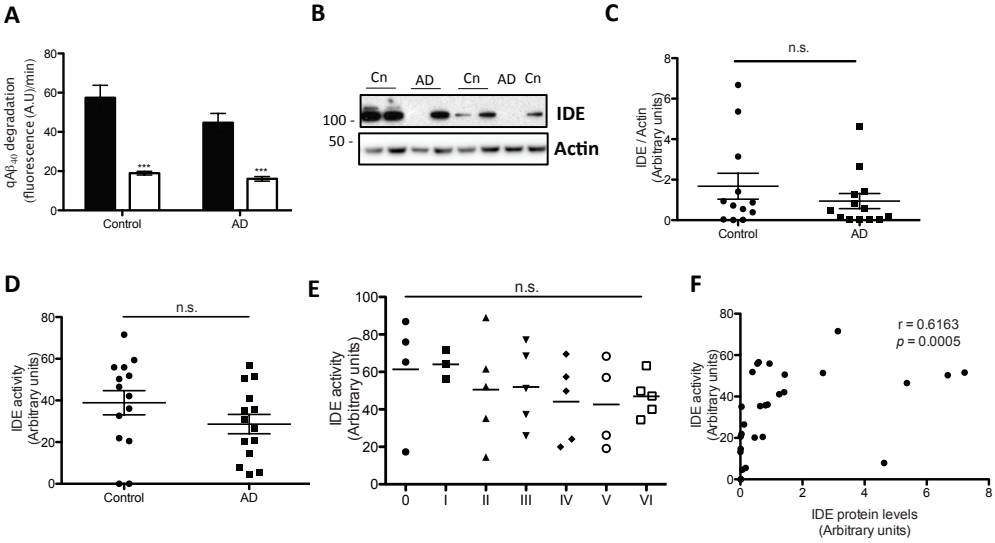

Fig 1. IDE protein concentration and activity in AD human hippocampus.

A, qAb_{40} degradation in post-mortem human hippocampal homogenates from controls and AD patients, without inhibitor (black bars), and with bacitracin (white bars), which indicates that IDE is the main peptidase degrading Ab. ***B,*** Representative western blot of IDE protein levels in hippocampus from Control (Cn) and AD cases. Actin analysis was used as a loading control. ***C,*** IDE reactivity in post-mortem human hippocampal homogenates from control (n = 14) and AD (n = 14) patients was quantified and corrected for actin levels. Data were compared based on pathological diagnosis. ***D,*** IDE reactivity in post-mortem human hippocampal homogenates from control (n = 14) and AD (n = 14) patients. ***E,*** IDE activity in post-mortem human hippocampal homogenates of cases separated by different Braak stages (from 0 to VI). ***F,*** Correlation analysis showed a significant correlation between the protein levels and activity of IDE. Error bars represent standard error of the mean. *** $p < 0.001$. n.s: non significant. Spearman's correlation coefficients and *p* values are presented in the inserts.

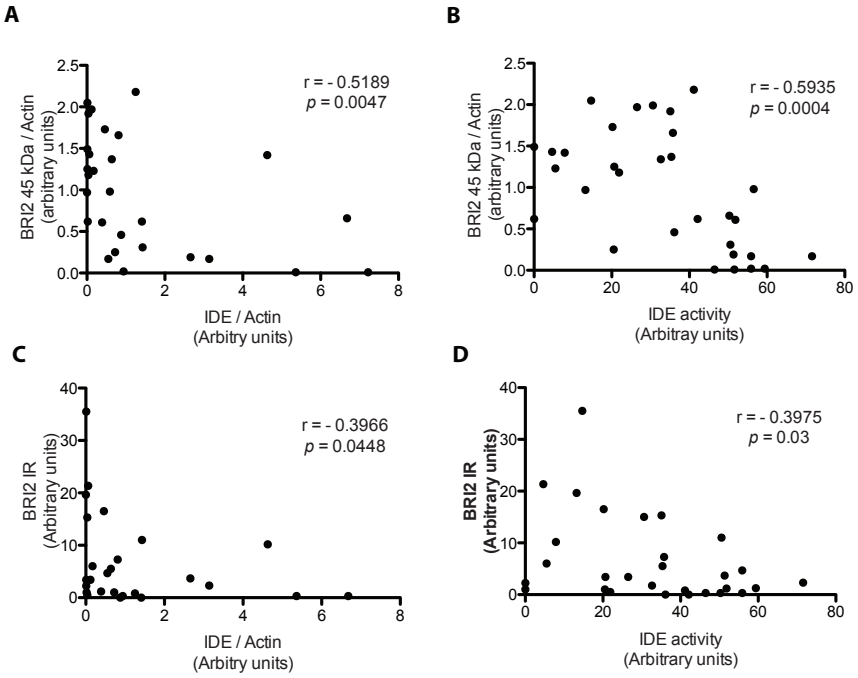

Fig 2. IDE protein concentration and activity inversely correlate with the formation of larger BRI2 form and BRI2 deposits in AD

A-D, Correlation analysis were performed between IDE protein levels (**A, C**) or activity (**B, D**) and the levels of the 45 kDa BRI2 form (**A, B**) or the formation of BRI2 deposits (BRI2 IR) **(C, D**) in post-mortem human hippocampus from control (n = 14) and AD patients (n = 14). Spearman's correlation coefficients and *p* values are presented in the inserts.

Discussion

BRI2 is a transmembrane protein that can regulate different proteins that are critically involved in the amyloid cascade hypothesis (reviewed in[19]). Indeed, BRI2 transfection in cell cultures increased the levels of secreted IDE[16], one of the main enzymes involved in Aβ clearance[24,25]. Our previous data suggested that an aberrant processing and subsequent accumulation of BRI2 could lead to a lack of BRI2 function, which may ultimately decrease the levels and activity of secreted IDE leading to a reduced clearance of Aβ in the parenchyma. In this study, we analyzed whether the changes on BRI2 as previously observed in early stages of AD[22], were related to changes in the protein levels and activity of IDE in human hippocampus.

In agreement with previous data, we confirmed that IDE is the main peptidase involved in the degradation of Aβ in human hippocampus[25]. Although a tendency for reduced protein levels and activity of IDE was observed in AD, no significant differences were

detected. These results are in line with previous data[28] but challenge one preceding study that detected a significant decrease in the activity of IDE along with AD development[25]. Importantly, the latter study, in which a considerably higher number of samples were used, focused its IDE analysis to separate Braak stages and detected a significant decrease already in Braak I and II. The usual inclusion of those Braak cases into the control group may hamper to find significant differences between control and AD patients. Indeed, in agreement with Stargardt et al.[25], we also observed a decreased IDE activity along with disease progression but the smaller sample size per Braak stage used in this analysis likely explains the lack of significant differences.

Interestingly, we observed a correlation between BRI2 changes and IDE. A previous in vitro study showed that BRI2 increased the levels of secreted IDE thereby reducing extracellular amyloid load. No changes in cytosolic IDE or other Aβ-degrading enzymes (i.e. neprilysin) were observed[16]. We previously hypothesized that the formation of BRI2 aggregates/deposits could affect the positive anti-amyloidogenic effects of BRI2[5,6,12–14], which was supported by the decreased formation of APP-BRI2 complexes observed in human AD hippocampus[22]. In the current study we additionally observed that the increased levels of the larger BRI2 45 kDa form as well as the development of BRI2 deposits inversely correlated not only with the protein levels of IDE but also with its Aβ degrading activity. It is important to note that the assays used do not differentiate between cytosolic IDE or secreted IDE. Considering that BRI2 can regulate only the levels of secreted IDE[16] we expect to detect stronger associations if the different IDE forms could be differentiated. Noteworthy, new studies in a dementia mouse model of FDD (FDD_{KI}) suggest that APP derived metabolites (such as the amino-terminal-soluble APPβ (sAPPβ) and β-carboxyl-terminal fragments (β-CTF)[29]) rather amyloid peptides, mediate synaptic failure and memory deficits[30,31]. Indeed FDD_{KI} mice, which had reduced levels of BRI2, developed cognitive deficits but not amyloidosis[18]. These data are not in line with our current results since reduced levels of BRI2 would decrease IDE function and thus increase Aβ load. Nevertheless, the study did not directly measure IDE activity or Aβ degradation and therefore, other possible compensatory mechanism may hamper Aβ increase. In addition, FDD_{KI} mouse still had one wild-type BRI2 allele, which might be sufficient to maintain homeostatic IDE and Aβ levels. It can neither be omitted that while FDD_{KI} mouse partially models FDD pathogenesis, other mechanisms might be additionally involved in AD.

Based on the current results, we suggest that the formation of BRI2 aggregates and consequent loss of BRI2 function may contribute to the reduced protein levels and activity of secreted IDE observed in AD. Reduced IDE activity likely impairs the clearance of monomeric Aβ, thereby promoting the subsequent oligomerization and extracellular accumulation of this amyloidogenic peptide[32]. Nevertheless, further in vitro and in vivo analysis are needed in order to get further insight in the underlying mechanisms

that links BRI2 aggregation, IDE activity and Aβ degradation. In conclusion, the results of this analysis further support that the BRI2 changes observed in AD may lead not only to impaired production and fibrillation of Aβ, but also affect the clearance of this amyloidogenic peptide.

Acknowledgment

This work was supported by the Erasmus Mundus Joint Doctorate Program (EMJD 2009-2013, Action 1B, Grant 159302-1-2009-1-NL-ERA, European Neuroscience Campus Network).

Disclosure statement

Dr. Teunissen serves on the advisory board of Fujirebio and Roche, received research consumables from Euroimmun, IBL, Fujirebio, Invitrogen and Mesoscale Discovery. None of the other authors has any competing interest.

Authors' contributions

MC designed the study, performed the experiments, analyzed the data and wrote the manuscript. AS performed the experiments and participate in manuscript writing, ER and RV provided material and participate in manuscript writing, CT directed the study, analyzed the data and participate in manuscript writing.

References

1. Vidal, R. *et al.* A stop-codon mutation in the BRI gene associated with familial British dementia. *Nature* **399,** 776–81 (1999).

2. Vidal, R. *et al.* A decamer duplication in the 3' region of the BRI gene originates an amyloid peptide that is associated with dementia in a Danish kindred. *Proc Natl Acad Sci U S A* **97,** 4920–5 (2000).

3. Rostagno, A. *et al.* Chromosome 13 dementias. *Cell Mol Life Sci* **62,** 1814–25 (2005).

4. Garringer, H. J., Murrell, J., D'Adamio, L., Ghetti, B. & Vidal, R. Modeling familial British and Danish dementia. *Brain Struct Funct* **214,** 235–44 (2010).

5. Fotinopoulou, A. *et al.* BRI2 interacts with amyloid precursor protein (APP) and regulates amyloid beta (Abeta) production. *J Biol Chem* **280,** 30768–72 (2005).

6. Matsuda, S. *et al.* The familial dementia BRI2 gene binds the Alzheimer gene amyloid-beta precursor protein and inhibits amyloid-beta production. *J Biol Chem* **280,** 28912–6 (2005).

7. Matsuda, S., Giliberto, L., Matsuda, Y., McGowan, E. M. & D'Adamio, L. BRI2 inhibits amyloid beta-peptide precursor protein processing by interfering with the docking of secretases to the substrate. *J Neurosci* **28,** 8668–76 (2008).

8. Matsuda, S., Matsuda, Y., Snapp, E. L. & D'Adamio, L. Maturation of BRI2 generates a specific inhibitor that reduces APP processing at the plasma membrane and in endocytic vesicles. *Neurobiol Aging* **32,** 1400–8 (2009).

9. Matsuda, S., Tamayev, R. & D'Adamio, L. Increased AβPP Processing in Familial Danish Dementia Patients. *J Alzheimers Dis* **27,** 385–91 (2011).

10. Tamayev, R., Matsuda, S., Giliberto, L., Arancio, O. & D'Adamio, L. APP heterozygosity averts memory deficit in knockin mice expressing the Danish dementia BRI2 mutant. *EMBO J* **30,** 2501–9 (2011).

11. Tamayev, R. & D'Adamio, L. Memory deficits of British Dementia knock-in mice are prevented by APP haploinsufficiency. *J Neurosci* **32,** 5481–5485 (2012).

12. Tsachaki, M. *et al.* BRI2 interacts with BACE1 and regulates its cellular levels by promoting its degradation and reducing its mRNA levels. *Curr Alzheimer Res* **10,** 532–41 (2013).

13. Willander, H. *et al.* BRICHOS Domains Efficiently Delay Fibrillation of Amyloid β-Peptide. *J Biol Chem* **287,** 31608–17 (2012).

14. Peng, S., Fitzen, M., Jörnvall, H. & Johansson, J. The extracellular domain of Bri2 (ITM2B) binds the ABri peptide (1-23) and amyloid beta-peptide (Abeta1-40): Implications for Bri2 effects on processing of amyloid precursor protein and Abeta aggregation. *Biochem Biophys Res Commun* **393,** 356–61 (2010).

15. Kim, J. *et al.* BRI2 (ITM2b) inhibits Abeta deposition in vivo. *J Neurosci* **28,** 6030–6 (2008).

16. Kilger, E. *et al.* BRI2 regulates {beta}-amyloid degradation by increasing levels of secreted insulin degrading enzyme (IDE). *J Biol Chem* **286,** 37446–37457 (2011).

17. Tamayev, R. *et al.* Memory Deficits Due to Familial British Dementia BRI2 Mutation Are Caused by Loss of BRI2 Function Rather than Amyloidosis. *J Neurosci* **30,** 14915–14924 (2010).

18. Tamayev, R., Matsuda, S., Fà, M., Arancio, O. & Adamio, L. D. Danish dementia mice suggest that loss of function and not the amyloid cascade causes synaptic plasticity and memory deficits. *PNAS* **107,** 20822–27 (2010).

19. Del Campo, M. & Teunissen, C. E. Role of BRI2 in dementia. *J Alzheimers Dis* **40,** 481–94 (2014).

20. Kim, S. H. *et al.* Furin mediates enhanced production of fibrillogenic ABri peptides in familial British dementia. *Nat Neurosci* **2,** 984–8 (1999).

21. Martin, L. *et al.* Regulated intramembrane proteolysis of Bri2 (Itm2b) by ADAM10 and SPPL2a/SPPL2b. *J Biol Chem* **283,** 1644–52 (2008).

22. Del Campo, M. *et al.* BRI2-BRICHOS is increased in human amyloid plaques in early stages of Alzheimer's disease. *Neurobiol Aging* **35,** 1596–604 (2014).

23. Del Campo, M. *et al.* BRI2 ectodomain affects Aβ42 fibrillation and tau truncation in human neuroblastoma cells. *Cell Mol Life Sci* (2014). doi:10.1007/s00018-014-1769-y

24. Miners, J. S. *et al.* Abeta-degrading enzymes in Alzheimer's disease. *Brain Pathol* **18,** 240–52 (2008).

25. Stargardt, A. *et al.* Reduced amyloid-β degradation in early Alzheimer's disease but not in the APPswePS1dE9 and 3xTg-AD mouse models. *Aging Cell* **12,** 499–507 (2013).

26. Zhao, J., Li, L. & Leissring, M. a. Insulin-degrading enzyme is exported via an unconventional protein secretion pathway. *Mol Neurodegener* **4,** 4 (2009).

27. Vekrellis, K. *et al.* Neurons Regulate Extracellular Levels of Amyloid -Protein via Proteolysis by Insulin-Degrading Enzyme. *J ne* **20,** 1657–1665 (2000).

28. Wang, S. *et al.* Expression and functional profiling of neprilysin, insulin-degrading enzyme, and endothelin-converting enzyme in prospectively studied elderly and Alzheimer's brain. *J Neurochem* **115,** 47–57 (2010).

29. Chow, V. W., Mattson, M. P., Wong, P. C. & Gleichmann, M. An Overview of APP Processing Enzymes and Products. *Neuromolecular Med* 1–12 (2009). doi:10.1007/s12017-009-8104-z

30. Tamayev, R. & D'Adamio, L. Inhibition of γ-secretase worsens memory deficits in a genetically congruous mouse model of Danish dementia. *Mol Neurodegener* **7,** 19 (2012).

31. Tamayev, R., Matsuda, S., Arancio, O. & D'Adamio, L. β- but not γ-secretase proteolysis of APP causes synaptic and memory deficits in a mouse model of dementia. *EMBO Mol Med* **4,** 171–9 (2012).

32. Mawuenyega, K. G. *et al.* Decreased Clearance of CNS Amyloid-β in Alzheimer's Disease. *Science (80-)* **330,** 1774 (2010).

Chapter 5

BRI2 ectodomain affects $A\beta_{42}$ fibrillation and tau truncation in human neuroblastoma cells.

Cell. Mol. Life Sci: 2015 Apr;72(8):1599-611.

Marta Del Campo
Catarina R. Oliveira
Wiep Scheper
Rob Zwart
Carsten Korth
Andreas Müller-Schiffmann
Geroge kostallas
Henrik Biverstal
Jenny Presto
Janne Johansson
Jeroen JM Hoozemans
Claudia F Pereira
Charlotte E. Teunissen

Abstract

Alzheimer's disease (AD) is pathologically characterized by the presence of misfolded proteins such as amyloid beta (Aβ) in senile plaques, and hyperphosphorylated tau and truncated tau in neurofibrillary tangles (NFT). The BRI2 protein inhibits Aβ aggregation via its BRICHOS domain and regulates critical proteins involved in initiating the amyloid cascade, which has been hypothesized to be central in AD pathogenesis. We recently detected the deposition of BRI2 ectodomain associated with Aβ plaques and concomitant changes in its processing enzymes in early stages of AD. Here, we aimed to investigate the effects of recombinant BRI2 ectodomain ($rBRI2_{76-266}$) on Aβ aggregation and on important molecular pathways involved in early stages of AD, including the unfolded protein response (UPR), phosphorylation and truncation of tau, as well as apoptosis. We found that $rBRI2_{76-266}$ delays Aβ fibril formation, although less efficiently than the BRI2 BRICHOS domain (BRI2 residues 113-231). In human neuroblastoma SH-SY5Y cells, $rBRI2_{76-266}$ slightly decreased cell viability and increased up to two-fold the Bax/Bcl-2 ratio and the subsequent activity of caspases 3 and 9, indicating activation of apoptosis. $rBRI2_{76-266}$ upregulated the chaperone BiP but did not modify the mRNA expression of other UPR markers (CHOP and Xbp-1). Strikingly, $rBRI2_{76-266}$ induced the activation of GSK3β but not the phosphorylation of tau. However, exposure to $rBRI2_{76-266}$ significantly induced the truncation of tau, indicating that BRI2 ectodomain can contribute to NFT formation. Since BRI2 can also regulate the metabolism of Aβ, the current data suggests that BRI2 ectodomain is a potential nexus between Aβ, tau pathology and neurodegeneration.

Key words: Alzheimer's disease, ITM2b, BRICHOS, aggregation, fibrillation, apoptosis

Introduction

Alzheimer's disease (AD), the most common form of dementia, is pathologically characterized by the accumulation and aggregation of misfolded proteins: the amyloid β peptide (Aβ) in senile plaques and hyperphosphorylated tau (p-Tau) in neurofibrillary tangles (NFTs)[1,2]. AD shares clinical and pathological similarities with familial British and Danish dementias (FBD and FDD). FBD and FDD originate from mutations in the BRI2 coding gene, causing amyloid angiopathy and NFTs similar to those observed in AD[3–6]. BRI2 is processed by different enzymes (furin[7], ADAM10 and SPPL2b[8]) leading to the secretion of peptides of different molecular weights. Although the physiological function of BRI2 remains unknown, BRI2 ectodomain contains a BRICHOS domain (BRI2-BRICHOS), which is able to delay Aβ fibrillation[9–11]. In addition, several studies have revealed that BRI2 can regulate the proteostasis of critical proteins involved in AD pathogenesis, such as the amyloid precursor protein (APP)[12–18], insulin degrading enzyme (IDE)[19] and β-secretase 1 (BACE1)[20]. BRI2 could have a key role in memory performance, since loss of wild-type BRI2 function rather than amyloidogenesis of the mutated BRI2 fragments correlated with memory deficits and impaired synaptic plasticity in FBD and FDD mice models[21,22]. Moreover, the recently characterized double-transgenic tg-FDD-tau model accumulated wild-type BRI2 and showed enhanced phosphorylation and truncation of tau before amyloid deposition[23], suggesting that BRI2 accumulation (or the subsequent loss of function) may facilitate NFT formation.

Taken together, previous studies suggest that the lack of BRI2 or reduced BRI2 functionality could play an important role in AD (reviewed in[24]). Interestingly, we recently found deposits of BRI2 ectodomain associated with Aβ plaques in early stages of AD[25]. In addition, the levels of BRI2-processing enzymes were also significantly changed in post-mortem hippocampus of AD patients compared to controls. Those results led us to hypothesize that in AD there is an aberrant BRI2 processing that promotes the secretion of the BRI2 ectodomain, leading to the formation of BRI2 aggregates, which may reduce BRI2 functionality as judged by the decrease of BRI2-APP complexes in AD hippocampus[25].

A common denominator in the pathogenesis of multiple neurodegenerative disorders is the abnormal folding, processing and/or clearance of different proteins leading to the formation of aberrant protein complexes. Those aberrant processes can influence protein activity promoting a pathological cascade via loss of physiological function, gain of toxic function or combination of both[26]. Thus, the presence of larger BRI2 forms in early stages of AD[25] besides influencing BRI2 physiological function may also have important direct effects on cell homeostasis, as shown for different protein aggregates (e.g. Aβ, α-synuclein, prion proteins)[27–32]. The presence of aggregated proteins and extracellular stimulus

can induce stress in the endoplasmic reticulum (ER) and the subsequent activation the unfolded protein response (UPR) in order to restore cell homeostasis[33,34]. When ER stress remains unmitigated, an apoptotic cell signalling cascade will be initiated, ultimately leading to cell death[33,35].

Thus, we investigated whether the BRI2 ectodomain can affect Aβ fibrillation and if exposure to recombinant BRI2 ectodomain disrupts cell homeostasis in vitro. In addition, we investigated the possible involvement of aggregated recombinant BRI2 accumulation in tau phosphorylation and truncation.

Materials and methods

Cell culture

Human neuroblastoma SH-SY5Y and SK-N-SH cells were cultured in Dulbecco's modified essential medium (DMEM)/Nutrient Mix F-12 (1:1; Gibco–BRL, Gaithersburg, MD, USA). Mouse neuroblastoma N2a cells were cultured in DMEM medium. Both mediums were supplemented with 10 IU penicillin/mL, 100 µg/mL streptomycin (Gibco–BRL), 10% fetal calf serum and 2 mM L- glutamine (Gibco–BRL). Cells were maintained at 37°C in a humidified incubator with 5% CO_2/95% air. Differentiation of SH-SY5Y and SK-N-SH cells was induced by incubation with 10 µM of retinoic acid (RA) for 5-6 days (Sigma, St Louis, MO, USA).

Expression and purification of recombinant BRI2$_{76-266}$ and BRI2 BRICHOS$_{113-231}$.

Recombinant human BRI2 ectodomain (76-266; rBRI2) was expressed and purified from E. coli as previously described[36]. A fragment corresponding to human BRI2 positions 113–231 was expressed as a soluble fusion protein together with His_6 and thioredoxin in *E. coli*. Bacteria were cultured in LB medium with 100 µg/ml ampicillin at 30 °C for 16 h, and protein expression was induced by adding 0.5 mM isopropylthiogalactoside (IPTG). After 4 h at 25 °C, cells were harvested by centrifugation, resuspended in 20 mM sodium phosphate buffer, pH 7.5 and stored at -20 °C. The cells were lysed by lysozyme (1 mg/ml) for 30 min and incubated with DNase and 2 mM $MgCl_2$ for 30 min on ice. The cell lysate was centrifuged at 6000 × g for 20 min, and the pellet was suspended in 2M urea in 20 mM sodium phosphate buffer, pH 7.5, and sonicated for 5 min. After centrifugation at 24000 × g for 30 min at 4 °C, the supernatant was filtered through a 5µm filter and loaded on a 2.5-ml nickel-agarose column (Qiagen, Ltd., West Sussex, UK). The column was washed with 50 ml of 2M urea in 20mM phosphate buffer, pH7.5, then with 50 ml of 1M urea in 20 mM sodium phosphate buffer, pH 7.5, and finally with 50 ml 20 mM sodium phosphate

buffer, 20 mM imidazole, pH 7.5. The protein was then eluted with 200 mM imidazole in 20 mM sodium phosphate buffer, pH 7.5, dialyzed against 20 mM sodium phosphate buffer, pH 7.5, cleaved by thrombin for 16 h at 4 °C (enzyme/substrate weight ratio of 0.002) to remove the thioredoxin and His_6 tag, and then reapplied to a Ni^{2+} column to remove the released tag. Concentration was determined from A_{280} using a molar extinction coefficient, $\varepsilon = 9065 \times M^{-1} \times cm^{-1}$.

$A\beta_{42}$ preparations

$A\beta_{42}$ peptide (American peptide, Sunnyvale, CA, USA) was reconstituted in MilliQ water to a final concentration of 225.5 µM. For aggregation kinetics, Met-Aβ1-42 (hereafter referred to as $A\beta_{42}$) was expressed in E. coli BL21 from synthetic genes and purified in batch format using ion exchange and size exclusion steps as previously described[37], which results in highly pure monomeric peptide. Purified peptide was aliquoted in low-bind Eppendorf tubes (Axygene) and stored at -20 °C. The peptide concentration was determined using an extinction coefficient of 1424 M^{-1} cm^{-1} for ($A_{280\text{-}300}$).

Coomassie staining

$rBRI2_{76\text{-}266}$ (1 mg) was prepared in sample buffer (100 mM Tris, 0.2% (w/v) bromophenol blue and 20% (v/v) glycerol) with or without dithiothreitol (DTT, 10mM) and/or 4% (v/v) of SDS to analyze the effects of different reducing and denaturing conditions. Samples prepared in complete buffer (+DTT/+SDS) or buffer without SDS (+DTT/-SDS) were boiled at 95ºC for 5 minutes. Proteins were separated by electrophoresis on 10% (w/v) SDS-polyacrylamide gel (SDS-PAGE) and gel was then incubated in fixing solution (50% ethanol, 10% acetic acid) during 30 minutes. For protein staining, gel was incubated during 2 hours with GelCodeÒBlue Stain Reagent (Thermo Scientific, Waltham, MA, USA). After washing with MilliQ water, gel was incubated overnight with destain solution (50% methanol, 10% acetic acid) until protein bands could be clearly detected.

Size Exclusion Chromatography

Size exclusion chromatography was performed on a Superdex200HR column (GE Healthcare) using an ÄKTA basic FPLC system (GE Healthcare). The column was equilibrated and operated in degassed buffer (20 mM sodium phosphate, pH 7.5). 70nmol recombinant $BRI2_{76\text{-}266}$ or BRI2 BRICHOS was injected from a 50µl loop and chromatograms recorded by monitoring the absorbance at 280 nm.

Aggregation kinetics

Aggregation kinetics was studied by recording the thioflavin T (ThT) fluorescence intensity as a function of time in a plate reader (FLUOStar Galaxy from BMG Labtech, Offenberg, Germany). The fluorescence was recorded using bottom optics in half-area 96-well polyethylene glycol-coated black polystyrene plates with clear bottom (Corning Glass, 3881) using a 440 nm excitation filter and a 490 nm emission filter. $A\beta_{42}$ monomer was isolated by size exclusion chromatography over a Superdex 75 column (GE Healthcare) in 20 mM sodium phosphate, 200 µM EDTA, 0.02% NaN_3 at pH 8, and kept on ice. Every sample was supplemented with 10 µM ThT from a 1 mM stock solution. To each well was added 80 µl of the ice-cold $A\beta_{42}$ solution, and the plate was immediately placed in the fluorescence reader at 37 °C, and incubated under quiescent conditions with readings made every 17 min. $A\beta_{42}$ (3 µM) was studied alone or coincubated with 0.6 µM of BRI2-BRICHOS or $BRI2_{76\text{-}266}$.

Cell viability test

The effect of $rBRI2_{76\text{-}266}$ on cell viability and on $A\beta_{42}$ induced toxicity was assessed by measuring residual cellular redox activity with 3-(4,5-dimethylthiazol-2-yl)-2,5-diphenyltetrazolium bromide (MTT; Sigma, St Louis, MO, USA) as previously described[38]. MTT assay is a sensitive and rapid indicator of amyloid toxicity[39].

Twenty-four hours after seeding (6×10^4 per well in a 48-well plate), medium was renewed by fresh medium containing $rBRI2_{76\text{-}266}$ at 0.2, 0.5 and 2 µM with or without 0.5 µM $A\beta_{42}$. After 24 h incubation, the conditioned medium was removed and cells were then incubated with 0.5 mg/ml MTT in Na-buffer (132 mM NaCl, 4 mM KCl, 1.2 mM Na_2HPO4, 1.4 mM $MgCl_2$, 6 mM glucose, 10 mM HEPES, and 1mM $CaCl_2$, pH 7.4) for 2 h at 37 °C. The blue formazan crystals formed were dissolved in an equal volume of 0.04 M HCl in isopropanol and quantified spectrophotometrically by measuring the absorbance at 570 nm using a microplater reader (SpectraMax Plus 384, Molecular Devices, California, USA). Results were normalized and expressed as the percentage of the absorbance determined in untreated cells (control) within each experiment.

Western blotting

To obtain lysates, SH-SY5Y cells (9×10^4 per well in a 24-well plate) were washed twice with PBS and scraped in ice-cold lysis buffer (25 mM HEPES, 1 mM EDTA, 1 mM EGTA, 2 mM $MgCl_2$, 100 µM PMSF, 2 mM DTT, 2mM Na_3VO_4, 50 mM NaF pH 7.5) containing 1:1000 of protein inhibitors cocktail (1 µg/ml leupeptin, pepstatin A, chymostatin and antipain). The cellular extracts immediately underwent three consecutive cycles of freezing/thawing

with liquid nitrogen. Cell lysates were then centrifuged for 10 minutes at 20,800 x g at 4°C and the supernatant was collected. Protein concentration was determined using a Bio-Rad protein assay (BIO-RAD, Hercules, California, USA). Equal amounts of protein (20 µg) were prepared in sample buffer (100 mM Tris, 100 mM DTT, 4% (v/v) SDS, 0.2% (w/v) bromophenol blue and 20% (v/v) glycerol), denatured at 95ºC for 5 minutes and proteins were separated by electrophoresis on 10% (w/v) SDS-polyacrylamide gel (SDS-PAGE). Proteins were then transferred to PVDF membranes, which were further blocked for 30 minutes at RT with 5% (w/v) BSA in Tris-buffered saline (150 mM NaCl, 50 mM Tris, pH 7.6) with 0.1% (w/v) Tween 20 (TBS-T) or Odyssey blocking buffer (LI-COR bioscience, Lincoln, Nebraska USA) for detection of tau isoforms. The membranes were next incubated overnight at 4 °C with the following primary monoclonal antibodies in TBS-T: mouse anti-GSK3β and anti-GSK-3β(pY216) (1:1,000; BD Biosciences, San José, CA, USA), anti-cleaved-Tau (Asp421) clone C3 and total TAU (Tau-5) (1:500; Life Technologies, Carlsbad, USA) or rabbit antibody anti-Bcl-2 or anti-Bax (1:1,000; Cell Signaling, Danvers, Massachusetts, USA). Control of protein loading was performed using a primary mouse anti-α-tubulin (1:20,000, Cell signaling) or anti-actin (clone AC-40, 1:1,000; Sigma-Aldrich, Saint Louis, MO, USA) antibodies. After washing, membranes were incubated for 1 hour at RT with an alkaline phosphatase (1:20,000; GE Healthcare, Amersham, UK) or biotinilyted (1:1,000 DAKO, Glostrup, Denmark) conjugated secondary anti-mouse or anti-rabbit antibody. Bands of immunoreactive proteins were visualized after incubation of the membrane with ECF™ substrate (GE Healthcare) during approximately 5 min on a Versa Doc 3000 Imaging System or after incubation with IRDye® Infrared Dye (1:15,000, LI-COR) for 45min on the LI-COR Odyssey scanner. Densitometric analysis was performed using ImageLab Software (Bio-Rad, Hercules, CA, USA) or ImageJ 1.45 (NIH, Bethesda, USA). The ratios between Bax/Bcl-2, P-GSK-3β/GSK-3β and TauC3/total tau were calculated and results were normalized to values in untreated cells.

Analysis of caspase-3 and -9 activities

In order to investigate the activation of caspases-3 and -9, cell lysates from SH-SY5Y cells treated with and without $rBRI2_{76-266}$ were prepared as described above, but in the absence of Na_3VO_4, and NaF. Cellular extracts containing 40 µg of protein were incubated with 0.1 mM Ac-DEVD-pNA (chromogenic substrate for caspase-3, Calbiochem, Darmstadt, Germany) or Ac-LEHD-pNA (chromogenic substrate for caspase-9, Calbiochem) in reaction buffer (25 mM HEPES-Na, 10% (w/v) sucrose, 10 mM DTT, and 0.1% (w/v) CHAPS, pH 7.4) for 2 h at 37 °C. Caspase activity was determined by measuring substrate cleavage at 405 nm in a microplate reader (SpectraMax Plus 384) and results were expressed relatively to the untreated cells.

RNA isolation and cDNA synthesis

For RNA isolation, SH-SY5Y cells (9×10^4 per well in a 24-well plate) were harvested and total RNA was isolated using TriPure isolation reagent (Roche Applied Science, Basel, Switzerland) following the manufacturer's specifications. RNA concentration and purity were assessed by OD measurements at 260 and 280 nm on a NanoDrop spectrophotometer (Thermo Scientific). cDNA synthesis was performed using 0.5 μg of RNA and 0.5 µg $Oligo(dT)_{12\text{-}18}$ primer (Life technologies, Carlsbad, California, U.S.) as previously described[40].

Real-time qPCR

Real-time qPCR was performed using the Light Cycler 480 system (Roche Applied Science). Oligonucleotide primers (Sigma, Saint Louis, MO, USA) used for qPCR are listed in Table 1. Eukaryotic Elongation factor (EEF), Binding immunoglobulin protein (BiP) and CCAAT-enhancer-binding protein homologous protein (CHOP) cDNA were measured using Fluorescent reporter probe method. Reaction was performed using 1 μl contained cDNA, 0.05 μl Universal Library probe (Roche Applied Science), 0.1 μl forward primer, 0.1 μl reverse primer and 2.5 μl 2 × LightCycler 480 Probes Master (Roche Applied Science). Unspliced and spliced X-box binding protein 1 (Xbp-1) cDNA were measured using SYBRGreen dsDNA dye. Reaction was performed using 1 μl cDNA, 0.25 μl forward primer, 0.25 μl reverse primer and 5μl 2 × SYBRGreen Master (Roche Applied Science). qPCR was performed as previously described[40]. Tunicamycin (0.1 µg/ml; Sigma) was used as a positive control for UPR activation. Data was analyzed using LightCycler Software (Roche).

Table 1. Primers and probes used for qPCR 480 Light Cycler

Gene	Primers (5'-3')	Probe no.
BiP	FW: GCTGGCCTAAATGTTATGAGGA	7
	RV: CCACCCAGGTCAAAC	
CHOP	FW: AAGGCACTGAGCGTATCATGT	21
	RV:TGAAGATACACTTCCTTCTTGAACA	
hEEF	FW: CAATGGCAAAATCTCACTGC	63
	RV: AACCTCATCTCTATTAAAAACACCAAA	
Xbp-1 (unspliced)	FW: GACAGAGAGCCAAGCTAATGTGG	Sybr.Green
	RV: ATCCAGTAGGCAGGAAGAT	
Xbp-1 (spliced)	FW: AAGACAGCGCTTGGGGATGG	Sybr.Green
	RV:CTGACCTGCTGCGGAC	

Probe numbers refer to numbers in the Roche universal probe library

Total tau and hyperphosphorylated tau

The concentration of total tau (t-Tau) and phosphorylated tau (p-Iau$_{181}$) in the cell lysates (2 and 20 µg respectively) was measured using INNOTEST® hTAU Ag or INNOTEST®PHOSPHO-TAU$_{(181P)}$ (Innogenetics, Gent, Belgium) ELISA Kits. Phosphorylation of tau$_{231}$ (p-Tau$_{231}$) was analyzed by Multi Array® PhosphoTau (Thr 231)/Total Tau immunosorbent assay (mesoscale discovery, MSD, Rockville, MD, USA). Assays were performed following manufacturer´s instructions. The ratio p-Tau/t-Tau was calculated and results were normalized to control values. Intra-assay coefficients of variation (CV) for t-Tau, p-Tau$_{181}$ and p-Tau$_{231}$ were 1.8%, 2.51% and 1.30% respectively.

Statistical analysis.

Data were expressed as means ± SEM of measurements from at least three independent experiments performed in duplicates or triplicates. Mean differences were analysed using non-parametric Mann–Whitney U test in GraphPad Prism Software (San Diego, CA, USA). Differences were considered significant for p values < 0.05.

Results

Characterization of recombinant BRI2 ectodomain.

Coomassie staining of rBRI2 ectodomain showed that rBRI2 ectodomain forms aggregates of different molecular weights as previously described[25] (Fig. 1*a*). Under reducing and denaturing conditions, rBRI2$_{76-266}$ was observed not only at its expected molecular weight of 25 kDa but also at 50 kDa. Larger complexes were observed under non-reducing conditions. Size exclusion chromatography showed that BRI2 BRICHOS elutes in several different fractions corresponding to complexes of different molecular weight (33, 80 336 and >600 kDa). However, rBRI2 ectodomain elutes only in one fraction at 6-8 ml, corresponding to larger complexes with a molecular mass higher than 600 kDa (Fig. 1*b*).

Recombinant BRI2 ectodomain delays $A\beta_{42}$ fibril formation less efficiently than BRI2 BRICHOS domain.

Thioflavin T (ThT) was used as a reporter for fibril formation in kinetic experiments of $A\beta_{42}$ alone or with different concentrations of the rBRI2 ectodomain and the BRI2 BRICHOS proteins. The midpoint of the aggregation process, $t_{1/2}$ were obtained by fitting a sigmoidal function to each kinetic trace and was plotted versus molar ratio of corresponding proteins/$A\beta_{42}$. The data showed that both rBRI2 ectodomain and BRI2-BRICHOS delayed

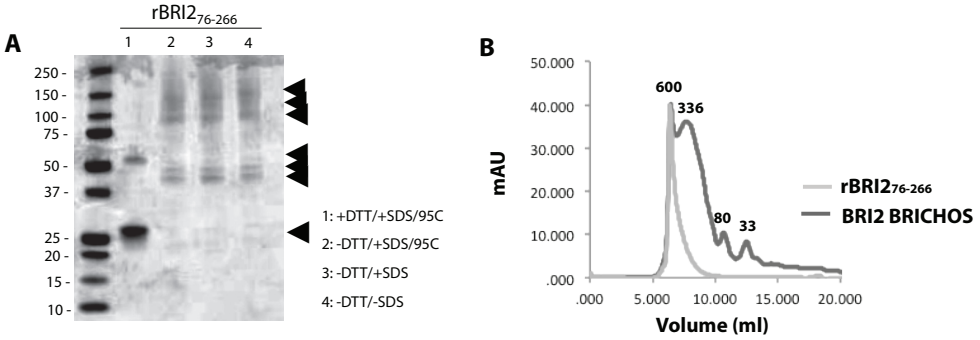

Fig. 1. Recombinant BRI2$_{76-266}$ form oligomeric aggregates of different molecular weights
a, Coomassie staining of rBRI2$_{76-266}$ in different reducing conditions showed several bands at different molecular weights. ***b,*** Gel filtration of rBRI2$_{76-266}$ and BRI2 BRICHOS shows peaks that elutes in the void volume indicating the formation of different complexes. Numbers indicate the molecular mass of the corresponding complex in kDa.

the aggregation of Aβ$_{42}$, and only substoichiometric amounts of the proteins are required (Fig. 2*a*). The half-times in the presence of BRICHOS were compared with the uninhibited case (Aβ$_{42}$ alone) (Fig. 2*b*). These experiments showed that while BRI2-BRICHOS domain efficiently prevented Aβ$_{42}$ conversion into ThT positive aggregates for more than 24 hours, ThT positive aggregates of Aβ$_{42}$ started to form already after 10 hours when the rBRI2 ectodomain was used (Fig. 2*a,b*).

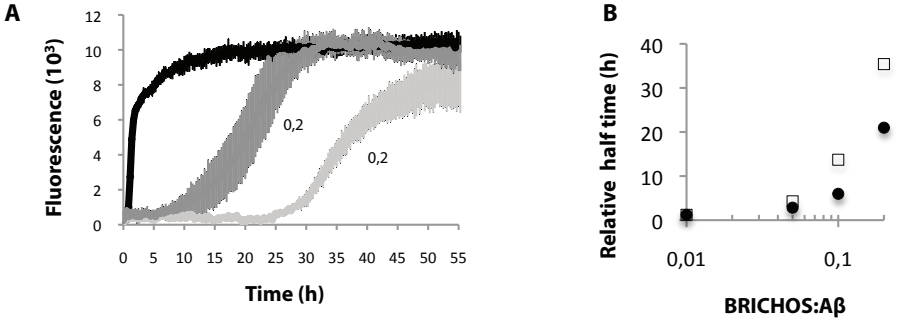

Fig. 2. Recombinant BRI2 ectodomain delays Aβ$_{42}$ less efficiently than BRI2 BRICHOS domain.
a, Aggregation kinetics as monitored by ThT fluorescence of 3 μM Aβ$_{42}$ in the absence (black) or presence of 0.2 (0.6 μM) equivalents of rBRI2$_{76-266}$ (dark grey) or BRI2-BRICHOS (light grey). Every kinetic trace is the average of 4 measurements with the standard deviations plotted as error bars on each time point. ***b,*** relative half-time of fibrillation versus molar ratio protein/Aβ$_{42}$ for rBRI2$_{76-266}$ (black dots) and Bri2 BRICHOS (open squares). Numbers are taken from the average of 4 kinetic traces, and the data are plotted relative to the half-time obtained in the absence of BRI2 protein.

Recombinant BRI2 ectodomain induced apoptotic cell death

The neurotoxicity of the rBRI2 ectodomain was investigated in SH-SY5Y human neuroblastoma cells. Incubation with rBRI2 ectodomain at 0.2, 0.5 and 2 μM for 24 hours decreased mildly, but significantly, MTT reduction by 10% in SH-SY5Y cells (Fig. 3*a*) and N2a cells (data not shown). Differentiated SH-SY5Y and SK-N-SH cells have been widely used to analyze the neurotoxic effects of Aβ[41,42]. The exposure of rBRI2 ectodomain to RA-differentiated SH-SY5Y (Fig. 3b) or SK-N-SH (data not shown) cells led also to a 10% decrease of MTT reduction indicating no differences between differentiated and non-differentiated cells. Therefore, subsequent experiments were performed only with undifferentiated SH-SY5Y cells. Since deposits of BRI2 were associated with Aβ plaques in the AD hippocampus[25], we investigated whether the co-incubation of rBRI2 ectodomain could modify the toxicity induced by $A\beta_{42}$ peptides. The decrease of MTT reduction induced by the $A\beta_{42}$ was not modified by the co-incubation with rBRI2 ectodomain (Fig. 3*c*).

Since a slight but significant reduction of cell viability was observed after $rBRI2_{76\text{-}266}$ exposure, we hypothesized that the rBRI2 ectodomain may promote the activation of apoptosis. Incubation of SH-SY5Y cells with 0.5 μM of $rBRI2_{76\text{-}266}$ led to a significant increase in the levels of the pro-apoptotic protein Bax (Fig. 3*d, e*), together with a decrease in the levels of the anti-apoptotic Bcl-2 protein (Fig. 3*d, f*) and a subsequent two-fold increase in the Bax/Bcl-2 ratio (Fig. 3*g*). To further investigate the role of BRI2 in apoptosis, we also analyzed the activity of caspases 3 and 9, which are downstream effectors of the apoptotic pathway[43]. The incubation with rBRI2 ectodomain led to a significant two-fold increase in the activity of both caspases 3 and 9 (Fig. 3*h, i)*. These data indicate rBRI2 ectodomain induced an apoptotic response in SH-SY5Y cells.

Recombinant BRI2 ectodomain increased the mRNA of BiP but did not modify the mRNA of CHOP or Xbp-1.

Since deposits of BRI2 ectodomain have been observed in early stages of AD, we investigated whether rBRI2 ectodomain activates the classical mediators involved in the UPR (BiP, CHOP and Xbp-1), which may explain the apoptotic response. Incubation of SH-SY5Y cells with rBRI2 ectodomain slightly increased the mRNA levels of BiP (Fig. 4*a*), but not the mRNA levels of CHOP and Xbp-1 (Fig. 4*b,c)*. Taken together, these data indicate that the UPR is not involved in the apoptotic cell death of SH-SY5Y observed upon rBRI2 exposure.

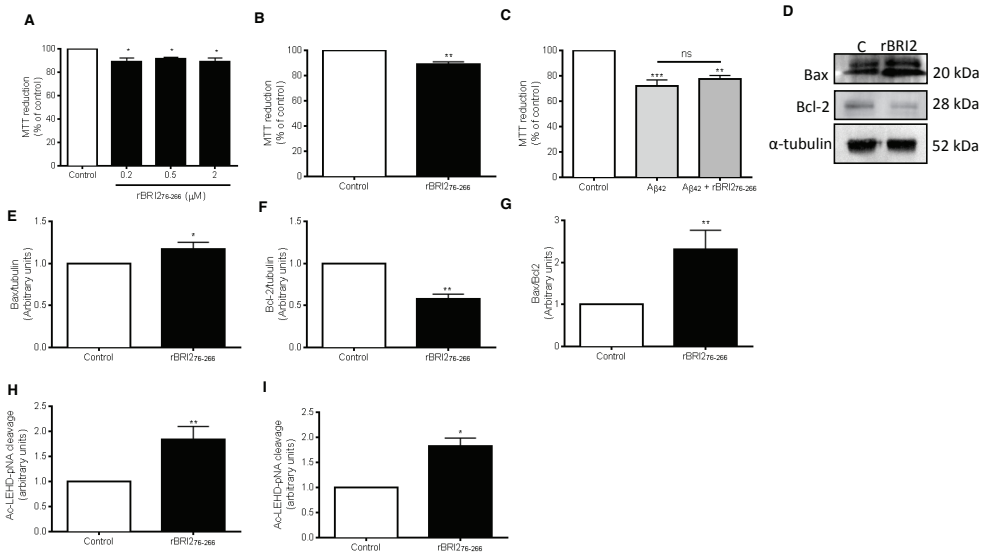

Fig. 3. Recombinant BRI2$_{76\text{-}266}$ induced the activation of the apoptosis pathway in human neuroblastoma cells.

a-c, Cell viability MTT assay after 24 hours incubation of (***a***) non-differentiated SH-SY5Y cells with 0.2, 0.5 or 2 µM rBRI2$_{76\text{-}266}$; (***b***) differentiated SH-SY5Y cells with 0.5 µM rBRI2$_{76\text{-}266}$; (***c***) non-differentiated SH-SY5Y cells with Aβ$_{42}$ peptide (0.5 µM) in the presence or absence of rBRI2$_{76\text{-}266}$ (0.5 µM) **. *d,*** Representative Western blot showing Bax and Bcl-2 expression in cell lysates from SH-SY5Y cells treated with rBRI2$_{76\text{-}266}$ (0.5 µM) during 24 hours. 20 µg of protein was loaded, and reactivity against α-tubulin was used as a loading control. Reactivity against Bax ***(e)*** and Bcl-2 ***(f)*** was quantified and corrected for α-tubulin levels. ***G,*** Bax/Bcl-2 ratio in control and treated cells. **h and i**: quantification of caspase-3 ***(h)*** and caspase-9 ***(i)***-like activities in cell lysates using the colorimetric substrates Ac-LEHD-pNA and Ac-DEVD-pNA respectively. Results were normalized to untreated cells (control) and represent the means ± SEM of at least four independent experiments. *p < 0.05, **p < 0.01**.**

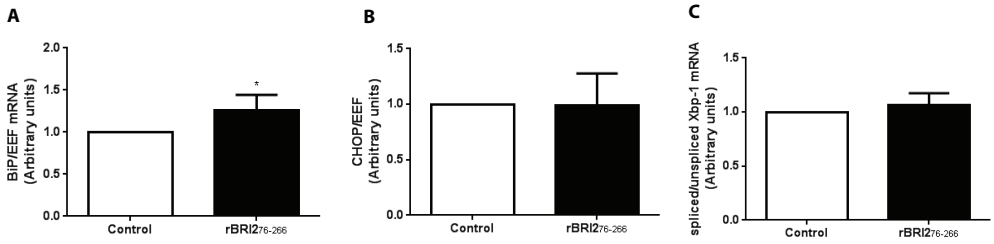

Fig. 4. Recombinant BRI2$_{76\text{-}266}$ did not induce the activation of the UPR in human neuroblastoma cells.

mRNA expression levels of BiP ***(a)***, CHOP ***(b)*** and spliced/unspliced Xbp-1 mRNA ratio ***(c)***. SH-SY5Y cells were treated with rBRI2$_{76\text{-}266}$ (0.5 µM) during 24 hours and mRNA was isolated as described in Materials and Methods. Relative mRNA of BiP, CHOP, spliced and unspliced Xbp-1 corrected EEF were determined using q-PCR. Results were normalized to untreated cells (control) within each experiment and represent the means ± SEM of at least four independent experiments. *p < 0.05.

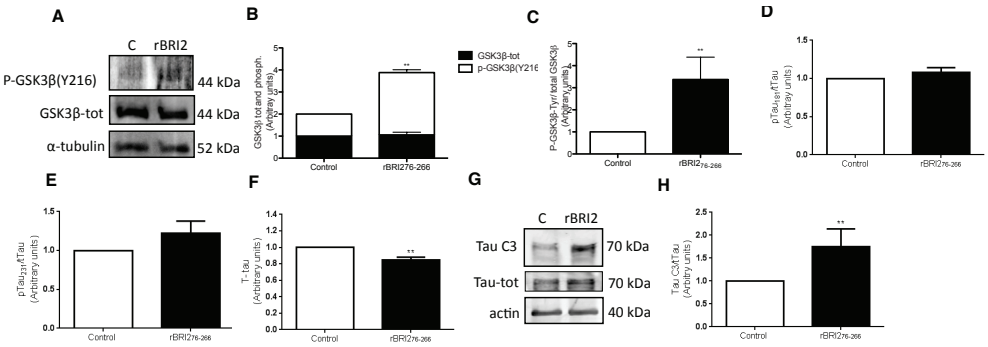

Fig. 5. Recombinant $BRI2_{76-266}$ induced the phosphorylation of GSK3β(Y216) and increased the levels of truncated tau at D421 in human neuroblastoma cells.

a, Western blot showing anti-GSK3β total and anti-p-GSK3β (Y216) expression in cell lysates from SH-SY5Y cells treated with $rBRI2_{76-266}$ (0.5 μM) during 24 hours. 20 μg protein were loaded, and reactivity against α-tubulin was used as a loading control. ***b,*** Reactivity against anti-GSK3β total and anti-p-GSK3β (Y216) was quantified and corrected for α-tubulin or actin levels. ***c,*** p-GSK3β/total-GSK3β ratio was calculated in control and treated cells. ***d-e,*** The corresponding p-Tau/t-Tau ratio for the levels of $p\text{-}Tau_{181}$ (***d***) or $p\text{-}Tau_{231}$ (***e***) were calculated in cell lysates from control and treated cells using highly specific ELISA and MSD kits respectively. ***f:*** Levels of t-Tau in cell lysates using specific ELISA kit***. g***: Western blot showing anti-tau total and anti-truncated tau at D421 (tau C3) expression in cell lysates from SH-SY5Y cells treated with $rBRI2_{76-266}$ (0.5 μM) during 24 hours. 20 μg protein was loaded, and reactivity against actin was used as a loading control. ***h:*** Reactivity against anti-total tau and anti-truncated tau C3 was quantified and corrected for actin levels. truncated/t-Tau ratio was calculated in control and treated cells. Results were normalized to untreated cells (control) and represent the means ± SEM of at least four independent experiments. **$p < 0.01$**.**

Recombinant BRI2 ectodomain induced the activation of GSK3β and increased the levels of truncated tau at D421.

Neurofibrillary tangles are mainly formed by aggregates of abnormal post translationally modified forms of tau such as hyper-phosphorylated tau and truncated tau[1,44]. Glycogen synthase kinase 3 beta (GSK3β) is the major kinase involved in tau phosphorylation and it is active after phosphorylation of its tyrosine at position 216 (p-GSK3β-Y216)[45,46]. We investigated whether incubation with rBRI2 ectodomain promoted activation of GSK3β and the subsequent phosphorylation of tau at threonine 181 and 231. We observed that incubation of SH-SY5Y cells with $rBRI2_{76-266}$ led to increased levels of p-GSK3β-Y216 and subsequent p-GSK3β-Y216/t-GSK3β ratio, indicating an activation of GSK3β (Fig. 5*a-c*). However, no differences in the levels of $p\text{-}Tau_{181}$ or $p\text{-}Tau_{231}$ were observed after incubation with rBRI2ectodomain (Fig. 5*d,e*) Strikingly, the levels of t-tau measured by the ELISA kit were mildly but significantly decreased in cells incubated with rBRI2 ectodomain (Fig. 5*f*). Interestingly, incubation with rBRI2 ectodomain led to increased levels of the truncated tau C3/total tau ratio (Fig. 5*g,h*), indicating that $rBRI2_{76-266}$ induced the truncation of tau at

D421. In summary, the results showed that rBRI2 ectodomain induced the activation of GSK3β, and increased the truncation of tau at D421.

Discussion

Protein conformation-dependent neurotoxicity is a common key molecular pathway involved in different neurodegenerative diseases including AD[47,48]. Several studies have shown that protein misfolding and aggregation (e.g. of Aβ, α-synuclein, prion protein) can lead to synaptic dysfunction and neuronal apoptosis[27–32]. Interestingly, we previously showed an accumulation of BRI2 ectodomain associated with Aβ plaques in early stages of AD[25]. We hypothesize that the observed decrease in the levels of the enzymes involved in the shedding of BRI2 ectodomain (furin and ADAM10[7,8,25,49,50]) leads to reduced cleavage of the BRI2 ectodomain. Together with the increased levels of SPPL2b[25], the enzyme cleaving in the BRI2 transmembrane domain[8], this may promote the release of an un-processed BRI2 ectodomain (BRI2 residues 76-266) instead of the shorter BRI2 peptides. The larger BRI2 fragment may then aggregate leading to the accumulation and loss of function of BRI2[25]. The analysis of $rBRI2_{76\text{-}266}$ under reducing and denaturing conditions showed not only the expected band at 25 kDa but also a band at 50 kDa, which suggest the formation of strong bonds similar to those observed in human hippocampus using an antibody raised against $rBRI2_{76\text{-}266}$[25]. Similar strong aggregates have been detected for other molecules such as the Aβ peptide[51]. The formation of BRI2 homodimers via covalent (i.e. disulfide bonds) and non-covalent interactions in the ectodomain have been previously reported[52]. Thus, the same interactions likely explain the larger BRI2 complexes that were also observed under non-reducing conditions. Further characterization of $rBRI2_{76\text{-}266}$ by size exclusion chromatography revealed that indeed $rBRI2_{76\text{-}266}$ forms large complexes > 600 kDa. These data further confirm the aggregation state of recombinant BRI2 ectodomain[25], as also seen for the recombinant form of BRI2 residues 90-236[9].

Previous studies showed that the BRI2-BRICHOS domain, which is part of the BRI2 protein fragment released after ADAM10 processing[8], inhibits Aβ aggregation and fibrillation very efficiently[9,11]. We previously suggested that the deposits/aggregates of BRI2 ectodomain observed in early stages of AD hippocampus could lead to a loss of BRI2 function[25], including its inhibitory function on Aβ aggregation and fibrillation. The results of this study further support this hypothesis since we observed that the anti-Aβ aggregation activity of rBRI2 ectodomain is significantly lower than that of the recombinant BRI2 BRICHOS domain (residues 113-231). However, despite both BRI2 containing BRICHOS domain (90-236)[9] and BRI2 BRICHOS domain (residues 113-231) form different larger complexes, they still act in delaying Aβ fibril formation. Thus, further studies are needed to reveal the

relation between BRI2 protein oligomeric states and activity. It should also be noted that $rBRI2_{76-266}$ includes the Bri23 peptide part, which is not the case for the fragments covering residues 90-236 or 113-231, and that it is still unknown to what extent this affects function. Similarly to aggregated proteins such as Aβ or α-synuclein, the accumulation of BRI2 ectodomain in AD may lead to a gain of toxic function and have a negative effect on cell homeostasis[27–29,53]. To address this question, we first analyzed the toxicity of rBRI2 ectodomain in neuronal cells using the MTT assay. In the current experimental setup, the addition of rBRI2 ectodomain led to a 10% decrease in cell viability indicating that BRI2 ectodomain can be slightly neurotoxic. More specific and sensitive analysis showed that $BRI2_{76-266}$ clearly induced an apoptotic response by increasing the levels of the pro-apoptotic protein Bax and decreasing the levels of the anti-apoptotic protein Bcl-2. The increased activity of caspases 3 and 9, downstream effectors in the apoptosis cascade[43], further confirm the pro-apoptotic effects of exposure to rBRI2 ectodomain. Strikingly, the cell viability changes observed after incubation with $rBRI2_{76-266}$ do not resemble the large changes observed in the survival and pro-apoptotic proteins. It is possible that the changes observed in the apoptotic pathway still in an early stage, which cannot be fully recognized by the MTT assay. In addition, the activation of compensatory mechanisms that ultimately may prevent cell death can neither be excluded.

Overexpression of a shorter BRI2 form (ITM2Bs, 1-210) also activated apoptosis in a murine T cell line, which was caused by the pro-apoptotic conserved BH3 domain in the cytosolic part of BRI2[54–56]. However, since $rBRI2_{76-266}$ does not contain the BH3 domain, we propose that the observed apoptosis is mediated by other causes, possibly conformation dependent mechanisms, as observed for Aβ[57,58]. Co-incubation of $rBRI2_{76-266}$ with $A\beta_{42}$ did not increase the toxicity induced by $A\beta_{42}$. On the contrary, co-incubation led to a slight but not significant decrease in the $A\beta_{42}$-induced toxicity. Since $rBRI2_{76-266}$ was able to delay $A\beta_{42}$ fibrillation in our experiments, their co-incubation may delay the aggregation and fibrillation of $A\beta_{42,}$ possibly mediating the decrease in the $A\beta_{42-}$induced toxicity. Whether recombinant BRI2 BRICHOS is similarly able to decrease $A\beta_{42}$-induced toxicity by delaying $A\beta_{42}$ aggregation and fibrillation remains to be investigated. Recently it was shown in a Drosophila model of Aβ aggregation and toxicity, that the BRICHOS domain of the lung surfactant protein C (proSP-C) prevents the toxic effect of expressed $A\beta_{42}$ in the fly brain[59]. Recombinant proSP-C BRICHOS domain has been shown to have a similar effect *in vitro* on Aβ fibril formation as BRI2 BRICHOS[11], which supports the hypothesis that the BRI2 BRICHOS domain is also capable of decreasing the $A\beta_{42}$-induced toxicity, and not only affect the fibrillation.

Misfolded proteins and extracellular stimuli can lead to ER stress and Ca^{2+} release, which can activate apoptosis[33,34]. ER stress induces the UPR, a coordinated adaptive cell response focused on restoring cell homeostasis[33,35]. Noteworthy, increased expression of UPR

markers has been observed in early stages of AD[60–62]. Compelling evidence suggests that Aβ can induce an ER stress-mediated apoptosis[63–66]. In a recent study, inhibition of the UPR prevented neurodegeneration independently of the primary pathogen in a mouse model of prion disease[67]. Thus, the UPR is an important response and a causative contributor to the pathogenesis of misfolded protein disorders[68]. In the UPR, misfolded proteins activate three independent pathways that ultimately lead to an increased transcription of several genes including the ER chaperone BiP, the pro-apoptotic protein CHOP and the cellular stress transcription factor Xbp-1[35]. Here, we showed that exogenous $rBRI2_{76\text{-}266}$ induced a slight up-regulation of BiP mRNA but it did not modify the mRNA levels of either CHOP or sXbp-1. Thus, the UPR presumably is not a major player during the apoptosis induced by exogenous rBRI2 ectodomain. However, the increase on BiP mRNA levels suggests that rBRI2 aggregates may initiate a mild stress of the ER and the subsequent release of Ca^{2+} similarly to Aβ[34,64]. It has been shown that apoptotic stimuli and ER-Ca^{2+} release in neuronal cells can also lead to the activation of GSK3β, providing an alternative pathway leading to neuronal death[69,70]. Interestingly, $rBRI2_{76\text{-}266}$ increased the phosphorylation and activation of GSK3β, suggesting that the apoptotic response induced by $rBRI2_{76\text{-}266}$ might be mediated via p-GSK3β-Y^{216}. Alternatively, apoptosis could be also mediated via cell surface death receptors or by other cytotoxic stress pathways (i.e. heat shock response)[71,72], which remains to be investigated.

We have previously shown that NFT formation correlated with the formation of BRI2 deposits in post-mortem human AD tissue[25], suggesting a close relationship between BRI2 accumulation and NFT development. NFTs are one of the classical neuropathological hallmarks in AD and consist of intracellular aggregates of abnormal hyperphosphorylated and truncated tau[1,44,73]. According to the amyloid cascade hypothesis, the observed association between Aβ deposits and NFTs suggests that amyloid-induced toxicity may trigger neurofibrillary pathology[74,75]. However, the exact mechanism by which amyloidosis may facilitate NFTs formation remains to be elucidated. In the last years, several studies suggested that truncation of tau by caspases (preferentially caspase-3) is an early and crucial event in tau pathogenesis[44,76,77]. However, it remains controversial whether tau truncation precedes tau hyperphosphorylation or if it occurs once NFT are formed[78]. Our data showed that while $rBRI2_{76\text{-}266}$ led to increased levels of p-GSK3β-Y^{216}, it did not modify the levels of p-Tau_{181} or p-Tau_{231} in SH-SY5Y cells. Besides tau phosphorylation, GSK3β can regulate other important proteins involved in AD pathogenesis such as presenilin 1 (PS1)[79,80] or BACE1[81], both involved in the processing of APP and production of Ab[82,83]. Intriguingly, previous studies have shown contradictory results when studying the effects of GSK3β in APP processing and Aβ production[79,84–86]. In addition GSK3β participates also in inflammatory mechanisms by promoting the secretion of different cytokines including IL-12[87], an inflammation pathway that regulated not only Aβ pathology but also spatial

memory in a transgenic mouse model[88,89]. Thus, future studies are needed to unravel whether rBRI2 ectodomain can modulate APP processing enzymes or inflammatory markers via activation of GSK3β.

Interestingly, in this experimental setup, incubation with $rBRI2_{76-266}$ led not only to an increased activity of caspase 3 but also to increased levels of truncated tau at D421. Importantly, truncation of tau at D421 has been observed in AD[90,91] and this truncated form has been suggested to have an important involvement in the formation of NFT[44,73,76,92]. Strikingly, decreased levels of t-Tau were found after incubation with rBRI2 ectodomain. We suggest that incubation with rBRI2 ectodomain and the subsequent increased activity of caspase 3 may promote the truncation and assembly of tau[93], masking some of the epitopes recognized by the antibodies of the t-Tau immunoassay and thus leading to the observed decrease levels in t-Tau. Thus, our results suggest that the presence of BRI2 aggregates may induce the truncation of tau at D421 and promote the formation of NFT in AD.

Taken together, our results reveal that the rBRI2 ectodomain was remarkably less efficient on preventing Aβ fibrillation than the BRI2 BRICHOS domain, supporting the hypothesis that un-processed BRI2 ectodomain and subsequent aggregation disrupts BRI2 functionality (i.e. easing amyloid fibrillation). Moreover, the rBRI2 ectodomain besides inducing an apoptotic response and activation of GSK3β, it also increased the levels of truncated tau at D421, suggesting that BRI2 ectodomain oligomers can be involved in NFT formation. Since BRI2 is able to regulate APP processing and Aβ load, we propose that modifications in BRI2 can play an important role of several aspects of AD pathogenesis. On one hand, the accumulation of BRI2 ectodomain in early stages of AD likely leads to a loss of BRI2 function [25], influencing APP processing and Aβ metabolism[11–13,19,20,94]. On top of that, our current results suggest that the presence BRI2 aggregates may participate in the neurodegenerative process through truncation of tau and an activation of the apoptosis pathway (Fig. 6). Nevertheless, it is important to define the specific conformational structure and sequencing of the BRI2 form that is modified in AD and thus, specific antibodies covering a wide range of the BRI2 protein need to be developed. In addition, other aspects need to be further investigated including a thorough analysis of the effects of aggregated BRI2 on AD related mechanisms (e.g. APP processing, ER-Ca^{2+} release and inflammation). The further understanding of BRI2 in AD may open new insight in the development of disease-modifying therapies trying to restore the normal function of BRI2.

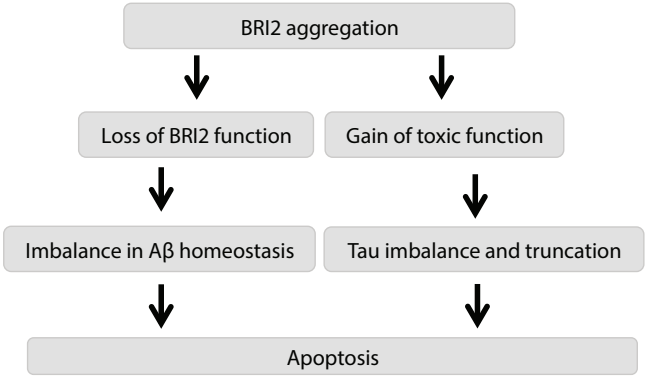

Fig. 6. Hypothetical model illustrating the possible consequences of aggregated BRI2 ectodomain.
Aggregated BRI2 ectodomain may have important consequences on the development of AD hallmarks as proposed in the "Discussion". However, it is important to note that exact characteristics of the larger BRI2 forms and deposits observed in human AD tissue remain to be clarified.

Acknowledgment

We acknowledge Kees van Uffelen, Dorine Wouters and Irina van Geffen from the Neurochemistry Laboratory of the Clinical Chemistry department at the VUmc for their technical assistance.

Funding

This work was supported by the Erasmus Mundus Joint Doctorate Program (EMJD 2009-2013, Action 1B, Grant 159302-1-2009-1-NL-ERA, European Neuroscience Campus Network) and the Swedish Research Council. We also acknowledge the grant from the German scientific network for dementia research BMBF KNDD rpAD (BMBF 01GI1010A) to C.K, and a grant from the Forschungskommission of the Medical Faculty Heinrich Heine University Düsseldorf to A.M.S.

Conflict of interest

None of the authors have any competing interest.

References

1. Grundke-Iqbal, I. *et al.* Abnormal phosphorylation of the microtubule-associated protein tau (tau) in Alzheimer cytoskeletal pathology. *Proc Natl Acad Sci U S A* **83,** 4913–7 (1986).

2. Selkoe, D. J. The Molecular of Alzheimer ' s Pathology Disease Review. *Neuron* **6,** 487–498 (1991).

3. Vidal, R. *et al.* A stop-codon mutation in the BRI gene associated with familial British dementia. *Nature* **399,** 776–81 (1999).

4. Vidal, R. *et al.* A decamer duplication in the 3′ region of the BRI gene originates an amyloid peptide that is associated with dementia in a Danish kindred. *Proc Natl Acad Sci U S A* **97,** 4920–5 (2000).

5. Rostagno, A. *et al.* Chromosome 13 dementias. *Cell Mol Life Sci* **62,** 1814–25 (2005).

6. Garringer, H. J., Murrell, J., D'Adamio, L., Ghetti, B. & Vidal, R. Modeling familial British and Danish dementia. *Brain Struct Funct* **214,** 235–44 (2010).

7. Kim, S. H. *et al.* Furin mediates enhanced production of fibrillogenic ABri peptides in familial British dementia. *Nat Neurosci* **2,** 984–8 (1999).

8. Martin, L. *et al.* Regulated intramembrane proteolysis of Bri2 (Itm2b) by ADAM10 and SPPL2a/SPPL2b. *J Biol Chem* **283,** 1644–52 (2008).

9. Peng, S., Fitzen, M., Jörnvall, H. & Johansson, J. The extracellular domain of Bri2 (ITM2B) binds the ABri peptide (1-23) and amyloid beta-peptide (Abeta1-40): Implications for Bri2 effects on processing of amyloid precursor protein and Abeta aggregation. *Biochem Biophys Res Commun* **393,** 356–61 (2010).

10. Willander, H., Hermansson, E., Johansson, J. & Presto, J. BRICHOS domain associated with lung fibrosis, dementia and cancer--a chaperone that prevents amyloid fibril formation? *FEBS J* **278,** 3893–904 (2011).

11. Willander, H. *et al.* BRICHOS Domains Efficiently Delay Fibrillation of Amyloid β-Peptide. *J Biol Chem* **287,** 31608–17 (2012).

12. Fotinopoulou, A. *et al.* BRI2 interacts with amyloid precursor protein (APP) and regulates amyloid beta (Abeta) production. *J Biol Chem* **280,** 30768–72 (2005).

13. Matsuda, S. *et al.* The familial dementia BRI2 gene binds the Alzheimer gene amyloid-beta precursor protein and inhibits amyloid-beta production. *J Biol Chem* **280,** 28912–6 (2005).

14. Matsuda, S., Giliberto, L., Matsuda, Y., McGowan, E. M. & D'Adamio, L. BRI2 inhibits amyloid beta-peptide precursor protein processing by interfering with the docking of secretases to the substrate. *J Neurosci* **28,** 8668–76 (2008).

15. Matsuda, S., Matsuda, Y., Snapp, E. L. & D'Adamio, L. Maturation of BRI2 generates a specific inhibitor that reduces APP processing at the plasma membrane and in endocytic vesicles. *Neurobiol Aging* **32,** 1400–8 (2009).

16. Matsuda, S., Tamayev, R. & D'Adamio, L. Increased AβPP Processing in Familial Danish Dementia Patients. *J Alzheimers Dis* **27,** 385–91 (2011).

17. Tamayev, R., Matsuda, S., Giliberto, L., Arancio, O. & D'Adamio, L. APP heterozygosity averts memory deficit in knockin mice expressing the Danish dementia BRI2 mutant. *EMBO J* **30,** 2501–9 (2011).

18. Tamayev, R. & D'Adamio, L. Memory deficits of British Dementia knock-in mice are prevented by APP haploinsufficiency. *J Neurosci* **32,** 5481–5485 (2012).

19. Kilger, E. *et al.* BRI2 regulates {beta}-amyloid degradation by increasing levels of secreted insulin degrading enzyme (IDE). *J Biol Chem* **286,** 37446–37457 (2011).

20. Tsachaki, M. *et al.* BRI2 interacts with BACE1 and regulates its cellular levels by promoting its degradation and reducing its mRNA levels. *Curr Alzheimer Res* **10,** 532–41 (2013).

21. Tamayev, R. *et al.* Memory Deficits Due to Familial British Dementia BRI2 Mutation Are Caused by Loss of BRI2 Function Rather than Amyloidosis. *J Neurosci* **30,** 14915–14924 (2010).

22. Tamayev, R., Matsuda, S., Fà, M., Arancio, O. & Adamio, L. D. Danish dementia mice suggest that loss of function and not the amyloid cascade causes synaptic plasticity and memory deficits. *PNAS* **107,** 20822–27 (2010).

23. Garringer, H. J. *et al.* Increased tau phosphorylation and tau truncation, and decreased synaptophysin levels in mutant BRI2/tau transgenic mice. *PLoS One* **8,** e56426 (2013).

24. Del Campo, M. & Teunissen, C. E. Role of BRI2 in dementia. *J Alzheimers Dis* **40,** 481–94 (2014).

25. Del Campo, M. *et al.* BRI2-BRICHOS is increased in human amyloid plaques in early stages of Alzheimer's disease. *Neurobiol Aging* **35,** 1596–604 (2014).

26. Winklhofer, K. F., Tatzelt, J. & Haass, C. The two faces of protein misfolding: gain- and loss-of-function in neurodegenerative diseases. *EMBO J* **27,** 336–49 (2008).

27. Klein, W. L. Synaptotoxic amyloid-β oligomers: a molecular basis for the cause, diagnosis, and treatment of Alzheimer's disease? *J Alzheimers Dis* **33 Suppl 1,** S49–65 (2013).

28. Brown, D. R. Oligomeric alpha-synuclein and its role in neuronal death. *IUBMB Life* **62,** 334–9 (2010).

29. Bossy-Wetzel, E., Schwarzenbacher, R. & Lipton, S. A. Molecular pathways to neurodegeneration. *Nat Med* **Suppl:S2-9,** (2004).

30. Forloni, G. *et al.* Neurotoxicity of a prion protein fragment. *Nature* **362,** 543–6 (1993).

31. El-Agnaf, O. M. *et al.* Aggregates from mutant and wild-type alpha-synuclein proteins and NAC peptide induce apoptotic cell death in human neuroblastoma cells by formation of beta-sheet and amyloid-like filaments. *FEBS Lett* **440,** 71–5 (1998).

32. El-Agnaf, O. M., Mahil, D. S., Patel, B. P. & Austen, B. M. Oligomerization and toxicity of beta-amyloid-42 implicated in Alzheimer's disease. *Biochem Biophys Res Commun* **273,** 1003–7 (2000).

33. Rutkowski, D. T. & Hegde, R. S. Regulation of basal cellular physiology by the homeostatic unfolded protein response. *J Cell Biol* **189,** 783–94 (2010).

34. Ferreiro, E., Oliveira, C. R. & Pereira, C. Involvement of endoplasmic reticulum Ca2+ release through ryanodine and inositol 1,4,5-triphosphate receptors in the neurotoxic effects induced by the amyloid-beta peptide. *J Neurosci Res* **76,** 872–80 (2004).

35. Walter, P. & Ron, D. The unfolded protein response: from stress pathway to homeostatic regulation. *Science* **334,** 1081–6 (2011).

36. Korth, C. *et al.* Prion (PrPSc)-specific epitope defined by a monoclonal antibody. *Nature* **390,** 74–7 (1997).

37. Walsh, D. M. *et al.* A facile method for expression and purification of the Alzheimer's disease-associated amyloid beta-peptide. *FEBS J* **276,** 1266–81 (2009).

38. Fonseca, A. C. R. G., Ferreiro, E., Oliveira, C. R., Cardoso, S. M. & Pereira, C. F. Activation of the endoplasmic reticulum stress response by the amyloid-beta 1-40 peptide in brain endothelial cells. *Biochim Biophys Acta* **1832,** 2191–203 (2013).

39. Liu, Y. & Schubert, D. Cytotoxic amyloid peptides inhibit cellular 3-(4,5-dimethylthiazol-2-yl)-2,5-diphenyltetrazolium bromide (MTT) reduction by enhancing MTT formazan exocytosis. *J Neurochem* **69,** 2285–93 (1997).

40. Nijholt, D. A. T. *et al.* Endoplasmic reticulum stress activates autophagy but not the proteasome in neuronal cells: implications for Alzheimer's disease. *Cell Death Differ* **18,** 1071–81 (2011).

41. Datki, Z. *et al.* Method for measuring neurotoxicity of aggregating polypeptides with the MTT assay on differentiated neuroblastoma cells. *Brain Res Bull* **62,** 223–9 (2003).

42. Chafekar, S. M., Baas, F. & Scheper, W. Oligomer-specific Abeta toxicity in cell models is mediated by selective uptake. *Biochim Biophys Acta* **1782,** 523–31 (2008).

43. Marsden, V. S. & Strasser, A. Control of apoptosis in the immune system: Bcl-2, BH3-only proteins and more. *Annu Rev Immunol* **21,** 71–105 (2003).

44. Rissman, R. A. *et al.* Caspase-cleavage of tau is an early event in Alzheimer disease tangle pathology. *J Clin Invest* **114,** 121–30 (2004).

45. Lovestone, S. *et al.* Alzheimer's disease-like phosphorylation of the microtubule-associated protein tau by glycogen synthase kinase-3 in transfected mammalian cells. *Curr Biol* **4,** 1077–1086 (1994).

46. Hughes, K., Nikolakaki, E., Plyte, S. E., Totty, N. F. & Woodgett, J. R. Modulation of the glycogen synthase Kinase-3 family by tyrosine phosphorilation. *EMBO J* **12,** 803–808 (1993).

47. Soto, C. & Estrada, L. Protein Misfolding and Neurodegeneration. *Arch Neurol* **65,** 184–189 (2008).

48. Soto, C. Unfolding the role of protein misfolding in neurodegenerative diseases. *Nat Rev Neurosci* **4,** 49–60 (2003).

49. Endres, K. & Fahrenholz, F. Regulation of alpha-secretase ADAM10 expression and activity. *Exp Brain Res* **217,** 343–52 (2012).

50. Tyler, S. J., Dawbarn, D., Wilcock, G. K. & Allen, S. J. alpha- and beta-secretase: profound changes in Alzheimer's disease. *Biochem Biophys Res Commun* **299,** 373–376 (2002).

51. Bouter, Y. *et al.* N-truncated amyloid β (Aβ) 4-42 forms stable aggregates and induces acute and long-lasting behavioral deficits. *Acta Neuropathol* **126,** 189–205 (2013).

52. Tsachaki, M., Ghiso, J., Rostagno, A. & Efthimiopoulos, S. BRI2 homodimerizes with the involvement of intermolecular disulfide bonds. *Neurobiol Aging* **31,** 88–98 (2010).

53. Bemporad, F. & Chiti, F. Protein misfolded oligomers: experimental approaches, mechanism of formation, and structure-toxicity relationships. *Chem Biol* **19,** 315–27 (2012).

54. Fleischer, A., Ayllón, V., Dumoutier, L., Renauld, J.-C. & Rebollo, A. Proapoptotic activity of ITM2B(s), a BH3-only protein induced upon IL-2-deprivation which interacts with Bcl-2. *Oncogene* **21,** 3181–9 (2002).

55. Fleischer, A., Ayllon, V. & Rebollo, A. ITM2BS regulates apoptosis by inducing loss of mitochondrial membrane potential. *Eur J Immunol* **32,** 3498–505 (2002).

56. Fleischer, A. & Rebollo, A. Induction of p53-independent apoptosis by the BH3-only protein ITM2Bs. *FEBS Lett* **557,** 283–287 (2004).

57. Lesné, S. E. *et al.* Brain amyloid-β oligomers in ageing and Alzheimer's disease. *Brain* **136,** 1383–98 (2013).

58. Zahs, K. R. & Ashe, K. H. β-Amyloid oligomers in aging and Alzheimer's disease. *Front Aging Neurosci* **5,** 28 (2013).

59. Hermansson, E. *et al.* The chaperone domain BRICHOS prevents CNS toxicity of amyloid-β peptide in Drosophila melanogaster. *Dis Model Mech* **7,** 659–65 (2014).

60. Unterberger, U. *et al.* Endoplasmic reticulum stress features are prominent in Alzheimer disease but not in prion diseases in vivo. *J Neuropathol Exp Neurol* **65,** 348–57 (2006).

61. Hoozemans, J. J. M., van Haastert, E. S., Nijholt, D. A. T., Rozemuller, A. J. M. & Scheper, W. Activation of the unfolded protein response is an early event in Alzheimer's and Parkinson's disease. *Neurodegener Dis* **10,** 212–5 (2012).

62. Hoozemans, J. J. M. *et al.* The unfolded protein response is activated in Alzheimer's disease. *Acta Neuropathol* **110,** 165–72 (2005).

63. Costa, R. O. *et al.* Amyloid β-induced ER stress is enhanced under mitochondrial dysfunction conditions. *Neurobiol Aging* **33,** 824.e5–16 (2012).

64. Resende, R., Ferreiro, E., Pereira, C. & Resende de Oliveira, C. Neurotoxic effect of oligomeric and fibrillar species of amyloid-beta peptide 1-42: involvement of endoplasmic reticulum calcium release in oligomer-induced cell death. *Neuroscience* **155,** 725–37 (2008).

65. Chafekar, S. M., Hoozemans, J. J. M., Zwart, R., Baas, F. & Scheper, W. Abeta 1-42 induces mild endoplasmic reticulum stress in an aggregation state-dependent manner. *Antioxid Redox Signal* **9,** 2245–54 (2007).

66. Ferreiro, E., Resende, R., Costa, R., Oliveira, C. R. & Pereira, C. M. F. An endoplasmic-reticulum-specific apoptotic pathway is involved in prion and amyloid-beta peptides neurotoxicity. *Neurobiol Dis* **23,** 669–78 (2006).

67. Moreno, J. A. *et al.* Oral treatment targeting the unfolded protein response prevents neurodegeneration and clinical disease in prion-infected mice. *Sci Transl Med* **5,** 206ra138 (2013).

68. Scheper, W. & Hoozemans, J. J. M. Endoplasmic reticulum protein quality control in neurodegenerative disease: the good, the bad and the therapy. *Curr Med Chem* **16,** 615–26 (2009).

69. Song, L., De Sarno, P. & Jope, R. S. Central role of glycogen synthase kinase-3beta in endoplasmic reticulum stress-induced caspase-3 activation. *J Biol Chem* **277,** 44701–8 (2002).

70. Jacobs, K. M. *et al.* GSK-3β: A Bifunctional Role in Cell Death Pathways. *Int J Cell Biol* **2012,** 11 (2012).

71. Wilhelmus, M. M. M. *et al.* Specific association of small heat shock proteins with the pathological hallmarks of Alzheimer's disease brains. *Neuropathol Appl Neurobiol* **32,** 119–30 (2006).

72. Milleron, R. S. & Bratton, S. B. Heat shock induces apoptosis independently of any known initiator caspase-activating complex. *J Biol Chem* **281,** 16991–7000 (2006).

73. Gamblin, T. C. *et al.* Caspase cleavage of tau: linking amyloid and neurofibrillary tangles in Alzheimer's disease. *Proc Natl Acad Sci U S A* **100,** 10032–7 (2003).

74. Reitz, C. Alzheimer's disease and the amyloid cascade hypothesis: a critical review. *Int J Alzheimers Dis* **2012,** 11 (2012).

75. Götz, J., Chen, F., van Dorpe, J. & Nitsch, R. M. Formation of neurofibrillary tangles in P301l tau transgenic mice induced by Abeta 42 fibrils. *Science* **293,** 1491–5 (2001).

76. De Calignon, A. *et al.* Caspase activation precedes and leads to tangles. *Nature* **464,** 1201–4 (2010).

77. Zhao, H., Zhao, W., Lok, K., Wang, Z. & Yin, M. A synergic role of caspase-6 and caspase-3 in Tau truncation at D421 induced by H2O 2. *Cell Mol Neurobiol* **34,** 369–78 (2014).

78. Gendron, T. F. & Petrucelli, L. The role of tau in neurodegeneration. *Mol Neurodegener* **4,** 13 (2009).

79. Uemura, K. *et al.* GSK3beta activity modifies the localization and function of presenilin 1. *J Biol Chem* **282,** 15823–32 (2007).

80. Twomey, C. & McCarthy, J. V. Presenilin-1 is an unprimed glycogen synthase kinase-3beta substrate. *FEBS Lett* **580,** 4015–20 (2006).

81. Ly, P. T. T. *et al.* Inhibition of GSK3 β -mediated BACE1 expression reduces Alzheimer-associated phenotypes. **123,** (2013).

82. Cai, H. *et al.* BACE1 is the major beta-secretase for generation of Abeta peptides by neurons. *Nat Neurosci* **4,** 233–4 (2001).

83. De Strooper, B. *et al.* A presenilin-1-dependent gamma-secretase-like protease mediates release of Notch intracellular domain. *Nature* **398,** 518–22 (1999).

84. Jaworski, T. *et al.* GSK-3α/β kinases and amyloid production in vivo. *Nature* **480,** E4–5; discussion E6 (2011).

85. Phiel, C. J., Wilson, C. A., Lee, V. M. & Klein, P. S. GSK-3 a regulates production of Alzheimer ' s disease amyloid- b peptides. **17,** 435–439 (2003).

86. Maesako, M. *et al.* Effect of glycogen synthase kinase 3 β-mediated presenilin 1 phosphorylation on amyloid β production is negatively regulated by insulin receptor cleavage. *Neuroscience* **177,** 298–307 (2011).

87. Martin, M., Rehani, K., Jope, R. S. & Michalek, S. M. Toll-like receptor-mediated cytokine production is differentially regulated by glycogen synthase kinase 3. *Nat Immunol* **6,** 777–84 (2005).

88. Vom Berg, J. *et al.* Inhibition of IL-12/IL-23 signaling reduces Alzheimer's disease-like pathology and cognitive decline. *Nat Med* **18,** 1812–9 (2012).

89. Tan, M.-S. *et al.* IL12/23 p40 inhibition ameliorates Alzheimer's disease-associated neuropathology and spatial memory in SAMP8 mice. *J Alzheimers Dis* **38,** 633–46 (2014).

90. Guillozet-Bongaarts, A. L. *et al.* Tau truncation during neurofibrillary tangle evolution in Alzheimer's disease. *Neurobiol Aging* **26,** 1015–22 (2005).

91. Basurto-Islas, G. *et al.* Accumulation of aspartic acid421- and glutamic acid391-cleaved tau in neurofibrillary tangles correlates with progression in Alzheimer disease. *J Neuropathol Exp Neurol* **67,** 470–83 (2008).

92. Zhang, Q., Zhang, X. & Sun, A. Truncated tau at D421 is associated with neurodegeneration and tangle formation in the brain of Alzheimer transgenic models. *Acta Neuropathol* **117,** 687–97 (2009).

93. Lee, S. & Shea, T. B. Caspase-mediated truncation of tau potentiates aggregation. *Int J Alzheimers Dis* **2012,** 731063 (2012).

94. Kim, J. *et al.* BRI2 (ITM2b) inhibits Abeta deposition in vivo. *J Neurosci* **28,** 6030–6 (2008).